Approximation of multivariate periodic functions by trigonometric polynomials based on rank-1 lattice sampling

Lutz Kämmerer* Daniel Potts* Toni Volkmer*

In this paper, we present algorithms for the approximation of multivariate periodic functions by trigonometric polynomials. The approximation is based on sampling of multivariate functions on rank-1 lattices. To this end, we study the approximation of periodic functions of a certain smoothness. Our considerations include functions from periodic Sobolev spaces of generalized mixed smoothness. Recently an algorithm for the trigonometric interpolation on generalized sparse grids for this class of functions was investigated in [12]. The main advantage of our method is that the algorithm based mainly on a single one-dimensional fast Fourier transform, and that the arithmetic complexity of the algorithm depends only on the cardinality of the support of the trigonometric polynomial in the frequency domain. Therefore, we investigate trigonometric polynomials with frequencies supported on hyperbolic crosses and energy norm based hyperbolic crosses in more detail. Furthermore, we present an algorithm for sampling multivariate functions on perturbed rank-1 lattices and show the numerical stability of the suggested method. Numerical results are presented up to dimension $d = 10$, which confirm the theoretical findings.

Keywords and phrases : approximation of multivariate functions, trigonometric polynomials, Taylor approximation, hyperbolic cross, lattice rule, fast Fourier transform

2000 AMS Mathematics Subject Classification : 65T40, 42A10,

*Technische Universität Chemnitz, Faculty of Mathematics, 09107 Chemnitz, Germany
{lutz.kaemmerer, daniel.potts, toni.volkmer}@mathematik.tu-chemnitz.de

Contents

1 Introduction

The approximation of high-dimensional functions is a fundamental problem in numerical analysis. It is a well known fact, that the discretisation of high-dimensional problems often leads to an exponential growth in the number of degrees of freedom. This is labeled as the curse of dimensions and the use of sparsity has become a very popular tool for handling such problems. For a wide range of moderately high-dimensional problems the use of sparse grids and the approximation of functions using approximants supported on hyperbolic crosses in Fourier domain has decreased the problem size dramatically from $\mathcal{O}(N^d)$ to $\mathcal{O}(N(\log N)^{d-1})$ while hardly deteriorating the approximation error, cf. e.g., [35, 37, 34, 5, 31]. Here d denotes the underlying problem's dimensionality and N is the number of nodes in one coordinate direction on the hyperbolic cross. Of course, an important issue is the adaption of efficient Fourier algorithms, which realize the map between the spatial domain and the hyperbolic crosses. Fast algorithms that realize the map between sparse grids in spatial domain and hyperbolic crosses in Fourier domain are known as the hyperbolic cross fast Fourier transform (HCFFT). Such algorithms were studied in [2, 15, 11, 19]. Recently, sparse grid based approaches have emerged as useful techniques to tackle higher dimensional problems, see e.g., the seminal paper of M. Griebel and J. Hamaekers [12], where the authors used trigonometric interpolation based on generalized sparse grids, especially so-called energy norm based sparse grids [4, 5], and developed the related hyperbolic cross fast Fourier transform. For the energy norm based sparse grids, only $C_d\, N$ degrees of freedom are necessary. Typically, one uses these techniques for the approximation of functions in periodic Sobolev spaces of generalized mixed smoothness.

In this paper, we use a sampling scheme based on sampling on rank-1 lattices in spatial domain and consider functions in subspaces of the Wiener algebra and periodic Sobolev spaces of generalized mixed smoothness. Lattice rules are well known for the integration of functions of many variables, cf. e.g., [32, 8] and the extensive reference list therein. Furthermore, there exist already comprehensive tractability results for numerical integration using rank-1 lattices, see [29].

The main tool of our approximation method is based on the observation that a trigonometric polynomial $p\colon \mathbb{T}^d := [0,1)^d \to \mathbb{C}$,

$$p(\boldsymbol{x}) = \sum_{\boldsymbol{k}\in I} \hat{p}_{\boldsymbol{k}}\, \mathrm{e}^{2\pi \mathrm{i} \boldsymbol{k}\boldsymbol{x}},\ \hat{p}_{\boldsymbol{k}} \in \mathbb{C},\ I \subset \mathbb{Z}^d, |I| < \infty, \tag{1.1}$$

with frequencies supported on an arbitrary index set I of finite cardinality can be fast evaluated at a rank-1 lattice by the one-dimensional FFT, cf. [23]. The scalar product $\boldsymbol{x}\boldsymbol{y}$ of two vectors $\boldsymbol{x} = (x_1, \ldots, x_d)^\top, \boldsymbol{y} = (y_1, \ldots, y_d)^\top \in \mathbb{R}^d$ is defined as usual by $\boldsymbol{x}\boldsymbol{y} = \sum_{t=1}^{d} x_t y_t$. On the other hand, a trigonometric polynomial p with frequencies supported on the index set I can be reconstructed from samples on a rank-1 lattice. It follows straightforward that for convex index sets I, there exists a rank-1 lattice of cardinality $M = \mathcal{O}(|I|)$, which allows for the unique reconstruction of the trigonometric polynomial p with frequencies supported on I. It is shown in [20] that for hyperbolic crosses as index set I, there exist rank-1 lattices of cardinality $M = \mathcal{O}(|I|^2)$. We end up with an algorithm with a complexity of $\mathcal{O}(|I|^2 \log |I|)$, which is very fast and simple, since it based mainly on a single one-dimensional fast Fourier transform. To this end, the first named author developed a component-by-component algorithm to find such rank-1 lattices, cf. [20]. This method is based on the component-by-component algorithm original developed for numerical integration in [6]. In contrast to possible stability

problems when sampling on sparse grids, see [22], our sampling method is perfectly stable. Furthermore, we develop an algorithm for sampling the multivariate function on a perturbed rank-1 lattice. The presented method is based on the Taylor approximation and on one-dimensional fast Fourier transforms, cf. [36]. Using these tools, we are in a position to prove stability results for such perturbed rank-1 lattices. Earlier work on nonequispaced hyperbolic cross fast Fourier transform [9] is based on the HCFFT and, hence, may suffer from stability problems.

The paper is organized as follows: We introduce the necessary notation in Section 2 and collect some known results. We present methods for the fast evaluation and fast reconstruction of trigonometric polynomials at a rank-1 lattice, see Subsection 2.2 and Subsection 2.3. In Subsection 2.4, we introduce subspaces of the Wiener algebra, which are characterized by its isotropic and dominating mixed smoothness, as well as the related frequency index sets. In Section 3, we address the problem of approximating the functions from these spaces by sampling on rank-1 lattices. For that purpose, we present Algorithm 2 and prove in Theorem 3.3 and in Theorem 3.4 the related approximation errors. The aim of Section 4 is twofold. On the one hand, we show that the fast evaluation and the fast reconstruction of trigonometric polynomials on perturbed rank-1 lattices is possible using Taylor expansion. To this end, we present Algorithm 3 and prove the stability results in Theorem 4.3. We remark that the complexity of the suggested algorithm depends exponentially on the dimension d and is therefore only practicable for moderate dimensions d. On the other hand, the theoretical results show the stability for our sampling scheme even for large dimensions d. In Section 5, we present the results for approximating the functions from the subspaces of the Wiener algebra by sampling on perturbed rank-1 lattices, see Theorem 5.1. Finally, we present extensive numerical tests in Section 6 in order to illustrate the theoretical results and we give some concluding remarks in Section 7.

2 Prerequisite

2.1 Reconstruction of trigonometric polynomials from sampling values

Let a frequency index set $I \subset \mathbb{Z}^d$ of finite cardinality be given. We want to reconstruct the Fourier coefficients $\hat{p}_{\boldsymbol{k}}$, $\boldsymbol{k} \in I$, of a trigonometric polynomial $p \in \Pi_I := \operatorname{span}\{\mathrm{e}^{2\pi\mathrm{i}\boldsymbol{k}\circ} : \boldsymbol{k} \in I\}$ with frequencies supported on I, $p(\boldsymbol{x}) := \sum_{\boldsymbol{k}\in I} \hat{p}_{\boldsymbol{k}}\, \mathrm{e}^{2\pi\mathrm{i}\boldsymbol{k}\boldsymbol{x}}$, from sampling values $p(\boldsymbol{y}_\ell)$, $\ell = 0, \ldots, L-1$. In matrix vector notation, we want to solve the linear system of equations

$$\boldsymbol{A}\hat{\boldsymbol{p}} = \boldsymbol{p}, \quad \boldsymbol{A} := (\mathrm{e}^{2\pi\mathrm{i}\boldsymbol{k}\boldsymbol{y}_\ell})_{\ell=0,\ldots,L-1;\, \boldsymbol{k}\in I}, \quad \hat{\boldsymbol{p}} := (\hat{p}_{\boldsymbol{k}})_{\boldsymbol{k}\in I}^{\top}, \quad \boldsymbol{p} := (p(\boldsymbol{y}_\ell))_{\ell=0,\ldots,L-1}^{\top}. \tag{2.1}$$

The sampling nodes $\boldsymbol{y}_\ell$ have to be chosen such that the *Fourier matrix* $\boldsymbol{A}$ has full column rank $|I|$, in particular we infer $L \geq |I|$. Then, we consider the system $\boldsymbol{A}\hat{\boldsymbol{p}} = \boldsymbol{p}$ as a normal equation of the first kind,

$$\boldsymbol{A}^{\mathrm{H}}\boldsymbol{A}\hat{\boldsymbol{p}} = \boldsymbol{A}^{\mathrm{H}}\boldsymbol{p}, \tag{2.2}$$

where $\boldsymbol{A}^{\mathrm{H}}$ denotes the adjoint of the matrix $\boldsymbol{A}$ and the square matrix $\left(\boldsymbol{A}^{\mathrm{H}}\boldsymbol{A}\right)$ is non-singular, i.e., a unique solution $\hat{\boldsymbol{p}} \in \mathbb{C}^{|I|}$ exists.

If we want to (approximately) solve the linear system of equations (2.2) without further assumptions, e.g., using a conjugate gradient like method, we have an algorithmic complexity of $\Omega(L|I|)$. In Section 2.3 and 4.3, possibilities to reduce this arithmetic complexity by sampling at nodes and perturbed nodes of a rank-1 lattice will be discussed.

2.2 Evaluation of trigonometric polynomials at rank-1 lattice nodes (rank-1 lattice FFT)

Let $M \in \mathbb{N}$, $\boldsymbol{z} \in \mathbb{Z}^d$ be given. We define the rank-1 lattice $\Lambda(\boldsymbol{z}, M) \subset \mathbb{T}^d$ of size M with generating vector $\boldsymbol{z} \in \mathbb{Z}^d$ by

$$\Lambda(\boldsymbol{z}, M) := \left\{ \boldsymbol{x}_j := \frac{j}{M}\boldsymbol{z} \bmod \mathbf{1} \colon j = 0, \ldots, M-1 \right\}.$$

We consider the evaluation of a trigonometric polynomial $p \in \Pi_I$, $p : \mathbb{T}^d \to \mathbb{C}$, $p(\boldsymbol{x}) := \sum_{\boldsymbol{k} \in I} \hat{p}_{\boldsymbol{k}} \, \mathrm{e}^{2\pi \mathrm{i} \boldsymbol{k}\boldsymbol{x}}$, where the Fourier coefficients $\hat{p}_{\boldsymbol{k}} \in \mathbb{C}$ are given, at rank-1 lattice nodes $\boldsymbol{x}_j \in \Lambda(\boldsymbol{z}, M)$. As presented in [27], we have

$$p(\boldsymbol{x}_j) = p\left(\frac{j}{M}\boldsymbol{z} \bmod \mathbf{1}\right) = \sum_{l=0}^{M-1} \left(\sum_{\substack{\boldsymbol{k} \in I \\ \boldsymbol{k}\boldsymbol{z} \equiv l \pmod M}} \hat{p}_{\boldsymbol{k}} \right) \mathrm{e}^{2\pi \mathrm{i} \frac{jl}{M}}$$

and the outer sum is a one-dimensional discrete Fourier transform of length M. Therefore, the multivariate trigonometric polynomial p can be evaluated at all rank-1 lattice nodes in $\mathcal{O}(M \log M + d|I|)$ arithmetic operations by using a single one-dimensional FFT, cf. Algorithm 1.

Note that setting the Fourier coefficients $\hat{p}_{\boldsymbol{k}}$ to $(2\pi \mathrm{i}\boldsymbol{k})^{\boldsymbol{\nu}} \hat{p}_{\boldsymbol{k}}$ allows the fast evaluation of the mixed derivative $D^{\boldsymbol{\nu}} p$ of the multivariate trigonometric polynomial p at all rank-1 lattice nodes $\boldsymbol{x}_j$, $j = 0, \ldots, M-1$, in $\mathcal{O}(M \log M + d|I|)$ arithmetic operations using a one-dimensional FFT.

Algorithm 1 Evaluation of a trigonometric polynomial p at a rank-1 lattice $\Lambda(\boldsymbol{z}, M)$.

Input:	$I \subset \mathbb{Z}^d$	frequency index set of finite cardinality
	$\Lambda(\boldsymbol{z}, M)$	rank-1 lattice of size M, generating vector $\boldsymbol{z} \in \mathbb{Z}^d$
	$\hat{\boldsymbol{p}} = (\hat{p}_{\boldsymbol{k}})_{\boldsymbol{k} \in I}$	Fourier coefficients of $p \in \Pi_I$
$\hat{\boldsymbol{g}} := (0)_{l=0}^{M-1}$		
for each $\boldsymbol{k} \in I$ ***do***		
$\hat{g}_{\boldsymbol{k}\boldsymbol{z} \bmod M} := \hat{g}_{\boldsymbol{k}\boldsymbol{z} \bmod M} + \hat{p}_{\boldsymbol{k}}$		
end for		
$\boldsymbol{p} := M \cdot \mathrm{iFFT\_1D}(\hat{\boldsymbol{g}})$		
Output:	$\boldsymbol{p} = \left(p\left(\frac{j\boldsymbol{z}}{M} \bmod \mathbf{1}\right)\right)_{j=0}^{M-1}$	function values of $p \in \Pi_I$
Complexity:	$\mathcal{O}\left(M \log M + d\|I\|\right)$	

2.3 Reconstruction of trigonometric polynomials by sampling at rank-1 lattice nodes

Using a suitable rank-1 lattice $\Lambda(\boldsymbol{z}, M)$, it is possible to perform an exact and perfectly stable reconstruction of the Fourier coefficients $\hat{p}_{\boldsymbol{k}} \in \mathbb{C}$ of a trigonometric polynomial $p \in \Pi_I$, $p(\boldsymbol{x}) := \sum_{\boldsymbol{k} \in I} \hat{p}_{\boldsymbol{k}} \, \mathrm{e}^{2\pi \mathrm{i} \boldsymbol{k}\boldsymbol{x}}$, by sampling at rank-1 lattice nodes $\boldsymbol{x}_j \in \Lambda(\boldsymbol{z}, M)$, $j = 0, \ldots, M-1$,

cf. [23]. To this end, we use a rank-1 lattice $\Lambda(\boldsymbol{z}, M)$, $M \geq |I|$, such that the Fourier matrix

$$\boldsymbol{F} := \left(\mathrm{e}^{2\pi \mathrm{i} j \boldsymbol{k}\boldsymbol{z}/M}\right)_{j=0,\ldots,M-1;\, \boldsymbol{k}\in I}$$

has full column rank. In particular $\boldsymbol{F}$ has orthogonal columns, $\boldsymbol{F}^{\mathrm{H}}\boldsymbol{F} = M\boldsymbol{I}$, i.e.,

$$\frac{1}{M}\left(\boldsymbol{F}^{\mathrm{H}}\boldsymbol{F}\right)_{\boldsymbol{h},\boldsymbol{k}} = \frac{1}{M}\sum_{j=0}^{M-1} \mathrm{e}^{2\pi \mathrm{i} j(\boldsymbol{k}-\boldsymbol{h})\boldsymbol{z}/M} = \begin{cases} 1 \text{ for } & \boldsymbol{k} = \boldsymbol{h}, \\ 0 \text{ for } & \boldsymbol{k} \neq \boldsymbol{h}, \end{cases} \qquad \forall\, \boldsymbol{k}, \boldsymbol{h} \in I. \tag{2.3}$$

This is the case if and only if

$$\boldsymbol{k}\boldsymbol{z} \not\equiv \boldsymbol{h}\boldsymbol{z} \pmod{M}\ \forall \boldsymbol{k}, \boldsymbol{h} \in I, \boldsymbol{k} \neq \boldsymbol{h}, \tag{2.4}$$

see [21, Section 2]. Introducing the difference set $\mathcal{D}(I)$ for the index set I, $\mathcal{D}(I) := \{\boldsymbol{k} - \boldsymbol{h} \colon \boldsymbol{k}, \boldsymbol{h} \in I\}$, we can rewrite the above conditions to

$$\boldsymbol{m}\boldsymbol{z} \not\equiv 0 \pmod{M}\ \forall \boldsymbol{m} \in \mathcal{D}(I) \setminus \{\boldsymbol{0}\}. \tag{2.5}$$

A rank-1 lattice $\Lambda(\boldsymbol{z}, M)$ which fulfills one of the equivalent *reconstruction properties* (2.3), (2.4) or (2.5) for a given frequency index set I will be called *reconstructing rank-1 lattice for* I and denoted by $\Lambda(\boldsymbol{z}, M, I)$. Using the nodes of such a reconstructing rank-1 lattice $\Lambda(\boldsymbol{z}, M, I)$ as sampling nodes, we obtain the Fourier coefficients $\hat{p}_{\boldsymbol{k}}$, $\boldsymbol{k} \in I$, by

$$\hat{p}_{\boldsymbol{k}} = \frac{1}{M}\sum_{j=0}^{M-1} p\left(\frac{j}{M}\boldsymbol{z} \bmod \boldsymbol{1}\right) \mathrm{e}^{-2\pi \mathrm{i} j \boldsymbol{k}\boldsymbol{z}/M},$$

i.e., we have the exact solution for the linear system of equations (2.1). Consequently, the Fourier coefficients $\hat{p}_{\boldsymbol{k}}$, $\boldsymbol{k} \in I$, can be computed in $\mathcal{O}(M \log M + d|I|)$ arithmetic operations by using a single one-dimensional FFT of length M and by computing the scalar products $\boldsymbol{k}\boldsymbol{z}$ for $\boldsymbol{k} \in I$.

One of the main difficulties is to determine reconstructing rank-1 lattices $\Lambda(\boldsymbol{z}, M, I)$ for a given frequency index set I. During the last years a lot of papers deal with (fast) component-by-component constructions of rank-1 lattices which are suitable for different quality measurements, cf. e.g., [33, 7, 6, 20]. In short, one determines a suitable lattice size M and constructs a corresponding generating vector $\boldsymbol{z}$ component–by–component. Based on [6], we developed algorithms in order to find reconstructing rank-1 lattices for arbitrary frequency index sets of finite cardinality, cf. [21].

Theorem 2.1. *For a given frequency index set $I \subset \mathbb{Z}^d$, $4 \leq |I| < \infty$, there always exists a reconstructing rank-1 lattice $\Lambda(\boldsymbol{z}, M, I)$ of size $\frac{|\mathcal{D}(I)|}{2} \leq M \leq |\mathcal{D}(I)|$ if $I \subset \mathbb{Z}^d \cap (-M/2, M/2)^d$. The generating vector $\boldsymbol{z}$ can be constructed using a component-by-component approach, see [21], and the construction requires no more than $2\,d^2\,|I|M \leq 2\,d^2\,|I|^3$ arithmetic operations if $I \subset \mathbb{Z}^d \cap (-M/2, M/2)^d$.*

Proof. This existence is a consequence from [21, Corollary 1] and Bertrand's postulate.
When searching for the component z_t, $t \in \{1, \ldots, d\}$, of the generating vector $\boldsymbol{z}$ in the component-by-component step t, the tests for the reconstruction property (2.4) for a given component z_t take no more than $t\,|I|$ multiplications, $(t-1)\,|I|$ additions as well as $|I|$ modulo

operations, and this yields $2\,t\,|I|$ many arithmetic operations. Due to this and since each component z_t, $t \in \{1,\ldots,d\}$, of the generating vector $\boldsymbol{z}$ can only have $M-1$ different values modulo M, we obtain that the construction requires no more than $2\,\frac{d(d+1)}{2}\,|I|(M-1) \leq 2\,d^2\,|I|M$ arithmetic operations in total. Due to $M \leq |\mathcal{D}(I)| \leq |I|^2$, this yields the assertion. ∎

In the numerical examples of this paper, we use the following simple strategy to determine reconstructing rank-1 lattices $\Lambda(\boldsymbol{z}, M, I)$ for a given frequency index set I, which is discussed in [21]. We set $M_0 = 1$ and search for small M_s such that $\Lambda(\boldsymbol{z} = (M_0,\ldots,M_{s-1})^\top, M = M_s)$ is a reconstructing rank-1 lattice for the frequency index set $\{(k_j)_{j=1}^s \in \mathbb{Z}^s\colon\ (k_j)_{j=1}^d \in I\}$. This approach guarantees that the result $\Lambda(\boldsymbol{z} = (M_0,\ldots,M_{d-1})^\top, M = M_d)$ is a reconstructing rank-1 lattice for I. However, the resulting reconstructing rank-1 lattice is neither necessarily optimal nor is the upper bound $M \leq |I|^2$ for the rank-1 lattice size from Theorem 2.1 guaranteed.

2.4 Function spaces and frequency index sets

This paper focuses on the approximation of functions $f\colon \mathbb{T}^d \to \mathbb{C}$ belonging to certain function spaces by sampling at rank-1 lattice nodes. We consider the subspaces

$$\mathcal{A}^{\alpha,\beta,\boldsymbol{\gamma}}(\mathbb{T}^d) := \left\{ f \in L^1(\mathbb{T}^d)\colon \|f|\mathcal{A}^{\alpha,\beta,\boldsymbol{\gamma}}(\mathbb{T}^d)\| := \sum_{\boldsymbol{k}\in\mathbb{Z}^d} \omega^{\alpha,\beta,\boldsymbol{\gamma}}(\boldsymbol{k})|\hat{f}_{\boldsymbol{k}}| < \infty \right\}$$

of the Wiener algebra and the periodic Sobolev spaces of generalized mixed smoothness

$$\mathcal{H}^{\alpha,\beta,\boldsymbol{\gamma}}(\mathbb{T}^d) := \left\{ f \in L^1(\mathbb{T}^d)\colon \|f|\mathcal{H}^{\alpha,\beta,\boldsymbol{\gamma}}(\mathbb{T}^d)\| := \sqrt{\sum_{\boldsymbol{k}\in\mathbb{Z}^d} \omega^{\alpha,\beta,\boldsymbol{\gamma}}(\boldsymbol{k})^2|\hat{f}_{\boldsymbol{k}}|^2} < \infty \right\}$$

with $\beta \geq 0$, $\alpha > -\beta$, where the weights $\omega^{\alpha,\beta,\boldsymbol{\gamma}}(\boldsymbol{k})$ are defined by

$$\omega^{\alpha,\beta,\boldsymbol{\gamma}}(\boldsymbol{k}) := \max(1,\|\boldsymbol{k}\|_1)^\alpha \prod_{s=1}^d \max(1,\gamma_s^{-1}|k_s|)^\beta, \quad \boldsymbol{k} := \begin{pmatrix} k_1 \\ \vdots \\ k_d \end{pmatrix}, \quad \boldsymbol{\gamma} := \begin{pmatrix} \gamma_1 \\ \vdots \\ \gamma_d \end{pmatrix} \in (0,1]^d. \tag{2.6}$$

The parameter α characterizes the isotropic smoothness and the parameter β the dominating mixed smoothness. Moreover, the parameter $\boldsymbol{\gamma}$ moderates the dependencies and importances of the different variables. We remark that one can use various equivalent weights which have different approximation properties for large dimensions d, cf. [25]. In general, functions from the subspaces $\mathcal{A}^{\alpha,\beta,\boldsymbol{\gamma}}(\mathbb{T}^d)$ of the Wiener algebra have continuous representatives and we always apply our sampling methods on these.

In the whole paper, we use embeddings of the function spaces $\mathcal{A}^{\alpha,\beta,\boldsymbol{\gamma}}(\mathbb{T}^d)$ and $\mathcal{H}^{\alpha,\beta,\boldsymbol{\gamma}}(\mathbb{T}^d)$ that are proved by the next lemma.

Lemma 2.2. *Let a function $f \in \mathcal{A}^{\alpha,\beta,\boldsymbol{\gamma}}(\mathbb{T}^d)$ be given, where $\alpha,\beta \in \mathbb{R}$, $\beta \geq 0$, $\alpha > -\beta$, and $\boldsymbol{\gamma}$ as stated in (2.6). Then, we have $\|f|\mathcal{H}^{\alpha,\beta,\boldsymbol{\gamma}}(\mathbb{T}^d)\| \leq \|f|\mathcal{A}^{\alpha,\beta,\boldsymbol{\gamma}}(\mathbb{T}^d)\|$. For a function $f \in \mathcal{H}^{\alpha,\beta+\lambda,\boldsymbol{\gamma}}(\mathbb{T}^d)$, where $\alpha,\beta \in \mathbb{R}$ and $\lambda > 1/2$, we have*

$$\|f|\mathcal{A}^{\alpha,\beta,\boldsymbol{\gamma}}(\mathbb{T}^d)\| \leq (1+2\zeta(2\lambda))^{\frac{d}{2}}\,\|f|\mathcal{H}^{\alpha,\beta+\lambda,\boldsymbol{\gamma}}(\mathbb{T}^d)\|, \tag{2.7}$$

where we denote by ζ the Riemann zeta function.

Proof. We infer $\|f|\mathcal{H}^{\alpha,\beta,\gamma}(\mathbb{T}^d)\|^2 \leq \left(\sum_{\boldsymbol{k}\in\mathbb{Z}^d} \omega^{\alpha,\beta,\gamma}(\boldsymbol{k})\,|\hat{f}_{\boldsymbol{k}}|\right)^2 = \|f|\mathcal{A}^{\alpha,\beta,\gamma}(\mathbb{T}^d)\|^2$. For arbitrary $\lambda > 1/2$, we apply the Cauchy-Schwarz inequality and obtain

$$\begin{aligned}
\|f|\mathcal{A}^{\alpha,\beta,\gamma}(\mathbb{T}^d)\| &= \sum_{\boldsymbol{k}\in\mathbb{Z}^d} \frac{\omega^{0,\lambda,\gamma}(\boldsymbol{k})}{\omega^{0,\lambda,\gamma}(\boldsymbol{k})} \quad \omega^{\alpha,\beta,\gamma}(\boldsymbol{k}) \left|\hat{f}_{\boldsymbol{k}}\right| \\
&\leq \left(\sum_{\boldsymbol{k}\in\mathbb{Z}^d} \frac{1}{\omega^{0,\lambda,\gamma}(\boldsymbol{k})^2}\right)^{\frac{1}{2}} \left(\sum_{\boldsymbol{k}\in\mathbb{Z}^d} \omega^{\alpha,\beta+\lambda,\gamma}(\boldsymbol{k})^2 \left|\hat{f}_{\boldsymbol{k}}\right|^2\right)^{\frac{1}{2}} \\
&= \left(\prod_{s=1}^{d} \sum_{l\in\mathbb{Z}} \frac{1}{\max(1,|l|)^{2\lambda}}\right)^{\frac{1}{2}} \|f|\mathcal{H}^{\alpha,\beta+\lambda,\gamma}(\mathbb{T}^d)\| \\
&= (1+2\zeta(2\lambda))^{\frac{d}{2}}\, \|f|\mathcal{H}^{\alpha,\beta+\lambda,\gamma}(\mathbb{T}^d)\|.
\end{aligned}$$

■

We are interested in the approximation of functions contained in $\mathcal{A}^{\alpha,\beta,\gamma}(\mathbb{T}^d)$ or $\mathcal{H}^{\alpha,\beta,\gamma}(\mathbb{T}^d)$ using trigonometric polynomials with frequencies supported on suitable frequency index sets I. Hence, let a parameter $T \in (-\infty, 1)$, a refinement $N \geq 1$ and a weight $\boldsymbol{\gamma}$ as specified in (2.6) be given. We define the weighted frequency index set $I_N^{d,T,\gamma}$ by

$$I_N^{d,T,\gamma} := \left\{ \boldsymbol{k} \in \mathbb{Z}^d \colon \omega^{-T,1,\gamma}(\boldsymbol{k}) = \max(1,\|\boldsymbol{k}\|_1)^{-T} \prod_{s=1}^{d} \max(1,\gamma_s^{-1}|k_s|) \leq N^{1-T} \right\}. \tag{2.8}$$

As a natural extension for $T = -\infty$, we define the weighted frequency index set $I_N^{d,-\infty,\gamma}$ as the d-dimensional ℓ_1-ball of size N,

$$I_N^{d,-\infty,\gamma} := \left\{ \boldsymbol{k} \in \mathbb{Z}^d \colon \max(1,\|\boldsymbol{k}\|_1) \leq N \right\}. \tag{2.9}$$

Later on, we need some embeddings of the weighted frequency index sets $I_N^{d,T,\gamma}$. First, we prove the embeddings into l_∞ balls, depending on the parameter T.

Lemma 2.3. *Let $N \in \mathbb{R}$, $N \geq 1$, $\boldsymbol{\gamma}$ as stated in (2.6), and $T \in [-\infty, 1)$ be given. The following inclusions hold*

$$I_N^{d,T,\gamma} \subset \begin{cases} \mathbb{Z}^d \cap [-N,N]^d, & \text{for } T \leq 0, \\ \mathbb{Z}^d \cap [-d^{\frac{T}{1-T}}N, d^{\frac{T}{1-T}}N]^d, & \text{for } 0 < T < 1. \end{cases} \tag{2.10}$$

Proof. In order to prove the inclusions, we use

$$\max(1,\|\boldsymbol{k}\|_\infty) \leq \prod_{s=1}^{d} \max(1,\gamma_s^{-1}|k_s|) \tag{2.11}$$

and

$$\max(1,\|\boldsymbol{k}\|_\infty) \leq \max(1,\|\boldsymbol{k}\|_1) \leq d\max(1,\|\boldsymbol{k}\|_\infty). \tag{2.12}$$

For $\boldsymbol{k} \in I_N^{d,T,\boldsymbol{\gamma}}$ and $T \in (-\infty, 1)$, we infer

$$\begin{aligned} N &\geq \left(\prod_{s=1}^{d} \max(1, \gamma_s^{-1}|k_s|) \right)^{\frac{1}{1-T}} \max(1, \|\boldsymbol{k}\|_1)^{-\frac{T}{1-T}} \\ &\geq \max(1, \|\boldsymbol{k}\|_\infty)^{\frac{1}{1-T}} \begin{cases} \max(1, \|\boldsymbol{k}\|_\infty)^{-\frac{T}{1-T}} & \text{for } -\frac{T}{1-T} \geq 0, \\ d^{-\frac{T}{1-T}} \max(1, \|\boldsymbol{k}\|_\infty)^{-\frac{T}{1-T}} & \text{for } -\frac{T}{1-T} < 0. \end{cases} \end{aligned}$$

Similarly, we estimate $N \geq \max(1, \|\boldsymbol{k}\|_1) \geq \max(1, \|\boldsymbol{k}\|_\infty)$ for $\boldsymbol{k} \in I_N^{d,-\infty,\boldsymbol{\gamma}}$. Thus, we have $\max(1, \|\boldsymbol{k}\|_\infty) \leq \left\{ \begin{array}{ll} N & \text{for } T \leq 0 \\ d^{\frac{T}{1-T}} N & \text{for } 0 < T < 1 \end{array} \right\}$ and this yields the assertion. ∎

Next, we show embeddings into "thicker" weighted frequency index sets $I_N^{d,\tilde{T},\boldsymbol{\gamma}}$, i.e., for parameters $\tilde{T} \leq T$.

Lemma 2.4. *Let $N \in \mathbb{R}$, $N \geq 1$, $\boldsymbol{\gamma}$ as stated in (2.6), and $-\infty \leq \tilde{T} \leq T < 1$ be given. Then, the following upper bound holds*

$$\max_{\boldsymbol{k} \in I_N^{d,T,\boldsymbol{\gamma}}} \omega^{-\frac{\tilde{T}}{1-\tilde{T}}, \frac{1}{1-\tilde{T}}, \boldsymbol{\gamma}}(\boldsymbol{k}) \leq \begin{cases} d^{\frac{T-\tilde{T}}{(1-T)(1-\tilde{T})}} N & \text{for } \tilde{T} > -\infty, \\ d^{\frac{1}{(1-T)}} N, & \text{for } \tilde{T} = -\infty, \end{cases}$$

where we define $\frac{\infty}{1+\infty} := 1$ and $\frac{1}{1+\infty} := 0$. This implies the following inclusion

$$I_N^{d,T,\boldsymbol{\gamma}} \subset \begin{cases} I^{d,\tilde{T},\boldsymbol{\gamma}}_{d^{(T-\tilde{T})/(1-T)/(1-\tilde{T})}N} & \text{for } \tilde{T} > -\infty, \\ I^{d,-\infty,\boldsymbol{\gamma}}_{d^{1/(1-T)}N} & \text{for } \tilde{T} = -\infty. \end{cases}$$

Proof. We observe by (2.8) that

$$I_N^{d,T,\boldsymbol{\gamma}} = \left\{ \boldsymbol{k} \in \mathbb{Z}^d \colon \max(1, \|\boldsymbol{k}\|_1)^{-\frac{T}{1-T}} \prod_{s=1}^{d} \max(1, \gamma_s^{-1}|k_s|)^{\frac{1}{1-T}} \leq N \right\}. \tag{2.13}$$

Let $\tilde{T} > -\infty$ and $\boldsymbol{k} \in I_N^{d,T,\boldsymbol{\gamma}}$. We estimate

$$\begin{aligned} N &\geq \omega^{-\frac{T}{1-T}, \frac{1}{1-T}, \boldsymbol{\gamma}}(\boldsymbol{k}) = \omega^{-\frac{T}{1-T} + \frac{T-\tilde{T}}{(1-T)(1-\tilde{T})}, \frac{1}{1-T} - \frac{T-\tilde{T}}{(1-T)(1-\tilde{T})}, \boldsymbol{\gamma}}(\boldsymbol{k}) \omega^{-\frac{T-\tilde{T}}{(1-T)(1-\tilde{T})}, \frac{T-\tilde{T}}{(1-T)(1-\tilde{T})}, \boldsymbol{\gamma}}(\boldsymbol{k}) \\ &= \omega^{-\frac{\tilde{T}}{1-\tilde{T}}, \frac{1}{1-\tilde{T}}, \boldsymbol{\gamma}}(\boldsymbol{k}) \left(\frac{\prod_{s=1}^{d} \max(1, \gamma_s^{-1}|k_s|)}{\max(1, \|\boldsymbol{k}\|_1)} \right)^{\frac{T-\tilde{T}}{(1-T)(1-\tilde{T})}}. \end{aligned}$$

Due to $\frac{T-\tilde{T}}{(1-T)(1-\tilde{T})} \geq 0$ and using the inequalities (2.11) and (2.12), we continue

$$N \geq \omega^{-\frac{\tilde{T}}{1-\tilde{T}}, \frac{1}{1-\tilde{T}}, \boldsymbol{\gamma}}(\boldsymbol{k}) \left(\frac{\prod_{s=1}^{d} \max(1, \gamma_s^{-1}|k_s|)}{d \prod_{s=1}^{d} \max(1, \gamma_s^{-1}|k_s|)} \right)^{\frac{T-\tilde{T}}{(1-T)(1-\tilde{T})}}$$

and obtain $d^{\frac{T-\tilde{T}}{(1-T)(1-\tilde{T})}} N \geq \omega^{-\frac{\tilde{T}}{1-\tilde{T}}, \frac{1}{1-\tilde{T}}, \boldsymbol{\gamma}}(\boldsymbol{k})$. This yields $\boldsymbol{k} \in I^{d,\tilde{T},\boldsymbol{\gamma}}_{d^{(T-\tilde{T})/(1-T)/(1-\tilde{T})}N}$.
In order to prove all inclusions from the assertion above, we have to deal separately with

$\tilde{T} = -\infty$. Obviously, for $T = \tilde{T} = -\infty$, the inclusion from above holds. So, let us assume $-\infty = \tilde{T} < T < 1$. Due to the inequalities (2.11) and (2.12), we estimate for $\boldsymbol{k} \in I_N^{d,T,\boldsymbol{\gamma}}$ and $T \in (-\infty, 1)$

$$\begin{aligned} N &\geq \left(\prod_{s=1}^{d} \max(1, \gamma_s^{-1} |k_s|) \right)^{\frac{1}{1-T}} \max(1, \|\boldsymbol{k}\|_1)^{-\frac{T}{1-T}} \\ &\geq \left(d^{-1} \max(1, \|\boldsymbol{k}\|_1) \right)^{\frac{1}{1-T}} \max(1, \|\boldsymbol{k}\|_1)^{-\frac{T}{1-T}} = d^{-\frac{1}{1-T}} \max(1, \|\boldsymbol{k}\|_1) \end{aligned}$$

and obtain $\boldsymbol{k} \in I^{d,-\infty,\boldsymbol{\gamma}}_{d^{\frac{1}{1-T}} N}$. The upper bound in the Lemma then follows. ■

Remark 2.5. If the weights $\boldsymbol{\gamma}$ are chosen $\boldsymbol{\gamma} = \mathbf{1} := (1, \ldots, 1)^\top$, the definition of the weighted frequency index set $I_N^{d,T,\boldsymbol{\gamma}}$ is related to the one of the index sets

$$\widetilde{I}_N^{d,T} := \left\{ \boldsymbol{k} \in \mathbb{Z}^d \colon (1 + \|\boldsymbol{k}\|_\infty)^{-T} \prod_{s=1}^{d} (1 + |k_s|) \leq (1+N)^{1-T} \right\}, \quad T \in (-\infty, 1), \qquad \text{and}$$

$$\widetilde{I}_N^{d,-\infty} := \left\{ \boldsymbol{k} \in \mathbb{Z}^d \colon \|\boldsymbol{k}\|_\infty \leq N \right\},$$

which was treated in [24, Section 3.3]. □

In order to estimate the cardinalities of the frequency index sets defined in (2.8) we show some useful embeddings.

Lemma 2.6. *Let a refinement $N \in \mathbb{R}$, $N \geq 1$, be given. In the case $0 \leq T < 1$, we have the inclusions*

$$I^{d,T,\mathbf{1}}_{(N+1)d^{-T/(1-T)}2^{-d/(1-T)}} \subset \widetilde{I}_N^{d,T} \subset I^{d,T,\mathbf{1}}_{(N+1)2^{T/(1-T)}}.$$

For $T < 0$, we have the inclusions

$$I^{d,T,\mathbf{1}}_{(N+1)2^{(T-d)/(1-T)}} \subset \widetilde{I}_N^{d,T} \subset I^{d,T,\mathbf{1}}_{(N+1)d^{-T/(1-T)}}.$$

Proof. For arbitrary $d \in \mathbb{N}$ and $\boldsymbol{k} \in \mathbb{Z}^d$, we have the inequalities

$$d^{-1} \max(1, \|\boldsymbol{k}\|_1) \leq 1 + \|\boldsymbol{k}\|_\infty \leq 2 \max(1, \|\boldsymbol{k}\|_1) \tag{2.14}$$

and $\prod_{s=1}^{d} \max(1, |k_s|) \leq \prod_{s=1}^{d} (1 + |k_s|) \leq 2^d \prod_{s=1}^{d} \max(1, |k_s|)$. Let $1 > T \geq 0$, we obtain

$$\begin{aligned} 2^{-T} \max(1, \|\boldsymbol{k}\|_1)^{-T} \prod_{s=1}^{d} \max(1, |k_s|) &\leq (1 + \|\boldsymbol{k}\|_\infty)^{-T} \prod_{s=1}^{d} (1 + |k_s|) \\ &\leq d^T \max(1, \|\boldsymbol{k}\|_1)^{-T} 2^d \prod_{s=1}^{d} \max(1, |k_s|). \end{aligned}$$

In the case of $-\infty < T < 0$, the inequality

$$\begin{aligned} d^T \max(1, \|\boldsymbol{k}\|_1)^{-T} \prod_{s=1}^{d} \max(1, |k_s|) &\leq (1 + \|\boldsymbol{k}\|_\infty)^{-T} \prod_{s=1}^{d} (1 + |k_s|) \\ &\leq 2^{-T} \max(1, \|\boldsymbol{k}\|_1)^{-T} 2^d \prod_{s=1}^{d} \max(1, |k_s|) \end{aligned}$$

arises. Finally, the assertion for the case $T = -\infty$ follows directly from (2.14). ■

In the following lemma, we give an asymptotic upper bound for the cardinality $|I_N^{d,T,\boldsymbol{\gamma}}|$ of the weighted frequency index set $I_N^{d,T,\boldsymbol{\gamma}}$.

Lemma 2.7. *The cardinality of the weighted frequency index set $I_N^{d,T,\boldsymbol{\gamma}}$ is bounded by*

$$|I_N^{d,T,\boldsymbol{\gamma}}| \leq \begin{cases} \mathcal{O}(N^d) & \text{for } T = -\infty, \\ \mathcal{O}(N^{\frac{T-1}{T/d-1}}) & \text{for } -\infty < T < 0, \\ \mathcal{O}(N \log^{d-1} N) & \text{for } T = 0, \\ \mathcal{O}(N) & \text{for } 0 < T < 1. \end{cases}$$

Proof. Due to $\boldsymbol{\gamma} \in (0,1]^d$, the inequality $\prod_{s=1}^d \max(1, |k_s|) \leq \prod_{s=1}^d \max(1, \gamma_s^{-1}|k_s|)$ and the embeddings

$$I_N^{d,T,\boldsymbol{\gamma}} \subset I_N^{d,T,\mathbf{1}} \subset I_{N+1}^{d,T,\mathbf{1}} \subset \begin{cases} \widetilde{I}^{d,T}_{2^{(d-T)/(1-T)}N} & \text{for } -\infty \leq T \leq 0, \\ \widetilde{I}^{d,T}_{Nd^{T/(1-T)}2^{d/(1-T)}} & \text{for } 0 < T < 1 \end{cases}$$

hold. Due to [13, Section 3.2 Lemma 1] and as stated in [24, Section 3.3 Lemma 2], the cardinality of the weighted frequency index set $\widetilde{I}_N^{d,T}$ is bounded by the terms indicated by the assertion. ∎

An alternative upper bound for the cardinality of the weighted symmetric hyperbolic crosses $I_N^{d,0,\boldsymbol{\gamma}}$ incorporating the weights $\boldsymbol{\gamma}$ is given by $|I_N^{d,0,\boldsymbol{\gamma}}| \leq N^\tau \prod_{s=1}^d (1 + 2\zeta(\tau)\gamma_s^\tau)$ for all $\tau > 1$, cf. [6], where ζ is the Riemann zeta function.

Figure 2.1 illustrates examples for weighted frequency index sets $I_N^{d,T,\boldsymbol{\gamma}}$ in the two-dimensional case for $N = 32$. For increasing parameter T and decreasing weights $\boldsymbol{\gamma}$, the weighted frequency index sets $I_N^{d,T,\boldsymbol{\gamma}}$ become "thinner". In particular, the index sets $I_N^{d,0,\boldsymbol{\gamma}}$ are weighted symmetric hyperbolic crosses.

3 Approximate reconstruction by sampling at rank-1 lattice nodes

As usual, we denote the Fourier coefficients

$$\hat{f}_{\boldsymbol{k}} := \int_{\mathbb{T}^d} f(\boldsymbol{x}) \mathrm{e}^{-2\pi \mathrm{i} \boldsymbol{k}\boldsymbol{x}} \mathrm{d}\boldsymbol{x}, \quad \boldsymbol{k} \in \mathbb{Z}^d \tag{3.1}$$

for functions $f \in \mathcal{A}^{\alpha,\beta,\boldsymbol{\gamma}}(\mathbb{T}^d)$ or $f \in \mathcal{H}^{\alpha,\beta,\boldsymbol{\gamma}}(\mathbb{T}^d)$, and formally approximate f by the Fourier partial sum

$$S_I f := \sum_{\boldsymbol{k} \in I} \hat{f}_{\boldsymbol{k}} \, \mathrm{e}^{2\pi \mathrm{i} \boldsymbol{k}\circ},$$

where $I \subset \mathbb{Z}^d$ is a frequency index set of finite cardinality. In general, we only compute approximations $\hat{\tilde{f}}_{\boldsymbol{k}}$ of the Fourier coefficients $\hat{f}_{\boldsymbol{k}}$ from (3.1) for all $\boldsymbol{k} \in I$. For this, we sample the function f at nodes $\boldsymbol{x}_j := \frac{j}{M}\boldsymbol{z} \bmod \mathbf{1}$, $j = 0, \ldots, M-1$, of a rank-1 lattice $\Lambda(\boldsymbol{z}, M)$. We compute the approximated Fourier coefficients $\hat{\tilde{f}}_{\boldsymbol{k}}$ by applying the lattice rule to the integrand in (3.1),

$$\hat{\tilde{f}}_{\boldsymbol{k}} := \frac{1}{M} \sum_{j=0}^{M-1} f\left(\frac{j}{M}\boldsymbol{z} \bmod \mathbf{1}\right) \mathrm{e}^{-2\pi \mathrm{i} j \boldsymbol{k}\boldsymbol{z}/M}, \qquad \boldsymbol{k} \in I, \tag{3.2}$$

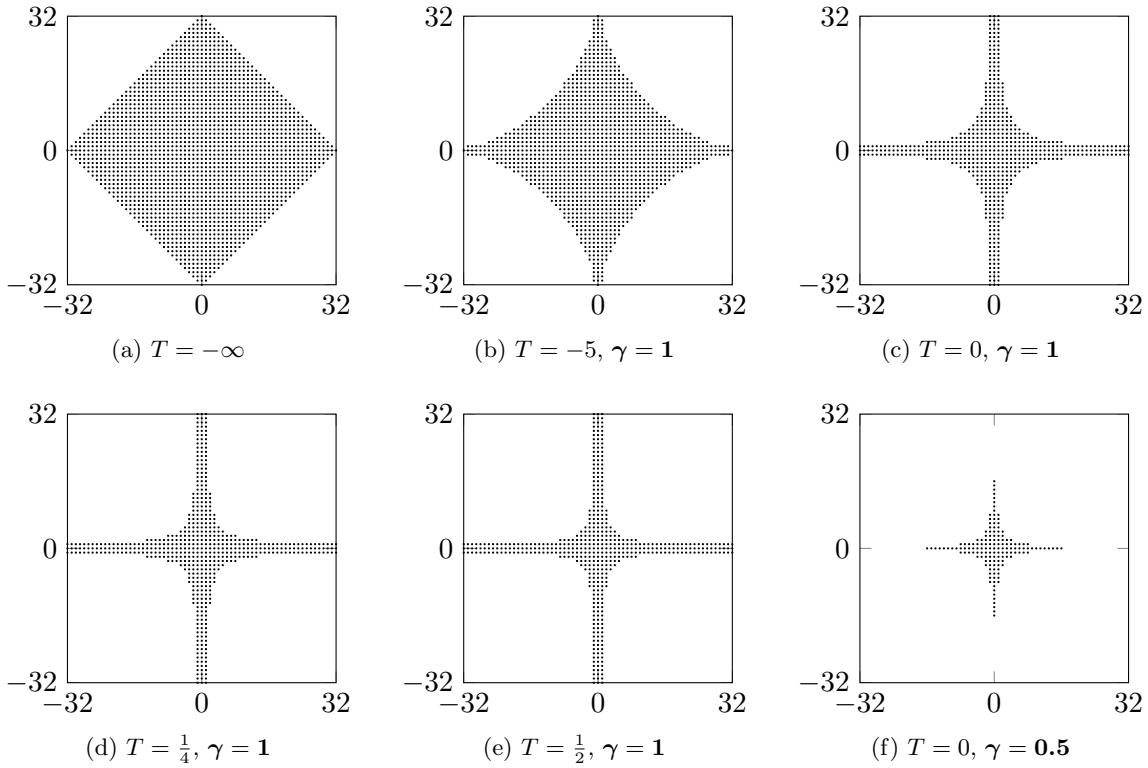

(a) $T = -\infty$ (b) $T = -5$, $\boldsymbol{\gamma} = \mathbf{1}$ (c) $T = 0$, $\boldsymbol{\gamma} = \mathbf{1}$

(d) $T = \frac{1}{4}$, $\boldsymbol{\gamma} = \mathbf{1}$ (e) $T = \frac{1}{2}$, $\boldsymbol{\gamma} = \mathbf{1}$ (f) $T = 0$, $\boldsymbol{\gamma} = \mathbf{0.5}$

Figure 2.1: Weighted frequency index sets $I_{32}^{2,T,\boldsymbol{\gamma}}$ for various parameters T and $\boldsymbol{\gamma}$.

Algorithm 2 Approximate reconstruction of a function $f \in \mathcal{A}^{\alpha,\beta,\boldsymbol{\gamma}}(\mathbb{T}^d)$ or $f \in \mathcal{H}^{\alpha,\beta,\boldsymbol{\gamma}}(\mathbb{T}^d)$ from sampling values on a reconstructing rank-1 lattice $\Lambda(\boldsymbol{z}, M, I)$.

Input:	$I \subset \mathbb{Z}^d$	frequency index set of finite cardinality
	$\Lambda(\boldsymbol{z}, M, I)$	reconstructing rank-1 lattice for I of size M with generating vector $\boldsymbol{z} \in \mathbb{Z}^d$
	$\boldsymbol{f} = \left(f\left(\frac{j\boldsymbol{z}}{M} \bmod \mathbf{1}\right)\right)_{j=0}^{M-1}$	function values of $f \in \mathcal{A}^{\alpha,\beta,\boldsymbol{\gamma}}(\mathbb{T}^d)$ or $f \in \mathcal{H}^{\alpha,\beta,\boldsymbol{\gamma}}(\mathbb{T}^d)$
$\hat{\boldsymbol{g}} = \mathrm{FFT\_1D}(\boldsymbol{f})$		
for each $\boldsymbol{k} \in I$ ***do***		
$\hat{\hat{f}}_{\boldsymbol{k}} = \frac{1}{M}\, \hat{g}_{\boldsymbol{k}\boldsymbol{z} \bmod M}$		
end for		
Output:	$\hat{\hat{\boldsymbol{f}}} = \left(\hat{\hat{f}}_{\boldsymbol{k}}\right)_{\boldsymbol{k} \in I}$	approximated Fourier coefficients of $f \in \mathcal{A}^{\alpha,\beta,\boldsymbol{\gamma}}(\mathbb{T}^d)$ or $f \in \mathcal{H}^{\alpha,\beta,\boldsymbol{\gamma}}(\mathbb{T}^d)$
Complexity:	$\mathcal{O}\left(M \log M + d\lvert I\rvert\right)$	

in $\mathcal{O}(M \log M + d|I|)$ arithmetic operations using a single one-dimensional FFT of length M, cf. Algorithm 2. Then, we define an approximation of the function f by the approximated

Fourier partial sum

$$\tilde{S}_I f := \sum_{\boldsymbol{k}\in I} \hat{\tilde{f}}_{\boldsymbol{k}}\, \mathrm{e}^{2\pi \mathrm{i}\boldsymbol{k}\circ}. \tag{3.3}$$

Lemma 3.1. *Let a function $f \in \mathcal{C}(\mathbb{T}^d) \cap \mathcal{A}^{\alpha,\beta,\boldsymbol{\gamma}}(\mathbb{T}^d)$, a frequency index set $I \subset \mathbb{Z}^d$ and a rank-1 lattice $\Lambda(\boldsymbol{z}, M)$ with nodes $\boldsymbol{x}_j := \frac{j}{M}\boldsymbol{z} \bmod \mathbf{1}$, $j = 0, \ldots, M-1$, be given, where $\alpha, \beta \in \mathbb{R}$, $\beta \geq 0$ and $\alpha > -\beta$. The approximated Fourier coefficients $\hat{\tilde{f}}_{\boldsymbol{k}}$, $\boldsymbol{k} \in I$, computed by applying the lattice rule (3.2), are aliased versions of the original Fourier coefficients $\hat{f}_{\boldsymbol{k}}$ of the function f, $\hat{\tilde{f}}_{\boldsymbol{k}} = \sum_{\substack{\boldsymbol{h}\in\mathbb{Z}^d \\ \boldsymbol{h}\boldsymbol{z}\equiv 0 \pmod M}} \hat{f}_{\boldsymbol{k}+\boldsymbol{h}}$, $\boldsymbol{k} \in I$, and the aliasing error is given by*

$$S_{I_N^{d,T,\boldsymbol{\gamma}}} f - \tilde{S}_{I_N^{d,T,\boldsymbol{\gamma}}} f = - \sum_{\boldsymbol{k}\in I_N^{d,T,\boldsymbol{\gamma}}} \sum_{\substack{\boldsymbol{h}\in\mathbb{Z}^d\setminus\{\mathbf{0}\} \\ \boldsymbol{h}\boldsymbol{z}\equiv 0 \pmod M}} \hat{f}_{\boldsymbol{k}+\boldsymbol{h}}\, \mathrm{e}^{2\pi\mathrm{i}\boldsymbol{k}\circ}. \tag{3.4}$$

Proof. Since we have $f(\frac{j}{M}\boldsymbol{z} \bmod \mathbf{1}) = \sum_{\boldsymbol{h}\in\mathbb{Z}^d} \hat{f}_{\boldsymbol{h}}\, \mathrm{e}^{2\pi\mathrm{i}j\boldsymbol{h}\boldsymbol{z}/M}$, we obtain

$$\hat{\tilde{f}}_{\boldsymbol{k}} = \frac{1}{M} \sum_{j=0}^{M-1} \sum_{\boldsymbol{h}\in\mathbb{Z}^d} \hat{f}_{\boldsymbol{h}}\, \mathrm{e}^{-2\pi\mathrm{i}\frac{j(\boldsymbol{k}-\boldsymbol{h})\boldsymbol{z}}{M}} = \sum_{\boldsymbol{h}\in\mathbb{Z}^d} \hat{f}_{\boldsymbol{h}}\, \frac{1}{M} \sum_{j=0}^{M-1} \mathrm{e}^{-2\pi\mathrm{i}\frac{j(\boldsymbol{k}-\boldsymbol{h})\boldsymbol{z}}{M}} = \sum_{\substack{\boldsymbol{h}\in\mathbb{Z}^d \\ \boldsymbol{h}\boldsymbol{z}\equiv 0 \pmod M}} \hat{f}_{\boldsymbol{k}+\boldsymbol{h}}$$

and the assertion follows. ∎

In order to avoid aliasing error within the frequency index set I, we use a reconstructing rank-1 lattice $\Lambda(\boldsymbol{z}, M, I)$ and this yields $\{\boldsymbol{h} \in \mathbb{Z}^d \setminus \{\mathbf{0}\} \colon \boldsymbol{h}\boldsymbol{z} \equiv 0 \pmod M\} \cap \mathcal{D}(I) = \emptyset$ due to the reconstruction property (2.5). Therefore, we only have aliasing from Fourier coefficients $\hat{f}_{\boldsymbol{k}}$ with $\boldsymbol{k} \in \mathbb{Z}^d \setminus I$.

We consider the approximation error $f - \tilde{S}_{I_N^{d,T,\boldsymbol{\gamma}}} f$ in different norms in the next sections. Preparing the statements therein, we estimate the maximum of the weight function of specific index sets in the following

Lemma 3.2. *Let $\tilde{\beta} \geq 0$, $\tilde{\alpha} > -\tilde{\beta}$ and a weighted frequency index set $I_N^{d,T,\boldsymbol{\gamma}}$ be given, where $N \geq 1$, $T \in [-\infty, 1)$ and $\boldsymbol{\gamma} \in (0,1]^d$. Then, we have*

$$\max_{\boldsymbol{k}\in\mathbb{Z}^d\setminus I_N^{d,T,\boldsymbol{\gamma}}} \omega^{-\tilde{\alpha},-\tilde{\beta},\boldsymbol{\gamma}}(\boldsymbol{k}) \leq N^{-(\tilde{\alpha}+\tilde{\beta})} \begin{cases} \left(N^{d-1} \prod_{s=1}^d \gamma_s^{-1}\right)^{\frac{T\tilde{\beta}+\tilde{\alpha}}{d-T}} & \text{for } T > -\frac{\tilde{\alpha}}{\tilde{\beta}}, \\ 1 & \text{for } T = -\frac{\tilde{\alpha}}{\tilde{\beta}}, \\ d^{-\frac{T\tilde{\beta}+\tilde{\alpha}}{1-T}} & \text{for } T < -\frac{\tilde{\alpha}}{\tilde{\beta}}. \end{cases}$$

Proof. We observe by (2.13) that

$$\mathbb{Z}^d \setminus I_N^{d,T,\boldsymbol{\gamma}} \;=\; \left\{ \boldsymbol{k} \in \mathbb{Z}^d \colon \max(1, \|\boldsymbol{k}\|_1)^{\frac{T}{1-T}} \prod_{s=1}^d \max(1, \gamma_s^{-1}|k_s|)^{-\frac{1}{1-T}} < N^{-1} \right\}.$$

Let $T > -\frac{\tilde{\alpha}}{\tilde{\beta}}$. We estimate dominating mixed smoothness by isotropic smoothness. Due to $\prod_{s=1}^d \max(1, \gamma_s^{-1}|k_s|) \leq \max(1, \|\boldsymbol{k}\|_\infty)^d \prod_{s=1}^d \gamma_s^{-1} \leq \max(1, \|\boldsymbol{k}\|_1)^d \prod_{s=1}^d \gamma_s^{-1}$ for $\boldsymbol{k} \in \mathbb{Z}^d$, we obtain

for all $\boldsymbol{k} \in \mathbb{Z}^d \setminus I_N^{d,T,\boldsymbol{\gamma}}$

$$\begin{aligned}
\omega^{-\tilde{\alpha},-\tilde{\beta},\boldsymbol{\gamma}}(\boldsymbol{k}) &= \max(1,\|\boldsymbol{k}\|_1)^{-\tilde{\alpha}} \prod_{s=1}^{d} \max(1,\gamma_s^{-1}|k_s|)^{-\tilde{\beta}-\frac{T\tilde{\beta}+\tilde{\alpha}}{d-T}+\frac{T\tilde{\beta}+\tilde{\alpha}}{d-T}} \\
&\leq \left(\prod_{s=1}^{d} \gamma_s^{-\frac{T\tilde{\beta}+\tilde{\alpha}}{d-T}}\right) \max(1,\|\boldsymbol{k}\|_1)^{-\tilde{\alpha}+d\frac{T\tilde{\beta}+\tilde{\alpha}}{d-T}} \prod_{s=1}^{d} \max(1,\gamma_s^{-1}|k_s|)^{-\tilde{\beta}-\frac{T\tilde{\beta}+\tilde{\alpha}}{d-T}} \\
&= \left(\prod_{s=1}^{d} \gamma_s^{-\frac{T\tilde{\beta}+\tilde{\alpha}}{d-T}}\right)\left(\max(1,\|\boldsymbol{k}\|_1)^{\frac{T}{1-T}} \prod_{s=1}^{d} \max(1,\gamma_s^{-1}|k_s|)^{-\frac{1}{1-T}}\right)^{\tilde{\alpha}+\tilde{\beta}-\frac{d-1}{d-T}(T\tilde{\beta}+\tilde{\alpha})}.
\end{aligned}$$

Consequently, we infer $\max_{\boldsymbol{k}\in\mathbb{Z}^d\setminus I_N^{d,T,\boldsymbol{\gamma}}} \omega^{-\tilde{\alpha},-\tilde{\beta},\boldsymbol{\gamma}}(\boldsymbol{k}) \overset{(2.13)}{\leq} \left(\prod_{s=1}^{d} \gamma_s^{-\frac{T\tilde{\beta}+\tilde{\alpha}}{d-T}}\right) N^{-(\tilde{\alpha}+\tilde{\beta})+\frac{d-1}{d-T}(T\tilde{\beta}+\tilde{\alpha})}$.
Let $T \leq -\frac{\tilde{\alpha}}{\tilde{\beta}}$ and $\tilde{\beta} > 0$. We estimate isotropic smoothness by dominating mixed smoothness. Using the inequalities (2.11) and (2.12), we obtain for all $\boldsymbol{k} \in \mathbb{Z}^d \setminus I_N^{d,T,\boldsymbol{\gamma}}$

$$\begin{aligned}
\omega^{-\tilde{\alpha},-\tilde{\beta},\boldsymbol{\gamma}}(\boldsymbol{k}) &= \max(1,\|\boldsymbol{k}\|_1)^{-\tilde{\alpha}-\frac{-\tilde{\alpha}-T\tilde{\beta}}{1-T}+\frac{-\tilde{\alpha}-T\tilde{\beta}}{1-T}} \prod_{s=1}^{d} \max(1,\gamma_s^{-1}|k_s|)^{-\tilde{\beta}} \\
&\leq d^{\frac{-\tilde{\alpha}-T\tilde{\beta}}{1-T}} \max(1,\|\boldsymbol{k}\|_1)^{-\tilde{\alpha}-\frac{-\tilde{\alpha}-T\tilde{\beta}}{1-T}} \prod_{s=1}^{d} \max(1,\gamma_s^{-1}|k_s|)^{\frac{-\tilde{\alpha}-T\tilde{\beta}}{1-T}-\tilde{\beta}} \\
&= d^{-\frac{T\tilde{\beta}+\tilde{\alpha}}{1-T}} \left(\max(1,\|\boldsymbol{k}\|_1)^{\frac{T}{1-T}} \prod_{s=1}^{d} \max(1,\gamma_s^{-1}|k_s|)^{-\frac{1}{1-T}}\right)^{\tilde{\alpha}+\tilde{\beta}}.
\end{aligned}$$

Thus, we infer $\max_{\boldsymbol{k}\in\mathbb{Z}^d\setminus I_N^{d,T,\boldsymbol{\gamma}}} \omega^{-\tilde{\alpha},-\tilde{\beta},\boldsymbol{\gamma}}(\boldsymbol{k}) \overset{(2.13)}{\leq} d^{-\frac{T\tilde{\beta}+\tilde{\alpha}}{1-T}} N^{-(\tilde{\alpha}+\tilde{\beta})}$.
Let $T = -\infty$ and $\tilde{\beta} = 0$. We have $\mathbb{Z}^d \setminus I_N^{d,-\infty,\boldsymbol{\gamma}} = \left\{\boldsymbol{k} \in \mathbb{Z}^d \colon \max(1,\|\boldsymbol{k}\|_1)^{-1} < N^{-1}\right\}$ due to (2.9) and thus, we infer $\max\limits_{\boldsymbol{k}\in\mathbb{Z}^d\setminus I_N^{d,-\infty,\boldsymbol{\gamma}}} \omega^{-\tilde{\alpha},0,\boldsymbol{\gamma}}(\boldsymbol{k}) = \max\limits_{\boldsymbol{k}\in\mathbb{Z}^d\setminus I_N^{d,-\infty,\boldsymbol{\gamma}}} \max(1,\|\boldsymbol{k}\|_1)^{-\tilde{\alpha}} \leq N^{-\tilde{\alpha}}$. ■

The next three subsections treat different kinds of approximation errors for functions f from the subspaces $\mathcal{A}^{\alpha,\beta,\boldsymbol{\gamma}}(\mathbb{T}^d)$ of the Wiener algebra. In Subsection 3.1 we consider the approximation error in the $L^\infty(\mathbb{T}^d)$ norm. Subsection 3.2 presents upper bounds on the approximation error in the norm of the periodic Sobolev spaces of generalized mixed smoothness $\mathcal{H}^{\alpha,\beta,\boldsymbol{\gamma}}(\mathbb{T}^d)$. The last Subsection 3.3 specifies a strategy to extend the approximation to an interpolation with similar error estimates.

3.1 Subspaces $\mathcal{A}^{\alpha,\beta,\boldsymbol{\gamma}}(\mathbb{T}^d)$ of the Wiener algebra

In this section, we estimate the approximation error $\|f - \tilde{S}_{I_N^{d,T,\boldsymbol{\gamma}}} f | L^\infty(\mathbb{T}^d)\|$ for functions f from the subspaces $\mathcal{A}^{\alpha,\beta,\boldsymbol{\gamma}}(\mathbb{T}^d)$ of the Wiener algebra.

Theorem 3.3. *Let a function $f \in \mathcal{C}(\mathbb{T}^d) \cap \mathcal{A}^{\alpha,\beta,\boldsymbol{\gamma}}(\mathbb{T}^d)$, a weighted frequency index set $I_N^{d,T,\boldsymbol{\gamma}}$ and a reconstructing rank-1 lattice $\Lambda(\boldsymbol{z}, M, I_N^{d,T,\boldsymbol{\gamma}})$ be given, where $N \geq 1$, $\beta \geq 0$, $\alpha > -\beta$,*

$T \in [-\infty, 1)$ *and* $\boldsymbol{\gamma}$ *as stated in* (2.6)*. Then, the approximation error is bounded by*

$$\begin{aligned} &\|f - \tilde{S}_{I_N^{d,T,\boldsymbol{\gamma}}} f | L^\infty(\mathbb{T}^d)\| \\ &\leq \; 2\, N^{-(\alpha+\beta)}\, \|f|\mathcal{A}^{\alpha,\beta,\boldsymbol{\gamma}}(\mathbb{T}^d)\| \begin{cases} \left(N^{d-1} \prod_{s=1}^d \gamma_s^{-1}\right)^{\frac{T\beta+\alpha}{d-T}} & \text{for } T > -\frac{\alpha}{\beta}, \\ 1 & \text{for } T = -\frac{\alpha}{\beta}, \\ d^{-\frac{T\beta+\alpha}{1-T}} & \text{for } T < -\frac{\alpha}{\beta}. \end{cases} \end{aligned} \tag{3.5}$$

Proof. Applying the triangle inequality in the $L^\infty(\mathbb{T}^d)$ norm, we estimate the approximation error by $\|f - \tilde{S}_{I_N^{d,T,\boldsymbol{\gamma}}} f | L^\infty(\mathbb{T}^d)\| \leq \|f - S_{I_N^{d,T,\boldsymbol{\gamma}}} f | L^\infty(\mathbb{T}^d)\| + \|S_{I_N^{d,T,\boldsymbol{\gamma}}} f - \tilde{S}_{I_N^{d,T,\boldsymbol{\gamma}}} f | L^\infty(\mathbb{T}^d)\|$, where the first term on the right hand side of this inequality is called truncation error and the second term is called aliasing error. Next, we estimate the truncation error. We have $f - S_{I_N^{d,T,\boldsymbol{\gamma}}} f = \sum_{\boldsymbol{k} \in \mathbb{Z}^d \setminus I_N^{d,T,\boldsymbol{\gamma}}} \hat{f}_{\boldsymbol{k}}\, \mathrm{e}^{2\pi \mathrm{i} \boldsymbol{k} \circ}$. Using the weights $\omega^{\alpha,\beta,\boldsymbol{\gamma}}(\boldsymbol{k})$, we obtain

$$\begin{aligned} &\|f - S_{I_N^{d,T,\boldsymbol{\gamma}}} f | L^\infty(\mathbb{T}^d)\| \\ &\leq \sum_{\boldsymbol{k} \in \mathbb{Z}^d \setminus I_N^{d,T,\boldsymbol{\gamma}}} |\hat{f}_{\boldsymbol{k}}| = \sum_{\boldsymbol{k} \in \mathbb{Z}^d \setminus I_N^{d,T,\boldsymbol{\gamma}}} \max(1, \|\boldsymbol{k}\|_1)^{-\alpha} \prod_{s=1}^d \max(1, \gamma_s^{-1}|k_s|)^{-\beta}\, \omega^{\alpha,\beta,\boldsymbol{\gamma}}(\boldsymbol{k})\, |\hat{f}_{\boldsymbol{k}}| \\ &\leq \max_{\boldsymbol{k} \in \mathbb{Z}^d \setminus I_N^{d,T,\boldsymbol{\gamma}}} \left(\max(1, \|\boldsymbol{k}\|_1)^{-\alpha} \prod_{s=1}^d \max(1, \gamma_s^{-1}|k_s|)^{-\beta} \right) \sum_{\boldsymbol{k} \in \mathbb{Z}^d \setminus I_N^{d,T,\boldsymbol{\gamma}}} \omega^{\alpha,\beta,\boldsymbol{\gamma}}(\boldsymbol{k})\, |\hat{f}_{\boldsymbol{k}}|. \end{aligned}$$

Applying Lemma 3.2 with $\tilde{\alpha} := \alpha$ and $\tilde{\beta} := \beta$ yields

$$\begin{aligned} &\|f - S_{I_N^{d,T,\boldsymbol{\gamma}}} f | L^\infty(\mathbb{T}^d)\| \\ &\leq \; N^{-(\alpha+\beta)} \sum_{\boldsymbol{k} \in \mathbb{Z}^d \setminus I_N^{d,T,\boldsymbol{\gamma}}} \omega^{\alpha,\beta,\boldsymbol{\gamma}}(\boldsymbol{k})\, |\hat{f}_{\boldsymbol{k}}| \begin{cases} \left(N^{d-1} \prod_{s=1}^d \gamma_s^{-1}\right)^{\frac{T\beta+\alpha}{d-T}} & \text{for } T > -\frac{\alpha}{\beta}, \\ 1 & \text{for } T = -\frac{\alpha}{\beta}, \\ d^{-\frac{T\beta+\alpha}{1-T}} & \text{for } T < -\frac{\alpha}{\beta}. \end{cases} \end{aligned} \tag{3.6}$$

Last, we estimate the aliasing error. Due to (3.4), we infer

$$\|S_{I_N^{d,T,\boldsymbol{\gamma}}} f - \tilde{S}_{I_N^{d,T,\boldsymbol{\gamma}}} f | L^\infty(\mathbb{T}^d)\| \leq \sum_{\boldsymbol{k} \in I_N^{d,T,\boldsymbol{\gamma}}} \sum_{\substack{\boldsymbol{h} \in \mathbb{Z}^d \setminus \{\boldsymbol{0}\} \\ \boldsymbol{h}\boldsymbol{z} \equiv 0 \pmod M}} |\hat{f}_{\boldsymbol{k}+\boldsymbol{h}}|.$$

Due to the reconstruction property (2.5), we have

$$\{\boldsymbol{k} + \boldsymbol{h} \in \mathbb{Z}^d \colon \boldsymbol{k} \in I_N^{d,T,\boldsymbol{\gamma}}, \boldsymbol{h} \in \mathbb{Z}^d \setminus \{\boldsymbol{0}\}, \boldsymbol{h}\boldsymbol{z} \equiv 0 \pmod M\} \subset \mathbb{Z}^d \setminus I_N^{d,T,\boldsymbol{\gamma}}. \tag{3.7}$$

Consequently, we obtain $\|S_{I_N^{d,T,\boldsymbol{\gamma}}} f - \tilde{S}_{I_N^{d,T,\boldsymbol{\gamma}}} f | L^\infty(\mathbb{T}^d)\| \leq \sum_{\boldsymbol{k} \in \mathbb{Z}^d \setminus I_N^{d,T,\boldsymbol{\gamma}}} |\hat{f}_{\boldsymbol{k}}|$ and proceed as in the estimate of the truncation error. This yields the assertion. ∎

As a consequence of Theorem 3.3, we can derive three cases for the relationship between the parameter T of a weighted frequency index set $I_N^{d,T,\boldsymbol{\gamma}}$ and the smoothness parameters α, β.

(I) The weighted frequency index set $I_N^{d,T,\boldsymbol{\gamma}}$ is "thinner" than required by the isotropic and dominating mixed smoothness parameters α and β, i.e., $T > -\alpha/\beta$.

(II) The weighted frequency index set $I_N^{d,T,\boldsymbol{\gamma}}$ fits the isotropic and dominating mixed smoothness parameters α and β, i.e., the parameter $T = -\alpha/\beta$.

(III) The weighted frequency index set $I_N^{d,T,\boldsymbol{\gamma}}$ is "thicker" than required by the isotropic and dominating mixed smoothness parameters α and β, i.e., $T < -\alpha/\beta$. Choosing the parameter T smaller than $-\alpha/\beta$ does not improve the estimate for the approximation error from the case (II).

3.2 Periodic Sobolev spaces of generalized mixed smoothness $\mathcal{H}^{\alpha,\beta,\boldsymbol{\gamma}}(\mathbb{T}^d)$

Next, we estimate the approximation error $f - \tilde{S}_{I_N^{d,T,\boldsymbol{\gamma}}} f$ of a continuous function $f \in \mathcal{A}^{\alpha,\beta,\boldsymbol{\gamma}}(\mathbb{T}^d) \subset \mathcal{H}^{\alpha,\beta,\boldsymbol{\gamma}}(\mathbb{T}^d)$ in the norm of the periodic Sobolev spaces of generalized mixed smoothness.

Theorem 3.4. *Let parameters $r, t, \alpha, \beta \in \mathbb{R}$, a function $f \in \mathcal{C}(\mathbb{T}^d) \cap \mathcal{A}^{\alpha,\beta,\boldsymbol{\gamma}}(\mathbb{T}^d)$, a weighted frequency index set $I_N^{d,T,\boldsymbol{\gamma}}$ and a reconstructing rank-1 lattice $\Lambda(\boldsymbol{z}, M, I_N^{d,T,\boldsymbol{\gamma}})$ be given, where $N \geq 1$, $\beta \geq t \geq 0$, $\alpha + \beta > r + t$, $\alpha > -\beta$, $\boldsymbol{\gamma}$ as stated in (2.6) and $T \in [-\frac{r}{t}, 1)$ with $-\frac{r}{t} := -\infty$ for $t = 0$. Then, the approximation error is bounded by*

$$\begin{aligned}
\|f - \tilde{S}_{I_N^{d,T,\boldsymbol{\gamma}}} f | \mathcal{H}^{r,t,\boldsymbol{\gamma}}(\mathbb{T}^d)\| &\leq N^{-(\alpha-r+\beta-t)} \\
&\cdot \left(\|f|\mathcal{H}^{\alpha,\beta,\boldsymbol{\gamma}}(\mathbb{T}^d)\| \begin{cases} \left(N^{d-1} \prod_{s=1}^d \gamma_s^{-1}\right)^{\frac{T(\beta-t)+\alpha-r}{d-T}} & \text{for } T > -\frac{\alpha-r}{\beta-t} \\ d^{-\frac{T(\beta-t)+\alpha-r}{1-T}} & \text{for } T \leq -\frac{\alpha-r}{\beta-t} \end{cases} \right. \\
&\left. + \|f|\mathcal{A}^{\alpha,\beta,\boldsymbol{\gamma}}(\mathbb{T}^d)\| \begin{cases} d^{\frac{Tt+r}{1-T}} \left(N^{d-1} \prod_{s=1}^d \gamma_s^{-1}\right)^{\frac{T\beta+\alpha}{d-T}} & \text{for } T > -\frac{\alpha}{\beta} \\ d^{-\frac{T(\beta-t)+\alpha-r}{1-T}} & \text{for } T \leq -\frac{\alpha}{\beta} \end{cases} \right). \quad (3.8)
\end{aligned}$$

Proof. For a function $f \in \mathcal{A}^{\alpha,\beta,\boldsymbol{\gamma}}(\mathbb{T}^d) \subset \mathcal{H}^{\alpha,\beta,\boldsymbol{\gamma}}(\mathbb{T}^d)$, we have $f - S_{I_N^{d,T,\boldsymbol{\gamma}}} f = \sum_{\boldsymbol{k} \in \mathbb{Z}^d \setminus I_N^{d,T,\boldsymbol{\gamma}}} \hat{f}_{\boldsymbol{k}}\, \mathrm{e}^{2\pi \mathrm{i} \boldsymbol{k} \circ}$. Using the weights $\omega^{\alpha,\beta,\boldsymbol{\gamma}}(\boldsymbol{k})$, we obtain

$$\begin{aligned}
\|f - S_{I_N^{d,T,\boldsymbol{\gamma}}} f | \mathcal{H}^{r,t,\boldsymbol{\gamma}}(\mathbb{T}^d)\|^2 &= \sum_{\boldsymbol{k} \in \mathbb{Z}^d \setminus I_N^{d,T,\boldsymbol{\gamma}}} \omega^{r,t,\boldsymbol{\gamma}}(\boldsymbol{k})^2 \, \frac{\omega^{\alpha,\beta,\boldsymbol{\gamma}}(\boldsymbol{k})^2}{\omega^{\alpha,\beta,\boldsymbol{\gamma}}(\boldsymbol{k})^2} \, |\hat{f}_{\boldsymbol{k}}|^2 \\
&\leq \max_{\boldsymbol{k} \in \mathbb{Z}^d \setminus I_N^{d,T,\boldsymbol{\gamma}}} \omega^{-(\alpha-r),-(\beta-t),\boldsymbol{\gamma}}(\boldsymbol{k})^2 \sum_{\boldsymbol{k} \in \mathbb{Z}^d \setminus I_N^{d,T,\boldsymbol{\gamma}}} \omega^{\alpha,\beta,\boldsymbol{\gamma}}(\boldsymbol{k})^2 \, |\hat{f}_{\boldsymbol{k}}|^2.
\end{aligned}$$

Next, we apply Lemma 3.2 with $\tilde{\alpha} := \alpha - r$ and $\tilde{\beta} := \beta - t$. This yields the first summand in (3.8), since we have $\sum_{\boldsymbol{k} \in \mathbb{Z}^d \setminus I_N^{d,T,\boldsymbol{\gamma}}} \omega^{\alpha,\beta,\boldsymbol{\gamma}}(\boldsymbol{k})^2 \, |\hat{f}_{\boldsymbol{k}}|^2 \leq \|f|\mathcal{H}^{\alpha,\beta,\boldsymbol{\gamma}}(\mathbb{T}^d)\|^2$.
For the aliasing error of a function $f \in \mathcal{C}(\mathbb{T}^d) \cap \mathcal{A}^{\alpha,\beta,\boldsymbol{\gamma}}(\mathbb{T}^d)$, we have (3.4) and, in consequence

of the concaveness of the square root function, we conclude

$$\begin{aligned}
\|S_{I_N^{d,T,\boldsymbol{\gamma}}} f - \tilde{S}_{I_N^{d,T,\boldsymbol{\gamma}}} f | \mathcal{H}^{r,t,\boldsymbol{\gamma}}(\mathbb{T}^d)\| &\leq \left(\sum_{\boldsymbol{k} \in I_N^{d,T,\boldsymbol{\gamma}}} \left| \sum_{\substack{\boldsymbol{h} \in \mathbb{Z}^d \setminus \{\boldsymbol{0}\} \\ \boldsymbol{h}\boldsymbol{z} \equiv 0 \pmod M}} \omega^{r,t,\boldsymbol{\gamma}}(\boldsymbol{k})\, \hat{f}_{\boldsymbol{k}+\boldsymbol{h}} \right|^2 \right)^{\frac{1}{2}} \\
&\leq \sum_{\boldsymbol{k} \in I_N^{d,T,\boldsymbol{\gamma}}} \left| \sum_{\substack{\boldsymbol{h} \in \mathbb{Z}^d \setminus \{\boldsymbol{0}\} \\ \boldsymbol{h}\boldsymbol{z} \equiv 0 \pmod M}} \omega^{r,t,\boldsymbol{\gamma}}(\boldsymbol{k})\, \hat{f}_{\boldsymbol{k}+\boldsymbol{h}} \right| \qquad (3.9) \\
&\leq \max_{\boldsymbol{k} \in I_N^{d,T,\boldsymbol{\gamma}}} \omega^{r,t,\boldsymbol{\gamma}}(\boldsymbol{k}) \sum_{\boldsymbol{k} \in I_N^{d,T,\boldsymbol{\gamma}}} \sum_{\substack{\boldsymbol{h} \in \mathbb{Z}^d \setminus \{\boldsymbol{0}\} \\ \boldsymbol{h}\boldsymbol{z} \equiv 0 \pmod M}} \left| \hat{f}_{\boldsymbol{k}+\boldsymbol{h}} \right|.
\end{aligned}$$

Since we have $\max\limits_{\boldsymbol{k} \in I_N^{d,T,\boldsymbol{\gamma}}} \left\{ \omega^{r,t,\boldsymbol{\gamma}}(\boldsymbol{k}) \right\} = \left\{ \begin{array}{ll} \max_{\boldsymbol{k} \in I_N^{d,T,\boldsymbol{\gamma}}} \left\{ \omega^{\frac{r/t}{1+r/t}, \frac{1}{1+r/t}, \boldsymbol{\gamma}}(\boldsymbol{k}) \right\}^{(1+r/t)t} & \text{for } t > 0 \\ \max_{\boldsymbol{k} \in I_N^{d,T,\boldsymbol{\gamma}}} \left\{ \omega^{1,0,\boldsymbol{\gamma}}(\boldsymbol{k}) \right\}^r & \text{for } t = 0 \end{array} \right\}$
and by applying Lemma 2.4 with $\tilde{T} = -\frac{r}{t}$, we estimate

$$\max_{\boldsymbol{k} \in I_N^{d,T,\boldsymbol{\gamma}}} \left\{ \omega^{r,t,\boldsymbol{\gamma}}(\boldsymbol{k}) \right\} \leq \left\{ \begin{array}{ll} (d^{(T+\frac{r}{t})/(1-T)/(1+\frac{r}{t})} N)^{t+r} & \text{for } t > 0 \\ (d^{1/(1-T)} N)^r & \text{for } t = 0 \end{array} \right\} = d^{(Tt+r)/(1-T)} N^{r+t}. \qquad (3.10)$$

Due to the reconstruction property (2.5), the inclusion (3.7) follows. Thus, we infer

$$\begin{aligned}
\|S_{I_N^{d,T,\boldsymbol{\gamma}}} f - \tilde{S}_{I_N^{d,T,\boldsymbol{\gamma}}} f | \mathcal{H}^{r,t,\boldsymbol{\gamma}}(\mathbb{T}^d)\| &\leq d^{\frac{Tt+r}{1-T}} N^{r+t} \sum_{\boldsymbol{k} \in \mathbb{Z}^d \setminus I_N^{d,T,\boldsymbol{\gamma}}} \frac{\omega^{\alpha,\beta,\boldsymbol{\gamma}}(\boldsymbol{k})}{\omega^{\alpha,\beta,\boldsymbol{\gamma}}(\boldsymbol{k})} \left| \hat{f}_{\boldsymbol{k}} \right| \\
&\leq d^{\frac{Tt+r}{1-T}} N^{r+t} \max_{\boldsymbol{k} \in \mathbb{Z}^d \setminus I_N^{d,T,\boldsymbol{\gamma}}} \frac{1}{\omega^{\alpha,\beta,\boldsymbol{\gamma}}(\boldsymbol{k})} \|f | \mathcal{A}^{\alpha,\beta,\boldsymbol{\gamma}}(\mathbb{T}^d)\|.
\end{aligned}$$

Applying Lemma 3.2 with $\tilde{\alpha} := \alpha$ and $\tilde{\beta} := \beta$ yields the second summand in (3.8). ∎

Using the inequality (2.7) we obtain the statement of Theorem 3.4 with the $\mathcal{H}^{\alpha,\beta+\lambda,\boldsymbol{\gamma}}(\mathbb{T}^d)$ norm on the right hand side for functions $f \in \mathcal{C}(\mathbb{T}^d) \cap \mathcal{H}^{\alpha,\beta+\lambda,\boldsymbol{\gamma}}(\mathbb{T}^d) \subset \mathcal{A}^{\alpha,\beta,\boldsymbol{\gamma}}(\mathbb{T}^d)$, $\lambda > 1/2$.

3.3 Approximate reconstruction by interpolation

Let a frequency index set $I_N^{d,T,\boldsymbol{\gamma}}$, $N \geq 1$, $T \in [-\infty, 1)$, $\boldsymbol{\gamma} \in (0,1]^d$, and a reconstructing rank-1 lattice $\Lambda(\boldsymbol{z}, M, I_N^{d,T,\boldsymbol{\gamma}})$ be given. When we approximate a function $f \in \mathcal{A}^{\alpha,\beta,\boldsymbol{\gamma}}(\mathbb{T}^d)$ or $f \in \mathcal{H}^{\alpha,\beta,\boldsymbol{\gamma}}(\mathbb{T}^d)$ by the approximated Fourier partial sum $\tilde{S}_{I_N^{d,T,\boldsymbol{\gamma}}} f(\boldsymbol{x})$ from (3.3), an interpolation condition $f(\boldsymbol{x}_j) = \tilde{S}_{I_N^{d,T,\boldsymbol{\gamma}}} f(\boldsymbol{x}_j)$, $\boldsymbol{x}_j \in \Lambda(\boldsymbol{z}, M, I_N^{d,T,\boldsymbol{\gamma}})$, $j = 0, \ldots, M-1$, does not hold in general and we only have $f(\boldsymbol{x}_j) \approx \tilde{S}_{I_N^{d,T,\boldsymbol{\gamma}}} f(\boldsymbol{x}_j)$, $j = 0, \ldots, M-1$. However, we can expand the frequency index set $I_N^{d,T,\boldsymbol{\gamma}}$ to an interpolation frequency index set $\widetilde{I} \supset I_N^{d,T,\boldsymbol{\gamma}}$ using a slightly modified version of the approach presented in [28] and obtain the interpolation condition

$$f(\boldsymbol{x}_j) = \tilde{S}_{\widetilde{I}} f(\boldsymbol{x}_j), \quad \boldsymbol{x}_j \in \Lambda(\boldsymbol{z}, M, I_N^{d,T,\boldsymbol{\gamma}}), \quad j = 0, \ldots, M-1.$$

The method for constructing the interpolation frequency index set $\widetilde{I}$ consists of the following steps.

1. Start with the index set $\widetilde{I} := I_N^{d,T,\gamma}$.
2. For $l = 0, \ldots, M-1$, if $\nexists \boldsymbol{k} \in \widetilde{I}\colon \boldsymbol{k}\boldsymbol{z} \equiv l \pmod M$, add a frequency $\boldsymbol{k}' \in \mathbb{Z}^d\colon \boldsymbol{k}'\boldsymbol{z} \equiv l \pmod M$ to the index set $\widetilde{I}$.

We have several possibilities for choosing $\boldsymbol{k}'$ in step 2. Subsequent to the following Theorem 3.5, we suggest a special choice.

After applying the two steps mentioned above, we have constructed an interpolation frequency index set $\widetilde{I}$, which has the properties $I_N^{d,T,\gamma} \subset \widetilde{I}$, $|\widetilde{I}| = M$ and $|\{\boldsymbol{k} \in \widetilde{I}\colon \boldsymbol{k}\boldsymbol{z} \equiv l \pmod M\}| = 1$ for all $l = 0, \ldots, M-1$. Due to this, the Fourier matrix $\boldsymbol{F} := \left(\mathrm{e}^{2\pi \mathrm{i} j\boldsymbol{k}\boldsymbol{z}/M}\right)_{j=0;\,\boldsymbol{k}\in\widetilde{I}}^{M-1}$ is a square matrix and identical to the one-dimensional Fourier matrix $\widetilde{\boldsymbol{F}} := \left(\mathrm{e}^{2\pi \mathrm{i} jl/M}\right)_{j,l=0}^{M-1}$ except for column permutations. Therefore, we compute the approximated Fourier coefficients $\hat{\tilde{f}}_{\boldsymbol{k}}$, $\boldsymbol{k} \in \widetilde{I}$, by $\left(\hat{\tilde{f}}_{\boldsymbol{k}}\right)_{\boldsymbol{k}\in\widetilde{I}} = \frac{1}{M}\, \boldsymbol{F}^{\mathrm{H}}\, (f(\boldsymbol{x}_j))_{j=0}^{M-1}$ in $\mathcal{O}(M(\log M + d))$ arithmetic operations using a single one-dimensional FFT as described in Section 2.3.

The following theorem states that we have identical error estimates as in Section 3.1, Theorem 3.3 and Section 3.2, Theorem 3.4.

Theorem 3.5. *Let parameters $r, t, \alpha, \beta \in \mathbb{R}$, a function $f \in \mathcal{C}(T^d) \cap \mathcal{A}^{\alpha,\beta,\gamma}(\mathbb{T}^d)$, a weighted frequency index set $I_N^{d,T,\gamma}$, a reconstructing rank-1 lattice $\Lambda(\boldsymbol{z}, M, I_N^{d,T,\gamma})$ and an interpolation frequency index set $\widetilde{I} \supset I_N^{d,T,\gamma}$ be given, where $N \geq 1$, $\beta \geq t \geq 0$, $\alpha + \beta > r + t$, $\alpha > -\beta$, $\boldsymbol{\gamma}$ as stated in (2.6), and $|\{\boldsymbol{k} \in \widetilde{I}\colon \boldsymbol{k}\boldsymbol{z} \equiv l \pmod M\}| = 1$ for all $l = 0, \ldots, M-1$. Then, the approximation error is bounded by (3.5) for $T \in [-\infty, 1)$ and by (3.8) for $T \in [-\frac{r}{t}, 1)$ with $-\frac{r}{t} := -\infty$ for $t = 0$.*

Proof. We use the inclusion $\mathbb{Z}^d \setminus \widetilde{I} \subset \mathbb{Z}^d \setminus I_N^{d,T,\gamma}$ and proceed as in the proofs of Theorem 3.3 and Theorem 3.4. ∎

In step 2 of the method for constructing the interpolation frequency index set $\widetilde{I}$, we suggest choosing $\boldsymbol{k}'$ as a smallest frequency index with respect to the weight $\omega^{-T,1,\gamma}(\boldsymbol{k})$, $\boldsymbol{k}' = \arg\min_{\substack{\boldsymbol{k}\in\mathbb{Z}^d \\ \boldsymbol{k}\boldsymbol{z}\equiv l \pmod M}} \omega^{-T,1,\gamma}(\boldsymbol{k})$, since this may reduce the approximation error $\|f - \tilde{S}_{I_N^{d,T,\gamma}} f | L^\infty(\mathbb{T}^d)\|$ or $\|f - \tilde{S}_{\widetilde{I}} f | \mathcal{H}^{r,t,\gamma}(\mathbb{T}^d)\|$ for a function $f \in \mathcal{C}(\mathbb{T}^d) \cap \mathcal{A}^{\alpha,\beta,\gamma}(\mathbb{T}^d)$ in general.

4 Fast evaluation and reconstruction of trigonometric polynomials using Taylor expansion and rank-1 lattices

We have already discussed the fast and exact evaluation of a trigonometric polynomial p with frequencies supported on an index set I at rank-1 lattice nodes $\boldsymbol{x}_j$ in Section 2.2 as well as the fast, exact and perfectly stable reconstruction of a trigonometric polynomial p by sampling at rank-1 lattice nodes $\boldsymbol{x}_j$ in Section 2.3. Based on these two results, we consider the case where the sampling values are not given exactly at the rank-1 lattice nodes $\boldsymbol{x}_j$ but at perturbed rank-1 lattice nodes. We are especially interested in the evaluation error and the stability of the reconstruction as a function of the perturbation parameter ε.

First, we consider in Section 4.1 the fast evaluation of a trigonometric polynomial p. As presented in [36] and based on the ideas in [1, 26], we evaluate a trigonometric polynomial p at nodes $\boldsymbol{y}_\ell \in \mathbb{T}^d$, $\ell = 0, \ldots, L-1$, using a Taylor expansion at a closest rank-1 lattice node $\boldsymbol{x}_{j'} \in \Lambda(\boldsymbol{z}, M)$ for each node $\boldsymbol{y}_\ell$. For evaluating the trigonometric polynomial p and its derivatives at the rank-1 lattice nodes, one-dimensional FFTs are used as described in Section 2.2. In Section 4.2, we develop error estimates for the approximation of the trigonometric polynomial p by the Taylor expansion. Then, we investigate the reconstruction of the trigonometric polynomial p from sampling values at perturbed rank-1 lattice nodes in Section 4.3. Thereby, we consider the stability of the reconstruction in dependence of the perturbation and prove upper bounds for the reconstruction error.

4.1 Fast evaluation of trigonometric polynomials using Taylor expansion and rank-1 lattices

We approximate a trigonometric polynomial $p : \mathbb{T}^d \to \mathbb{C}$ by

$$p(\boldsymbol{x}) \approx s_m(\boldsymbol{x}) := \sum_{0 \le |\boldsymbol{\nu}| < m} \frac{D^{\boldsymbol{\nu}} p(\boldsymbol{a})}{\boldsymbol{\nu}!} (\boldsymbol{x} - \boldsymbol{a})^{\boldsymbol{\nu}},$$

where $m \in \mathbb{N}$, $D^{\boldsymbol{0}} p := p$, $D^{\boldsymbol{\nu}} p := \frac{\partial^{\nu_1}}{\partial {x_1}^{\nu_1}} \ldots \frac{\partial^{\nu_d}}{\partial {x_d}^{\nu_d}} p$, $\boldsymbol{x} := (x_1, \ldots, x_d)^\top$, $\boldsymbol{\nu} := (\nu_1, \ldots, \nu_d) \in \mathbb{N}_0^d$, $|\boldsymbol{\nu}| := |\nu_1| + \ldots + |\nu_d|$, $\boldsymbol{\nu}! := \nu_1! \cdot \ldots \cdot \nu_d!$, $\boldsymbol{x}^{\boldsymbol{\nu}} := {x_1}^{\nu_1} \cdot \ldots \cdot {x_d}^{\nu_d}$. For a trigonometric polynomial $p \in \Pi_I$, we have $D^{\boldsymbol{\nu}} p(\boldsymbol{x}) = \sum_{\boldsymbol{k} \in I} (2\pi \mathrm{i} \boldsymbol{k})^{\boldsymbol{\nu}} \, \hat{p}_{\boldsymbol{k}} \, \mathrm{e}^{2\pi \mathrm{i} \boldsymbol{k} \boldsymbol{x}}$ and thus,

$$s_m(\boldsymbol{x}) = \sum_{0 \le |\boldsymbol{\nu}| < m} \frac{(\boldsymbol{x} - \boldsymbol{a})^{\boldsymbol{\nu}}}{\boldsymbol{\nu}!} \sum_{\boldsymbol{k} \in I} (2\pi \mathrm{i} \boldsymbol{k})^{\boldsymbol{\nu}} \, \hat{p}_{\boldsymbol{k}} \, \mathrm{e}^{2\pi \mathrm{i} \boldsymbol{k} \boldsymbol{a}}. \tag{4.1}$$

Let a frequency index set $I \subset \mathbb{Z}^d$ of finite cardinality and a rank-1 lattice $\Lambda(\boldsymbol{z}, M) \subset \mathbb{T}^d$ of size M with generating vector $\boldsymbol{z} \in \mathbb{Z}^d$ be given. Furthermore, we define the metric $\rho(\boldsymbol{x}, \boldsymbol{y}) := \min_{\boldsymbol{h} \in \mathbb{Z}^d} \|\boldsymbol{x} - \boldsymbol{y} + \boldsymbol{h}\|_\infty$ for $\boldsymbol{x}, \boldsymbol{y} \in \mathbb{T}^d$. For the expansion point $\boldsymbol{a} \in \mathbb{T}^d$ in (4.1), we use a closest rank-1 lattice point $\boldsymbol{x}_{j'} \in \Lambda(\boldsymbol{z}, M)$, $\boldsymbol{x}_{j'} := \arg\min_{\boldsymbol{x}_j \in \Lambda(\boldsymbol{z}, M)} \rho(\boldsymbol{x}, \boldsymbol{x}_j)$, for each $\boldsymbol{x} \in \mathbb{T}^d$, and we approximate the trigonometric polynomial $p(\boldsymbol{x}) := \sum_{\boldsymbol{k} \in I} \hat{p}_{\boldsymbol{k}} \, \mathrm{e}^{2\pi \mathrm{i} \boldsymbol{k} \boldsymbol{x}}$ by (4.1).

Assuming that the index $\mu_\ell \in \{0, \ldots, M-1\}$ of a closest rank-1 lattice node $\boldsymbol{x}_{\mu_\ell} = \arg\min_{\boldsymbol{x}_j \in \Lambda(\boldsymbol{z}, M)} \rho(\boldsymbol{y}_\ell, \boldsymbol{x}_j)$ is known for each sampling node $\boldsymbol{y}_\ell$, $\ell = 0, \ldots, L-1$, Algorithm 3 demonstrates that the approximation of the trigonometric polynomial p by s_m can be realized in $\mathcal{O}\left(m^d (L + M \log M + d|I|)\right)$ arithmetic operations for L sampling nodes $\boldsymbol{y}_\ell$.

We write the evaluation of $s_m(\boldsymbol{x})$ at sampling nodes $\boldsymbol{y}_\ell$, $\ell = 0, \ldots, L-1$, in matrix-vector notation as

$$(s_m(\boldsymbol{y}_\ell))_{\ell=0}^{L-1} = \boldsymbol{A}_{m-1} \hat{\boldsymbol{p}} = \sum_{0 \le |\boldsymbol{\nu}| \le m-1} \boldsymbol{B}_{\boldsymbol{\nu}} \boldsymbol{F} \boldsymbol{D}_{\boldsymbol{\nu}} \hat{\boldsymbol{p}}, \tag{4.2}$$

where $\hat{\boldsymbol{p}} := (\hat{p}_{\boldsymbol{k}})_{\boldsymbol{k} \in I} \in \mathbb{C}^{|I|}$ is the vector of the Fourier coefficients,
$\boldsymbol{D}_{\boldsymbol{\nu}} := \operatorname{diag}\left(((2\pi \mathrm{i} \boldsymbol{k})^{\boldsymbol{\nu}})_{\boldsymbol{k} \in I}\right) \in \mathbb{C}^{|I| \times |I|}$ is a diagonal matrix, $\boldsymbol{F} := \left(\mathrm{e}^{2\pi \mathrm{i} j \boldsymbol{k} \boldsymbol{z} / M}\right)_{j=0;\, \boldsymbol{k} \in I}^{M-1} \in \mathbb{C}^{M \times |I|}$ is the Fourier matrix from Section 2.3, and $\boldsymbol{B}_{\boldsymbol{\nu}} \in \mathbb{R}^{L \times M}$ is a sparse matrix with at most one non-zero entry $\frac{(\boldsymbol{y}_\ell - \boldsymbol{x}_{\mu_\ell})^{\boldsymbol{\nu}}}{\boldsymbol{\nu}!}$ at column μ_ℓ in each row $\ell = 0, \ldots, L-1$.

Algorithm 3 Fast evaluation of a trigonometric polynomial p at nodes $\boldsymbol{y}_\ell \in \mathbb{T}^d$, $\ell = 0, \ldots, L-1$.

Input:	$I \subset \mathbb{Z}^d$	frequency index set of finite cardinality
	$\hat{p}_{\boldsymbol{k}} \in I$	Fourier coefficients
	$\Lambda(\boldsymbol{z}, M)$	rank-1 lattice of size M, generating vector $\boldsymbol{z} \in \mathbb{Z}^d$
	$m \in \mathbb{N}$	Taylor expansion degree
	$\boldsymbol{y}_\ell \in \mathbb{T}^d$, $\ell = 0, \ldots, L-1$	nodes
	$\mu_\ell \in 0, \ldots, M-1$	index of rank-1 lattice node closest to $\boldsymbol{y}_\ell$

1: Set $\tilde{s}(\boldsymbol{y}_\ell) := 0$, $\ell = 0, \ldots, L-1$.
2: ***forall*** $\boldsymbol{\nu} \in \{\boldsymbol{\alpha} \in \mathbb{N}_0^d \colon 0 \leq |\boldsymbol{\alpha}| < m\}$ ***do***
3: $\quad \hat{\boldsymbol{g}} := \left(\sum_{\boldsymbol{k} \in I, \boldsymbol{k}\boldsymbol{z} \equiv l \pmod M} (2\pi \mathrm{i} \boldsymbol{k})^{\boldsymbol{\nu}} \, \hat{p}_{\boldsymbol{k}} \right)_{l=0}^{M-1}$
4: $\quad \boldsymbol{g} = (g_j)_{j=0}^{M-1} := M \cdot \mathrm{iFFT\_1D}(\hat{\boldsymbol{g}})$.
5: $\quad \tilde{s}(\boldsymbol{y}_\ell) := \tilde{s}(\boldsymbol{y}_\ell) + \frac{(\boldsymbol{y}_\ell - \boldsymbol{x}_{\mu_\ell})^{\boldsymbol{\nu}}}{\boldsymbol{\nu}!} g_{\mu_\ell}$, $\ell = 0, \ldots, L-1$.
6: ***end for***

Output:	$s_m(\boldsymbol{y}_\ell) := \tilde{s}(\boldsymbol{y}_\ell)$, $\ell = 0, \ldots, L-1$	approximation to the values $p(\boldsymbol{y}_\ell)$
Complexity:	$\mathcal{O}\left(m^d (L + M \log M + d\lvert I \rvert)\right)$	

4.2 Error estimates for the evaluation of trigonometric polynomials at perturbed rank-1 lattice nodes

In this section, we establish error bounds for the approximate evaluation of a trigonometric polynomial $p \in \Pi_I$ by a Taylor expansion s_m from (4.1) for nodes $\boldsymbol{y} \in \mathcal{Y}_\varepsilon$ from the set of admissible evaluation nodes $\mathcal{Y}_\varepsilon := \{\boldsymbol{x} \in \mathbb{T}^d \colon \exists \boldsymbol{x}_{j'} \in \Lambda(\boldsymbol{z}, M)$ such that $\rho(\boldsymbol{x}, \boldsymbol{x}_{j'}) \leq \varepsilon\}$ with perturbation parameter $\varepsilon \geq 0$. The results for the error bounds in Theorem 4.1 are similar to the ones in [36, Theorem III.1]. However, in the latter one, we allowed arbitrary evaluation nodes $\boldsymbol{x} \in \mathbb{T}^d$ and used the so-called mesh norm δ, whereas we restrict the evaluation nodes $\boldsymbol{y}$ here to the set $\mathcal{Y}_\varepsilon$, i.e., to those nodes from $\mathbb{T}^d$ which are close to the rank-1 lattice $\Lambda(\boldsymbol{z}, M)$ with respect to the perturbation parameter ε.

Theorem 4.1. *Let a weighted frequency index set $I_N^{d,T,\boldsymbol{\gamma}}$ and a trigonometric polynomial $p : \mathbb{T}^d \to \mathbb{C}$ supported on $I_N^{d,T,\boldsymbol{\gamma}}$, $p(\boldsymbol{x}) := \sum_{\boldsymbol{k} \in I_N^{d,T,\boldsymbol{\gamma}}} \hat{p}_{\boldsymbol{k}} \, \mathrm{e}^{2\pi \mathrm{i} \boldsymbol{k}\boldsymbol{x}}$, be given by its Fourier coefficients $\hat{p}_{\boldsymbol{k}} \in \mathbb{C}$, where $N \geq 1$, $T \in [-\infty, 1)$ and $\boldsymbol{\gamma} \in (0,1]^d$. Furthermore, let $\Lambda(\boldsymbol{z}, M)$ be a rank-1 lattice and $\mathcal{Y}_\varepsilon$ be a special set of admissible evaluation nodes for a perturbation parameter $\varepsilon \geq 0$. Additionally, let a parameter $m \in \mathbb{N}$, a dominating mixed smoothness parameter $\beta \geq 0$ and an isotropic smoothness parameter α be given, where $0 \leq \alpha + \beta \leq m$. Then, for the approximate evaluation of the trigonometric polynomial p by a truncated Taylor series $s_m(\boldsymbol{y}) := \sum_{|\boldsymbol{\nu}|=0}^{m-1} \frac{D^{\boldsymbol{\nu}} p(\boldsymbol{x}_{j'})}{\boldsymbol{\nu}!} (\boldsymbol{y} - \boldsymbol{x}_{j'})^{\boldsymbol{\nu}}$ of degree $m-1$ at nodes $\boldsymbol{y} \in \mathcal{Y}_\varepsilon$, where $m \in \mathbb{N}$ and $\boldsymbol{x}_{j'} = \arg\min_{\boldsymbol{x}_j \in \Lambda(\boldsymbol{z}, M)} \rho(\boldsymbol{y}, \boldsymbol{x}_j)$, the remainder $R_m := p - s_m$ is bounded by*

$$|R_m(\boldsymbol{y})| \quad \leq \quad \frac{(2\pi)^m}{m!} d^{\frac{m-\alpha-T\beta}{1-T}} \varepsilon^m N^{m-\alpha-\beta} \sum_{\boldsymbol{k} \in I_N^{d,T,\boldsymbol{\gamma}}} |\hat{p}_{\boldsymbol{k}}| \, \omega^{\alpha,\beta,\boldsymbol{\gamma}}(\boldsymbol{k}).$$

Proof. First we show $|R_m(\boldsymbol{y})| \leq \frac{(2\pi)^m}{m!} \varepsilon^m \sum_{\boldsymbol{k} \in I_N^{d,T,\boldsymbol{\gamma}}} |\hat{p}_{\boldsymbol{k}}| \, \|\boldsymbol{k}\|_1^m$ for all $\boldsymbol{y} \in \mathcal{Y}_\varepsilon$ and therefor,

we follow the major steps of the proof of [36, Theorem III.1]. Let $\boldsymbol{\xi}(t) := \boldsymbol{x}_{j'} + t(\boldsymbol{y} - \boldsymbol{x}_{j'})$, $t \in [0,1]$. The remainder $R_m(\boldsymbol{y})$ can be written in the form

$$R_m(\boldsymbol{y}) = m \int_0^1 (1-t)^{m-1} \sum_{|\boldsymbol{\nu}|=m} D^{\boldsymbol{\nu}} p(\boldsymbol{\xi}(t)) \frac{(\boldsymbol{y} - \boldsymbol{x}_{j'})^{\boldsymbol{\nu}}}{\boldsymbol{\nu}!} \mathrm{d}t$$

and we estimate $|R_m(\boldsymbol{y})| \leq \max_{t\in[0,1]} \sum_{|\boldsymbol{\nu}|=m} \left| \sum_{\boldsymbol{k}\in I_N^{d,T,\boldsymbol{\gamma}}} (2\pi \mathrm{i}\boldsymbol{k})^{\boldsymbol{\nu}} \hat{p}_{\boldsymbol{k}} \, \mathrm{e}^{2\pi\mathrm{i}\boldsymbol{k}(\boldsymbol{\xi}(t))} \right| \frac{|(\boldsymbol{y}-\boldsymbol{x}_{j'})^{\boldsymbol{\nu}}|}{\boldsymbol{\nu}!}$. Since we have $\rho(\boldsymbol{y}, \boldsymbol{x}_{j'}) \leq \varepsilon$ and by applying the multinomial theorem, we get

$$\begin{aligned}
|R_m(\boldsymbol{y})| &\leq \max_{t\in[0,1]} \sum_{|\boldsymbol{\nu}|=m} \frac{\varepsilon^{|\boldsymbol{\nu}|}}{\boldsymbol{\nu}!} \sum_{\boldsymbol{k}\in I_N^{d,T,\boldsymbol{\gamma}}} |(2\pi\mathrm{i}\boldsymbol{k})^{\boldsymbol{\nu}}| \, |\hat{p}_{\boldsymbol{k}}| \, |\mathrm{e}^{2\pi\mathrm{i}\boldsymbol{k}(\boldsymbol{\xi}(t))}| \\
&\leq 2^m \pi^m \varepsilon^m \sum_{\boldsymbol{k}\in I_N^{d,T,\boldsymbol{\gamma}}} |\hat{p}_{\boldsymbol{k}}| \sum_{|\boldsymbol{\nu}|=m} \frac{|k_1|^{\nu_1} \cdot \ldots \cdot |k_d|^{\nu_d}}{\boldsymbol{\nu}!} = \frac{2^m \pi^m}{m!} \, \varepsilon^m \sum_{\boldsymbol{k}\in I_N^{d,T,\boldsymbol{\gamma}}} |\hat{p}_{\boldsymbol{k}}| \, \|\boldsymbol{k}\|_1^m
\end{aligned}$$

for arbitrary $\boldsymbol{y} \in \mathcal{Y}_\varepsilon$.
Next, we remark that $\|\boldsymbol{k}\|_1^m \leq \max(1, \|\boldsymbol{k}\|_1)^m = \omega^{m,0,\boldsymbol{\gamma}}(\boldsymbol{k})$, $m > 0$, follows directly from definition. Furthermore, we estimate parts of the isotropic smoothness in terms of the dominating mixed smoothness, $\omega^{\frac{m-\alpha-T\beta}{1-T},0,\boldsymbol{\gamma}}(\boldsymbol{k}) \leq d^{\frac{m-\alpha-T\beta}{1-T}} \, \omega^{0,\frac{m-\alpha-T\beta}{1-T},\boldsymbol{\gamma}}(\boldsymbol{k})$ for all $\boldsymbol{k} \in \mathbb{Z}^d$, using the inequalities (2.11) and (2.12). Therefore, we have

$$\begin{aligned}
\omega^{m,0,\boldsymbol{\gamma}}(\boldsymbol{k}) &= \omega^{m-\alpha-\frac{m-\alpha-T\beta}{1-T},-\beta,\boldsymbol{\gamma}}(\boldsymbol{k}) \, \omega^{\frac{m-\alpha-T\beta}{1-T},0,\boldsymbol{\gamma}}(\boldsymbol{k}) \, \omega^{\alpha,\beta,\boldsymbol{\gamma}}(\boldsymbol{k}) \\
&\leq \omega^{m-\alpha-\frac{m-\alpha-T\beta}{1-T},-\beta,\boldsymbol{\gamma}}(\boldsymbol{k}) \, d^{\frac{m-\alpha-T\beta}{1-T}} \, \omega^{0,\frac{m-\alpha-T\beta}{1-T},\boldsymbol{\gamma}}(\boldsymbol{k}) \, \omega^{\alpha,\beta,\boldsymbol{\gamma}}(\boldsymbol{k}) \\
&= d^{\frac{m-\alpha-T\beta}{1-T}} \, \omega^{-\frac{T}{1-T}(m-\alpha-\beta),\frac{1}{1-T}(m-\alpha-\beta),\boldsymbol{\gamma}}(\boldsymbol{k}) \quad \omega^{\alpha,\beta,\boldsymbol{\gamma}}(\boldsymbol{k})
\end{aligned}$$

for $\boldsymbol{k} \in \mathbb{Z}$. Consequently, we infer

$$|R_m(\boldsymbol{y})| \leq \frac{(2\pi)^m}{m!} \, d^{\frac{m-\alpha-T\beta}{1-T}} \, \varepsilon^m \max_{\boldsymbol{k}\in I_N^{d,T,\boldsymbol{\gamma}}} \left(\omega^{-\frac{T}{1-T},\frac{1}{1-T},\boldsymbol{\gamma}}(\boldsymbol{k}) \right)^{m-\alpha-\beta} \sum_{\boldsymbol{k}\in I_N^{d,T,\boldsymbol{\gamma}}} \omega^{\alpha,\beta,\boldsymbol{\gamma}}(\boldsymbol{k}) \, |\hat{p}_{\boldsymbol{k}}|. \quad (4.3)$$

Due to (2.13), we obtain $\max_{\boldsymbol{k}\in I_N^{d,T,\boldsymbol{\gamma}}} \left(\omega^{-\frac{T}{1-T},\frac{1}{1-T},\boldsymbol{\gamma}}(\boldsymbol{k}) \right)^{m-\alpha-\beta} \leq N^{m-\alpha-\beta}$ and this yields the assertion. ∎

As a consequence of Theorem 4.1, we have several possibilities to ensure a small approximation error for fixed Taylor expansion degree $m-1$ and increasing refinement N.

(I) Choose the perturbation parameter ε like $\sim 1/N^{\frac{m-\alpha-\beta}{m}}$ or smaller and restrict evaluation nodes to the set $\mathcal{Y}_\varepsilon$, i.e., permit only relatively small perturbations to the nodes $\boldsymbol{x}_j$ of the rank-1 lattice.

(II) Allow arbitrarily chosen evaluation nodes $\boldsymbol{x} \in \mathbb{T}^d$ and use trigonometric polynomials with a certain decay of the Fourier coefficients $\hat{p}_{\boldsymbol{k}}$. For instance, choose $\alpha + \beta = m$ and ensure that the Fourier coefficients $\hat{p}_{\boldsymbol{k}}$ decay at least like $\sim 1/\omega^{\alpha,\beta,\boldsymbol{\gamma}}(\boldsymbol{k})$ or faster.

4.3 Approximate reconstruction of trigonometric polynomials by sampling at perturbed rank-1 lattice nodes

Let a frequency index set $I \subset \mathbb{Z}^d \cap [-N, N]^d$, $N \geq 1$, be given. In addition, let a reconstructing rank-1 lattice $\Lambda(\boldsymbol{z}, M, I)$ of size $M \geq |I|$ be given that allows for an exact and perfectly stable reconstruction of the Fourier coefficients $\hat{p}_{\boldsymbol{k}} \in \mathbb{C}$ of a trigonometric polynomial $p \in \Pi_I$, $p(\boldsymbol{x}) := \sum_{\boldsymbol{k} \in I} \hat{p}_{\boldsymbol{k}} \, \mathrm{e}^{2\pi \mathrm{i} \boldsymbol{k} \boldsymbol{x}}$, i.e., condition (2.3) is fulfilled.

Our aim is now to approximately reconstruct the Fourier coefficients $\hat{p}_{\boldsymbol{k}}$, $\boldsymbol{k} \in I$, from sampling values $p(\boldsymbol{y}_\ell)$, $\ell = 0, \ldots, L-1$, using the approach from Section 4.1. In the matrix-vector notation this problem reads as follows: Solve the linear system of equations $\boldsymbol{A}_{m-1} \, \hat{\hat{\boldsymbol{p}}} = \boldsymbol{p}$ in the least-squares sense,

$$\hat{\hat{\boldsymbol{p}}} := \operatorname*{arg\,min}_{\hat{\boldsymbol{g}} \in \mathbb{C}^{\left|I_N^{d,T,\boldsymbol{\gamma}}\right|}} \| \boldsymbol{A}_{m-1} \, \hat{\boldsymbol{g}} - \boldsymbol{p} \|_2, \tag{4.4}$$

where $\boldsymbol{A}_{m-1} := \sum_{|\boldsymbol{\nu}| \leq m-1} \boldsymbol{B}_{\boldsymbol{\nu}} \boldsymbol{F} \boldsymbol{D}_{\boldsymbol{\nu}} \in \mathbb{C}^{M \times |I|}$ is the approximated Fourier matrix, see (4.2), $\hat{\hat{\boldsymbol{p}}} := (\hat{\hat{p}}_{\boldsymbol{k}})_{\boldsymbol{k} \in I_N^{d,T,\boldsymbol{\gamma}}}$ is the vector of approximated Fourier coefficients and $\boldsymbol{p} := (p(\boldsymbol{y}_\ell))_{\ell=0,\ldots,L-1}$ is the vector of sampling values. Assuming that the approximated Fourier matrix $\boldsymbol{A}_{m-1}$ has full column rank, we expect a unique solution of (4.4) solving the normal equation of the first kind, $\boldsymbol{A}_{m-1}^{\mathrm{H}} \boldsymbol{A}_{m-1} \, \hat{\hat{\boldsymbol{p}}} = \boldsymbol{A}_{m-1}^{\mathrm{H}} \, \boldsymbol{p}$.

In the following, we investigate the condition number $\kappa(\boldsymbol{A}_{m-1}) := \frac{\sigma_1(\boldsymbol{A}_{m-1})}{\sigma_{|I|}(\boldsymbol{A}_{m-1})}$ of the approximated Fourier matrix $\boldsymbol{A}_{m-1}$, where $\sigma_1(\boldsymbol{A}_{m-1})$ and $\sigma_{|I|}(\boldsymbol{A}_{m-1})$ are the largest and smallest singular values of $\kappa(\boldsymbol{A}_{m-1})$, respectively. We assume that the number L of sampling nodes $\boldsymbol{y}_\ell$ is equal to the rank-1 lattice size M and that each rank-1 lattice node $\boldsymbol{x}_j$ is a closest one for the sampling node $\boldsymbol{y}_j$, $j = 0, \ldots, M-1$. Then, the sparse matrix $\boldsymbol{B}_{\boldsymbol{\nu}}$ from (4.2) is a diagonal matrix,

$$\boldsymbol{B}_{\boldsymbol{\nu}} = \operatorname{diag}\left(\left[\frac{(\boldsymbol{y}_j - \boldsymbol{x}_j)^{\boldsymbol{\nu}}}{\boldsymbol{\nu}!} \right]_{j=0,\ldots,M-1} \right) \in \mathbb{R}^{M \times M}, \quad \boldsymbol{\nu} \in \mathbb{N}_0^d. \tag{4.5}$$

Theorem 4.2. *Let a frequency index set $I \subset \mathbb{Z}^d \cap [-N, N]^d$, $N \geq 1$, and a corresponding reconstructing rank-1 lattice $\Lambda(\boldsymbol{z}, M, I)$ be given as well as a parameter $m \in \mathbb{N}$. Let the sparse matrix $\boldsymbol{B}_{\boldsymbol{\nu}}$ from* (4.2) *be a diagonal matrix of form* (4.5) *and $\|\boldsymbol{y}_j - \boldsymbol{x}_j\|_\infty \leq \varepsilon$, $j = 0, \ldots, M-1$, for fixed perturbation parameter ε, $0 \leq \varepsilon < \frac{\ln 2}{2\pi d N}$. Then, the condition number $\kappa(\boldsymbol{A}_{m-1})$ can be estimated by*

$$\kappa(\boldsymbol{A}_{m-1}) \leq \frac{1 + \sum_{r=1}^{m-1} \frac{(2\pi d N \varepsilon)^r}{r!}}{1 - \sum_{r=1}^{m-1} \frac{(2\pi d N \varepsilon)^r}{r!}} \leq \frac{\mathrm{e}^{2\pi d N \varepsilon}}{2 - \mathrm{e}^{2\pi d N \varepsilon}}.$$

Proof. For the case $m = 1$, we obtain $\boldsymbol{A}_0^{\mathrm{H}} \boldsymbol{A}_0 = \boldsymbol{D}_{\boldsymbol{0}}^{\mathrm{H}} \boldsymbol{F}^{\mathrm{H}} \boldsymbol{B}_{\boldsymbol{0}}^{\mathrm{H}} \boldsymbol{B}_{\boldsymbol{0}} \boldsymbol{F} \boldsymbol{D}_{\boldsymbol{0}}$. Since $\boldsymbol{D}_{\boldsymbol{0}} = \boldsymbol{I}_{|I|}$ and $\boldsymbol{B}_{\boldsymbol{0}} = \boldsymbol{I}_M$ are identity matrices, it follows from condition (2.3) that $\boldsymbol{A}_0^{\mathrm{H}} \boldsymbol{A}_0 = \boldsymbol{F}^{\mathrm{H}} \boldsymbol{F} = M \boldsymbol{I}_M$ and thus, all singular values $\sigma_1(\boldsymbol{A}_0) = \ldots = \sigma_{|I|}(\boldsymbol{A}_0) = \sqrt{M}$. Therefore, the condition number $\kappa(\boldsymbol{A}_0) = \frac{\sigma_1(\boldsymbol{A}_0)}{\sigma_{|I|}(\boldsymbol{A}_0)} = 1$. In the following, we consider the case $m > 1$. For the largest singular value $\sigma_1(\boldsymbol{A}_{m-1})$, we have

$$\sigma_1(\boldsymbol{A}_{m-1}) \leq \|\boldsymbol{B}_{\boldsymbol{0}} \boldsymbol{F} \boldsymbol{D}_{\boldsymbol{0}}\|_2 + \left\| \sum_{1 \leq |\boldsymbol{\nu}| \leq m-1} \boldsymbol{B}_{\boldsymbol{\nu}} \boldsymbol{F} \boldsymbol{D}_{\boldsymbol{\nu}} \right\|_2 = \sqrt{M} + \sigma_1 \left(\sum_{1 \leq |\boldsymbol{\nu}| \leq m-1} \boldsymbol{B}_{\boldsymbol{\nu}} \boldsymbol{F} \boldsymbol{D}_{\boldsymbol{\nu}} \right). \tag{4.6}$$

Next, we show an upper bound for $\sigma_1\left(\sum_{1\le|\boldsymbol{\nu}|\le m-1}\boldsymbol{B_\nu F D_\nu}\right)$. We have

$$\begin{aligned}\sigma_1\left(\sum_{1\le|\boldsymbol{\nu}|\le m-1}\boldsymbol{B_\nu F D_\nu}\right) &\le \sum_{1\le|\boldsymbol{\nu}|\le m-1}\|\boldsymbol{B_\nu F D_\nu}\|_2 \le \sum_{1\le|\boldsymbol{\nu}|\le m-1}\|\boldsymbol{B_\nu}\|_2\|\boldsymbol{F}\|_2\|\boldsymbol{D_\nu}\|_2\\ &= \sum_{1\le|\boldsymbol{\nu}|\le m-1}\sigma_1(\boldsymbol{B_\nu})\,\sigma_1(\boldsymbol{F})\,\sigma_1(\boldsymbol{D_\nu}).\end{aligned} \tag{4.7}$$

Since $\boldsymbol{B_\nu} = \operatorname{diag}\left(\left[\frac{(\boldsymbol{y}_j-\boldsymbol{x}_j)^{\boldsymbol{\nu}}}{\boldsymbol{\nu}!}\right]_{j=0,\dots,M-1}\right)\in\mathbb{R}^{M\times M}$, $\boldsymbol{F}\in\mathbb{C}^{M\times|I|}$ has orthogonal columns and $\boldsymbol{D_\nu} = \operatorname{diag}\left([(2\pi\mathrm{i}\boldsymbol{k})^{\boldsymbol{\nu}}]_{\boldsymbol{k}\in I}\right)\in\mathbb{C}^{|I|\times|I|}$, we obtain $\sigma_1(\boldsymbol{B_\nu})\le\frac{\varepsilon^{|\boldsymbol{\nu}|}}{\boldsymbol{\nu}!}$, $\sigma_1(\boldsymbol{F}) = \sqrt{M}$ and $\sigma_1(\boldsymbol{D_\nu})\le(2\pi N)^{|\boldsymbol{\nu}|}$. Due to this fact and by applying the multinomial theorem

$$(\xi_1+\ldots+\xi_d)^r = \sum_{|\boldsymbol{\nu}|=r}\frac{r!}{\boldsymbol{\nu}!}\boldsymbol{\xi}^{\boldsymbol{\nu}},\qquad \boldsymbol{\xi}:=(\xi_1,\dots,\xi_d)^\top,$$

on $\sum_{|\boldsymbol{\nu}|=r}\frac{1^{|\boldsymbol{\nu}|}}{\boldsymbol{\nu}!} = \sum_{|\boldsymbol{\nu}|=r}\frac{(1,\dots,1)^{\boldsymbol{\nu}}}{\boldsymbol{\nu}!} = \frac{d^r}{r!}$, we infer

$$\begin{aligned}\sigma_1\left(\sum_{1\le|\boldsymbol{\nu}|\le m-1}\boldsymbol{B_\nu F D_\nu}\right) &\overset{(4.7)}{\le} \sum_{1\le|\boldsymbol{\nu}|\le m-1}\frac{(2\pi N\varepsilon)^{|\boldsymbol{\nu}|}}{\boldsymbol{\nu}!}\sqrt{M} = \sqrt{M}\sum_{r=1}^{m-1}(2\pi N\varepsilon)^r\sum_{|\boldsymbol{\nu}|=r}\frac{1^{|\boldsymbol{\nu}|}}{\boldsymbol{\nu}!}\\ &= \sqrt{M}\sum_{r=1}^{m-1}\frac{(2\pi dN\varepsilon)^r}{r!}\le\sqrt{M}\,(\mathrm{e}^{2\pi dN\varepsilon}-1).\end{aligned}$$

With (4.6), we obtain $\sigma_1(\boldsymbol{A}_{m-1})\le\sqrt{M}+\sqrt{M}\sum_{r=1}^{m-1}\frac{(2\pi dN\varepsilon)^r}{r!}\le\sqrt{M}\mathrm{e}^{2\pi dN\varepsilon}$.
Next, we estimate the smallest singular values $\sigma_{|I|}(\boldsymbol{A}_{m-1})$. Therefor, we use the well-known inequality for the singular values (cf. [18, Theorem 3.3.16]) for arbitrary matrices $\boldsymbol{E},\boldsymbol{G}\in\mathbb{C}^{r\times s}$,

$$\sigma_{p+q-1}(\boldsymbol{E}+\boldsymbol{G})\le\sigma_p(\boldsymbol{E})+\sigma_q(\boldsymbol{G})\quad\text{if}\quad p+q-1\le\min(r,s).$$

Setting $\boldsymbol{E}:=\boldsymbol{A}_{m-1}=\sum_{|\boldsymbol{\nu}|\le m-1}\boldsymbol{B_\nu F D_\nu}$, $\boldsymbol{G}:=-\sum_{1\le|\boldsymbol{\nu}|\le m-1}\boldsymbol{B_\nu F D_\nu}$, $p=|I|$ and $q=1$, this yields

$$\begin{aligned}\sigma_{|I|}(\boldsymbol{A}_{m-1}) &\ge \sigma_{|I|}(\boldsymbol{B_0 F D_0}) - \sigma_1\left(-\sum_{1\le|\boldsymbol{\nu}|\le m-1}\boldsymbol{B_\nu F D_\nu}\right)\\ &\ge \sqrt{M}-\sqrt{M}\sum_{r=1}^{m-1}\frac{(2\pi dN\varepsilon)^r}{r!}\ge\sqrt{M}\left(2-\mathrm{e}^{2\pi dN\varepsilon}\right).\end{aligned} \tag{4.8}$$

The condition $\varepsilon<\frac{\ln 2}{2\pi dN}$ guarantees $\sigma_1\left(\sum_{1\le|\boldsymbol{\nu}|\le m-1}\boldsymbol{B_\nu F D_\nu}\right)<\sqrt{M}$ for all $m>1$ and thus, we have $\sigma_{|I|}(\boldsymbol{A}_{m-1})>0$. Altogether, this yields the assertion. ∎

Similar statements can be found in [14, 10, 30] with the same maximal and minimal singular values. However, in these papers, the approximated Fourier coefficients $\hat{\tilde{\boldsymbol{p}}}$ are not the solution of the (unweighted) optimization problem (4.4) but of a weighted problem. Furthermore, they

assume that the so called mesh-norm of the sampling set $\{\boldsymbol{y}_\ell\}_{\ell=0}^{L-1}$ has the upper bound $\frac{\ln 2}{2\pi d N}$, while we assume in Theorem 4.2 that the perturbation parameter ε has this upper bound.

Based on the evaluation error of Algorithm 3 and based on the stability results from Theorem 4.2, we consider the error for the fast and approximate reconstruction of trigonometric polynomials $p \in \Pi_{I_N^{d,T,\boldsymbol{\gamma}}}$ by sampling at perturbed nodes $\boldsymbol{y}_j$, $j = 0, \ldots, M-1$, of a reconstructing rank-1 lattice $\Lambda(\boldsymbol{z}, M, I_N^{d,T,\boldsymbol{\gamma}})$. The following theorem states that we obtain a similar error bound as in Theorem 3.4 for the trigonometric polynomial p with the additional constant $C(d, T, \alpha, \beta, m)$ and the additional stability term $\frac{1}{2-\mathrm{e}^{2\pi\left(d^{1+\max\left(0,\frac{T}{1-T}\right)}\right)N\varepsilon}}$ in the aliasing error. The truncation error is now zero since we have a trigonometric polynomial with frequencies supported on the index set $I_N^{d,T,\boldsymbol{\gamma}}$. We will use Theorem 4.3 later to show an error bound for functions $f \in \mathcal{A}^{\alpha,\beta,\boldsymbol{\gamma}}(\mathbb{T}^d)$ in the proof of Theorem 5.1.

Theorem 4.3. *Let a weighted frequency index set $I_N^{d,T,\boldsymbol{\gamma}}$ and a trigonometric polynomial $p \in \Pi_{I_N^{d,T,\boldsymbol{\gamma}}}$, $p(\boldsymbol{x}) := \sum_{\boldsymbol{k}\in I_N^{d,T,\boldsymbol{\gamma}}} \hat{p}_{\boldsymbol{k}}\, \mathrm{e}^{2\pi\mathrm{i}\boldsymbol{k}\boldsymbol{x}}$, be given by its Fourier coefficients $\hat{p}_{\boldsymbol{k}} \in \mathbb{C}$, where $N \geq 1$, $T \in [-\infty, 1)$ and $\boldsymbol{\gamma} \in (0,1]^d$. Furthermore, let a parameter $m \in \mathbb{N}$, a reconstructing rank-1 lattice $\Lambda(\boldsymbol{z}, M, I_N^{d,T,\boldsymbol{\gamma}})$ and a set of sampling nodes $\mathcal{Y} = \{\boldsymbol{y}_j\}_{j=0}^{M-1}$ be given, where $\|\boldsymbol{y}_j - \boldsymbol{x}_j\|_\infty \leq \varepsilon$, $j = 0, \ldots, M-1$, for fixed perturbation parameter ε, $0 \leq \varepsilon < \left(2\pi\left(d^{1+\max\left(0,\frac{T}{1-T}\right)}\right)N\right)^{-1} \ln 2$. Then, the error of the approximation $\tilde{S}_{I_N^{d,T,\boldsymbol{\gamma}}} p(\boldsymbol{x}) = \sum_{\boldsymbol{k}\in I_N^{d,T,\boldsymbol{\gamma}}} \hat{\tilde{p}}_{\boldsymbol{k}} \mathrm{e}^{2\pi\mathrm{i}\boldsymbol{k}\boldsymbol{x}}$ of the trigonometric polynomial p with $\left(\hat{\tilde{p}}_{\boldsymbol{k}}\right)_{\boldsymbol{k}\in I_N^{d,T,\boldsymbol{\gamma}}} := \underset{\hat{\boldsymbol{g}}\in\mathbb{C}^{\left|I_N^{d,T,\boldsymbol{\gamma}}\right|}}{\arg\min} \|\boldsymbol{A}_{m-1}\,\hat{\boldsymbol{g}} - \boldsymbol{p}\|_2$ and $\boldsymbol{p} := p(\boldsymbol{y}_j)_{j=0}^{M-1}$ is bounded by*

$$\|p - \tilde{S}_{I_N^{d,T,\boldsymbol{\gamma}}} p | L^2(\mathbb{T}^d)\| \quad \leq \quad \frac{C(d,T,\alpha,\beta,m)}{2-\mathrm{e}^{2\pi\left(d^{1+\max\left(0,\frac{T}{1-T}\right)}\right)N\varepsilon}}\, N^{-(\alpha+\beta)} \sum_{\boldsymbol{k}\in I_N^{d,T,\boldsymbol{\gamma}}} \omega^{\alpha,\beta,\boldsymbol{\gamma}}(\boldsymbol{k})\, |\hat{p}_{\boldsymbol{k}}|,$$

where the constant $C(d,T,\alpha,\beta,m) := d^{\frac{\min(0,Tm)-\alpha-T\beta}{1-T}} \frac{(\ln 2)^m}{m!}$ and the parameters $\alpha, \beta \in \mathbb{R}$, $\beta \geq 0$, $0 < \alpha + \beta \leq m$.

Proof. By Parseval's identity, we have $\|p - \tilde{S}_{I_N^{d,T,\boldsymbol{\gamma}}} p | L^2(\mathbb{T}^d)\| = \left\|(\hat{p}_{\boldsymbol{k}} - \hat{\tilde{p}}_{\boldsymbol{k}})_{\boldsymbol{k}\in I_N^{d,T,\boldsymbol{\gamma}}}\right\|_2$. Based on the normal equation $\boldsymbol{A}_{m-1}^{\mathrm{H}} \boldsymbol{A}_{m-1} \left(\hat{\tilde{p}}_{\boldsymbol{k}}\right)_{\boldsymbol{k}\in I_N^{d,T,\boldsymbol{\gamma}}} = \boldsymbol{A}_{m-1}^{\mathrm{H}} \boldsymbol{p}$, we obtain

$$\boldsymbol{A}_{m-1}^{\mathrm{H}} \boldsymbol{A}_{m-1} \left(\hat{\tilde{p}}_{\boldsymbol{k}} - \hat{p}_{\boldsymbol{k}}\right)_{\boldsymbol{k}\in I_N^{d,T,\boldsymbol{\gamma}}} = \boldsymbol{A}_{m-1}^{\mathrm{H}} \left(\boldsymbol{p} - \boldsymbol{A}_{m-1} \left(\hat{p}_{\boldsymbol{k}}\right)_{\boldsymbol{k}\in I_N^{d,T,\boldsymbol{\gamma}}}\right).$$

Since we have (2.10) by Lemma 2.3 and $\varepsilon < \left(2\pi\left(d^{1+\max\left(0,\frac{T}{1-T}\right)}\right)N\right)^{-1} \ln 2$, the smallest singular value $\sigma_{|I|}\left(\boldsymbol{A}_{m-1}^{\mathrm{H}} \boldsymbol{A}_{m-1}\right) = \sigma_{|I|}\left(\boldsymbol{A}_{m-1}\right)^2 > 0$ by (4.8) in the proof of Theorem 4.2 Consequently, the matrix $\boldsymbol{A}_{m-1}^{\mathrm{H}} \boldsymbol{A}_{m-1}$ is invertible. Therefore, we obtain

$$\left(\hat{\tilde{p}}_{\boldsymbol{k}} - \hat{p}_{\boldsymbol{k}}\right)_{\boldsymbol{k}\in I_N^{d,T,\boldsymbol{\gamma}}} = \left(\boldsymbol{A}_{m-1}^{\mathrm{H}} \boldsymbol{A}_{m-1}\right)^{-1} \boldsymbol{A}_{m-1}^{\mathrm{H}} \left(\boldsymbol{p} - \boldsymbol{A}_{m-1} \left(\hat{p}_{\boldsymbol{k}}\right)_{\boldsymbol{k}\in I_N^{d,T,\boldsymbol{\gamma}}}\right).$$

This yields the estimate

$$\left\|(\hat{p}_{\boldsymbol{k}} - \hat{\tilde{p}}_{\boldsymbol{k}})_{\boldsymbol{k}\in I_N^{d,T,\boldsymbol{\gamma}}}\right\|_2 \leq \left\|(\boldsymbol{A}_{m-1}^{\mathrm{H}} \boldsymbol{A}_{m-1})^{-1} \boldsymbol{A}_{m-1}^{\mathrm{H}}\right\|_2 \left\|\boldsymbol{p} - \boldsymbol{A}_{m-1} \left(\hat{p}_{\boldsymbol{k}}\right)_{\boldsymbol{k}\in I_N^{d,T,\boldsymbol{\gamma}}}\right\|_2. \tag{4.9}$$

According to [3, Subsection 1.4.3], we have $\left\|(\boldsymbol{A}_{m-1}^{\mathrm{H}}\boldsymbol{A}_{m-1})^{-1}\boldsymbol{A}_{m-1}^{\mathrm{H}}\right\|_2 = \frac{1}{\sigma_{|I_N^{d,T,\boldsymbol{\gamma}}|}(\boldsymbol{A}_{m-1})}$. Thus, we obtain $\left\|(\boldsymbol{A}_{m-1}^{\mathrm{H}}\boldsymbol{A}_{m-1})^{-1}\boldsymbol{A}_{m-1}^{\mathrm{H}}\right\|_2 \leq \frac{1}{\sqrt{M}\left(2-\mathrm{e}^{2\pi\left(d^{1+\max\left(0,\frac{T}{1-T}\right)}\right)N\varepsilon}\right)}$ by (4.8) in the proof of Theorem 4.2. Furthermore, we have $\left\|\boldsymbol{p}-\boldsymbol{A}_{m-1}\left(\hat{p}_{\boldsymbol{k}}\right)_{\boldsymbol{k}\in I_N^{d,T,\boldsymbol{\gamma}}}\right\|_2 \leq \sqrt{M}\ \left\|\boldsymbol{p}-\boldsymbol{A}_{m-1}\left(\hat{p}_{\boldsymbol{k}}\right)_{\boldsymbol{k}\in I_N^{d,T,\boldsymbol{\gamma}}}\right\|_\infty = \sqrt{M}\left\|\left(R_m(\boldsymbol{y}_j)\right)_{j=0}^{M-1}\right\|_\infty$, where R_m is the remainder from Theorem 4.1. We apply Theorem 4.1 and infer

$$\begin{aligned}\left\|\left(R_m(\boldsymbol{y}_j)\right)_{j=0}^{M-1}\right\|_\infty &\leq \frac{(2\pi)^m}{m!}\, d^{\frac{m-\alpha-T\beta}{1-T}}\varepsilon^m\, N^{m-\alpha-\beta}\sum_{\boldsymbol{k}\in I_N^{d,T,\boldsymbol{\gamma}}}|\hat{p}_{\boldsymbol{k}}|\,\omega^{\alpha,\beta,\boldsymbol{\gamma}}(\boldsymbol{k})\\ &\leq \frac{(\ln 2)^m}{m!}\,\underbrace{d^{\frac{m-\alpha-T\beta}{1-T}}\left(d^{1+\max\left(0,\frac{T}{1-T}\right)}\right)^{-m}}_{=d^{\frac{\min(0,Tm)-\alpha-T\beta}{1-T}}}N^{-\alpha-\beta}\sum_{\boldsymbol{k}\in I_N^{d,T,\boldsymbol{\gamma}}}|\hat{p}_{\boldsymbol{k}}|\,\omega^{\alpha,\beta,\boldsymbol{\gamma}}(\boldsymbol{k}).\end{aligned}$$

Altogether, this yields the assertion. ∎

5 Approximate reconstruction of multivariate periodic functions by sampling at perturbed rank-1 lattice nodes

In Section 4.3, we have dealt with the fast and stable approximate reconstruction of trigonometric polynomials by sampling at perturbed nodes $\boldsymbol{y}_j$, $j=0,\ldots,M-1$, of a reconstructing rank-1 lattice $\Lambda(\boldsymbol{z},M,I_N^{d,T,\boldsymbol{\gamma}})$. Based on these results and the results from Section 3, we consider the approximate reconstruction of functions $f\in\mathcal{C}(\mathbb{T}^d)\cap\mathcal{A}^{\alpha,\beta,\boldsymbol{\gamma}}(\mathbb{T}^d)$ by sampling at perturbed rank-1 lattice nodes $\boldsymbol{y}_j$, $j=0,\ldots,M-1$. We compute the approximated Fourier coefficients

$$\hat{\hat{\boldsymbol{f}}} := \operatorname*{arg\,min}_{\hat{\boldsymbol{g}}\in\mathbb{C}^{\left|I_N^{d,T,\boldsymbol{\gamma}}\right|}}\|\boldsymbol{A}_{m-1}\,\hat{\boldsymbol{g}}-\boldsymbol{f}\|_2 \tag{5.1}$$

by solving the normal equation $\boldsymbol{A}_{m-1}^{\mathrm{H}}\boldsymbol{A}_{m-1}\hat{\hat{\boldsymbol{f}}} = \boldsymbol{A}_{m-1}^{\mathrm{H}}\boldsymbol{f}$, where $\hat{\hat{\boldsymbol{f}}} := \left(\hat{\hat{f}}_{\boldsymbol{k}}\right)_{\boldsymbol{k}\in I_N^{d,T,\boldsymbol{\gamma}}}$ and $\boldsymbol{f} := f(\boldsymbol{y}_j)_{j=0}^{M-1}$. Using the LSQR algorithm [3] in combination with Algorithm 3 and its adjoint version, we obtain an approximation $\hat{\hat{\boldsymbol{h}}}$ of the approximated Fourier coefficients $\hat{\hat{\boldsymbol{f}}}$ in $\mathcal{O}\left(K\ m^d(M\log M+d|I|)\right)$ arithmetic operations, where K is the maximal number of iterations of the LSQR algorithm. Choosing $K=\left\lceil\frac{\log(2\,\kappa(\boldsymbol{A}_{m-1}))-\log\delta}{\log(\kappa(\boldsymbol{A}_{m-1})+1)-\log(\kappa(\boldsymbol{A}_{m-1})-1)}\right\rceil$ guarantees a relative error $\frac{\|\hat{\hat{\boldsymbol{f}}}-\hat{\hat{\boldsymbol{h}}}\|_2}{\|\hat{\hat{\boldsymbol{f}}}\|_2}\leq\delta$, cf. [3, Sec. 7.4.4], where $\kappa(\boldsymbol{A}_{m-1})$ denotes the condition number of the approximated Fourier matrix $\boldsymbol{A}_{m-1}$. If this condition number is unknown, we may use an upper bound of $\kappa(\boldsymbol{A}_{m-1})$, for instance the upper bound from Theorem 4.2. We stress the fact that the LSQR algorithm [3] in combination with Algorithm 3 and its adjoint version indicates a fast reconstruction algorithm for moderate dimensionality d and moderate Taylor expansion degree m.

The following theorem states that we obtain the same error bound as in Theorem 3.4 up to the additional constant $C(d,T,m)$ and the additional stability term $\frac{1}{2-\mathrm{e}^{2\pi\left(d^{1+\max\left(0,\frac{T}{1-T}\right)}\right)N\varepsilon}}$ in the aliasing error.

Theorem 5.1. *Let $r, t, \alpha, \beta \geq 0$, $\beta \geq t \geq 0$, $\alpha + \beta > r + t$, $T \in [-\frac{r}{t}, 1)$ with $-\frac{r}{t} := -\infty$ for $t = 0$, a weighted frequency index set $I_N^{d,T,\boldsymbol{\gamma}}$ and a reconstructing rank-1 lattice $\Lambda(\boldsymbol{z}, M, I_N^{d,T,\boldsymbol{\gamma}})$ be given, where $N \geq 1$, $0 < \alpha+\beta \leq m \in \mathbb{N}$, and $\boldsymbol{\gamma} \in (0,1]^d$. Furthermore, let a set of sampling nodes $\mathcal{Y} = \{\boldsymbol{y}_j\}_{j=0}^{M-1}$ be given, where $\|\boldsymbol{y}_j - \boldsymbol{x}_j\|_\infty \leq \varepsilon$, $j = 0, \ldots, M-1$, for fixed perturbation parameter ε, $0 \leq \varepsilon < \left(2\pi\left(d^{1+\max\left(0,\frac{T}{1-T}\right)}\right)N\right)^{-1} \ln 2$. Then, the error of the approximation $\tilde{S}_{I_N^{d,T,\boldsymbol{\gamma}}} f(\boldsymbol{x}) = \sum_{\boldsymbol{k} \in I_N^{d,T,\boldsymbol{\gamma}}} \hat{\tilde{f}}_{\boldsymbol{k}} \, \mathrm{e}^{2\pi \mathrm{i} \boldsymbol{k}\boldsymbol{x}}$ of a function $f \in \mathcal{C}(\mathbb{T}^d) \cap \mathcal{A}^{\alpha,\beta,\boldsymbol{\gamma}}(\mathbb{T}^d)$ with $\left(\hat{\tilde{f}}_{\boldsymbol{k}}\right)_{\boldsymbol{k} \in I_N^{d,T,\boldsymbol{\gamma}}}$ from (5.1) is bounded by*

$$\begin{aligned}
&\|f - \tilde{S}_{I_N^{d,T,\boldsymbol{\gamma}}} f | \mathcal{H}^{r,t,\boldsymbol{\gamma}}(\mathbb{T}^d)\| \leq N^{-(\alpha-r+\beta-t)} \\
&\cdot \left(\|f|\mathcal{H}^{\alpha,\beta,\boldsymbol{\gamma}}(\mathbb{T}^d)\| \begin{cases} \left(N^{d-1} \prod_{s=1}^{d} \gamma_s^{-1}\right)^{\frac{T(\beta-t)+\alpha-r}{d-T}} & \text{for } T > -\frac{\alpha-r}{\beta-t} \\ d^{-\frac{T(\beta-t)+\alpha-r}{1-T}} & \text{for } T \leq -\frac{\alpha-r}{\beta-t} \end{cases} \right. \\
&\left. + \frac{C(d,T,m)}{2 - \mathrm{e}^{2\pi\left(d^{1+\max\left(0,\frac{T}{1-T}\right)}\right)N\varepsilon}} \, \|f|\mathcal{A}^{\alpha,\beta,\boldsymbol{\gamma}}(\mathbb{T}^d)\| \begin{cases} d^{\frac{Tt+r}{1-T}} \left(N^{d-1} \prod_{s=1}^{d} \gamma_s^{-1}\right)^{\frac{T\beta+\alpha}{d-T}} & \text{for } T > -\frac{\alpha}{\beta} \\ d^{-\frac{T(\beta-t)+\alpha-r}{1-T}} & \text{for } T \leq -\frac{\alpha}{\beta} \end{cases} \right),
\end{aligned} \tag{5.2}$$

where $C(d,T,M) := 1 + \frac{\left(d^{\frac{T}{1-T}} \ln 2\right)^m}{m!}$.

Proof. We apply the triangle inequality on $\|f - \tilde{S}_{I_N^{d,T,\boldsymbol{\gamma}}} f | \mathcal{H}^{r,t,\boldsymbol{\gamma}}(\mathbb{T}^d)\|$ and estimate the truncation error $\|f - S_{I_N^{d,T,\boldsymbol{\gamma}}} f | \mathcal{H}^{r,t,\boldsymbol{\gamma}}(\mathbb{T}^d)\|$ as in the proof of Theorem 3.4.
Next, we estimate the aliasing error $\|S_{I_N^{d,T,\boldsymbol{\gamma}}} f - \tilde{S}_{I_N^{d,T,\boldsymbol{\gamma}}} f | \mathcal{H}^{r,t,\boldsymbol{\gamma}}(\mathbb{T}^d)\|$. Based on the normal equation $\boldsymbol{A}_{m-1}^{\mathrm{H}} \boldsymbol{A}_{m-1} \hat{\tilde{\boldsymbol{f}}} = \boldsymbol{A}_{m-1}^{\mathrm{H}} \boldsymbol{f}$, we calculate

$$\boldsymbol{D}\left(\hat{\tilde{f}}_{\boldsymbol{k}} - \hat{f}_{\boldsymbol{k}}\right)_{\boldsymbol{k} \in I_N^{d,T,\boldsymbol{\gamma}}} = \boldsymbol{D}\left(\boldsymbol{A}_{m-1}^{\mathrm{H}} \boldsymbol{A}_{m-1}\right)^{-1} \boldsymbol{A}_{m-1}^{\mathrm{H}} \left(\boldsymbol{f} - \boldsymbol{A}_{m-1}\left(\hat{f}_{\boldsymbol{k}}\right)_{\boldsymbol{k} \in I_N^{d,T,\boldsymbol{\gamma}}}\right)$$

where $\boldsymbol{D} := \operatorname{diag}\left(\omega^{r,t,\boldsymbol{\gamma}}(\boldsymbol{k})\right)_{\boldsymbol{k} \in I_N^{d,T,\boldsymbol{\gamma}}}$, Consequently, we obtain

$$\begin{aligned}
&\left\| S_{I_N^{d,T,\boldsymbol{\gamma}}} f - \tilde{S}_{I_N^{d,T,\boldsymbol{\gamma}}} f | \mathcal{H}^{r,t,\boldsymbol{\gamma}}(\mathbb{T}^d) \right\| = \left\| \boldsymbol{D}\left(\hat{\tilde{f}}_{\boldsymbol{k}} - \hat{f}_{\boldsymbol{k}}\right)_{\boldsymbol{k} \in I_N^{d,T,\boldsymbol{\gamma}}} \right\|_2 \\
\leq \; & \|\boldsymbol{D}\|_2 \left\| (\boldsymbol{A}_{m-1}^{\mathrm{H}} \boldsymbol{A}_{m-1})^{-1} \boldsymbol{A}_{m-1}^{\mathrm{H}} \right\|_2 \left\| \boldsymbol{f} - \boldsymbol{A}_{m-1}\left(\hat{f}_{\boldsymbol{k}}\right)_{\boldsymbol{k} \in I_N^{d,T,\boldsymbol{\gamma}}} \right\|_2
\end{aligned}$$

and we proceed as in the proof of Theorem 4.3 for $\left\|(\boldsymbol{A}_{m-1}^{\mathrm{H}} \boldsymbol{A}_{m-1})^{-1} \boldsymbol{A}_{m-1}^{\mathrm{H}}\right\|_2$. We infer

$$\begin{aligned}
&\left\| \boldsymbol{f} - \boldsymbol{A}_{m-1}\left(\hat{f}_{\boldsymbol{k}}\right)_{\boldsymbol{k} \in I_N^{d,T,\boldsymbol{\gamma}}} \right\|_2 \leq \sqrt{M} \left\| \boldsymbol{f} - \boldsymbol{A}_{m-1}\left(\hat{f}_{\boldsymbol{k}}\right)_{\boldsymbol{k} \in I_N^{d,T,\boldsymbol{\gamma}}} \right\|_\infty \\
\leq \; & \sqrt{M} \left(\left\| \boldsymbol{f} - \boldsymbol{A}\left(\hat{f}_{\boldsymbol{k}}\right)_{\boldsymbol{k} \in I_N^{d,T,\boldsymbol{\gamma}}} \right\|_\infty + \left\| (\boldsymbol{A} - \boldsymbol{A}_{m-1})\left(\hat{f}_{\boldsymbol{k}}\right)_{\boldsymbol{k} \in I_N^{d,T,\boldsymbol{\gamma}}} \right\|_\infty \right) \\
= \; & \sqrt{M} \left(\left\| \left(\sum_{\boldsymbol{k} \in \mathbb{Z}^d \setminus I_N^{d,T,\boldsymbol{\gamma}}} \hat{f}_{\boldsymbol{k}} \, \mathrm{e}^{2\pi \mathrm{i} \boldsymbol{k} \boldsymbol{y}_j} \right)_{j=0}^{M-1} \right\|_\infty + \left\| \left(R_m(\boldsymbol{y}_j)\right)_{j=0}^{M-1} \right\|_\infty \right),
\end{aligned} \tag{5.3}$$

where $R_m(\boldsymbol{y}_j) = \sum_{\boldsymbol{k}\in I_N^{d,T,\boldsymbol{\gamma}}} \hat{f}_{\boldsymbol{k}}\ \mathrm{e}^{2\pi\mathrm{i}\boldsymbol{k}\boldsymbol{y}_j} - \sum_{|\boldsymbol{\nu}|=0}^{m-1} \frac{D^{\boldsymbol{\nu}}\left(\sum_{\boldsymbol{k}\in I_N^{d,T,\boldsymbol{\gamma}}} \hat{f}_{\boldsymbol{k}}\ \mathrm{e}^{2\pi\mathrm{i}\boldsymbol{k}\boldsymbol{x}_j}\right)}{\boldsymbol{\nu}!}(\boldsymbol{y}-\boldsymbol{x}_{j'})^{\boldsymbol{\nu}}$. Now, we apply inequality (3.6) from the proof of Theorem 3.3 on the first summand and Theorem 4.1 on the second summand in (5.3). Last, we obtain $\|\boldsymbol{D}\|_2 = \max_{\boldsymbol{k}\in I_N^{d,T,\boldsymbol{\gamma}}} \left\{\omega^{r,t,\boldsymbol{\gamma}}(\boldsymbol{k})\right\} \leq d^{(r+Tt)/(1-T)} N^{r+t}$ due to (3.10) in the proof of Theorem 3.4. Altogether, this yields the assertion. ∎

As in Section 3.2, we may use the inequality (2.7) in order to obtain the statement of Theorem 5.1 with the $\mathcal{H}^{\alpha,\beta+\lambda,\boldsymbol{\gamma}}(\mathbb{T}^d)$ norm on the right hand side for functions $f \in \mathcal{C}(\mathbb{T}^d) \cap \mathcal{H}^{\alpha,\beta+\lambda,\boldsymbol{\gamma}}(\mathbb{T}^d)$, $\lambda > 1/2$.

6 Numerical tests

In the following, we verify the theoretical results from Section 3 and Section 5 in numerical tests. All numerical algorithms were implemented in MATLAB and all numerical tests were run in MATLAB using double precision arithmetic on a computer with an Intel Xeon X5690 3.47GHz CPU and 144 GB RAM.

Similar to [12], we define the functions $g_{3,4}(x) := n_{3,4}(4 + \operatorname{sgn}(x-1/2)\sin(2\pi x)^3 + \operatorname{sgn}(x-1/2)\sin(2\pi x)^4)$, where $n_{3,4}$ denotes a normalization factor such that $\|g_{3,4}|L^2(\mathbb{T})\| = 1$ and sgn denotes the signum function, $\operatorname{sgn}(x) := \frac{x}{|x|}$ for $x \neq 0$ and $\operatorname{sgn}(0) := 0$. In our numerical tests, we consider the tensor product function $G_{3,4}^d\colon \mathbb{T}^d \to \mathbb{C}$, defined by $G_{3,4}^d(\boldsymbol{x}) := \prod_{s=1}^d g_{3,4}(x_s)$, The Fourier coefficients of the function $g_{3,4}^d$ are given by

$$(\widehat{g_{3,4}})_k = n_{3,4} \begin{cases} \frac{-12}{(k-3)(k-1)(k+1)(k+3)\pi} & \text{for } k \in 2\mathbb{Z}\setminus\{0\}, \\ \frac{48\mathrm{i}}{(k-4)(k-2)k(k+2)(k+4)\pi} & \text{for } k \text{ odd}, \\ 4 - \frac{4}{3\pi} & \text{for } k = 0, \end{cases}$$

and $(\widehat{G_{3,4}})_{\boldsymbol{k}} \neq 0$ for all $\boldsymbol{k} \in \mathbb{Z}^d$ follows. Note, that we have $\|G_{3,4}^d|L^2(\mathbb{T}^d)\| = 1$ and $G_{3,4}^d \in \mathcal{H}^{0,\frac{7}{2}-\epsilon,\mathbf{1}}(\mathbb{T}^d)$ for $\epsilon > 0$. Furthermore, as in [12], we define the functions $g_p\colon \mathbb{T} \to \mathbb{C}$ by $g_p(x) := n_p(2 + \operatorname{sgn}(x-1/2)\sin(2\pi x)^p)$, $p \in \mathbb{N}$, where n_p denotes a normalization factor such that $\|g_p|L^2(\mathbb{T})\| = 1$. Based on these univariate functions g_p, we define the tensor-product functions $G_p^d\colon \mathbb{T}^d \to \mathbb{R}$ by $G_p^d(\boldsymbol{x}) := \prod_{s=1}^d g_p(x_s)$. Note, that we have $\|G_p^d|L^2(\mathbb{T}^d)\| = 1$ and $G_p^d \in \mathcal{H}^{0,\frac{1}{2}+p-\epsilon,\mathbf{1}}(\mathbb{T}^d)$ for $\epsilon > 0$, cf. [12]. In our numerical tests, we consider the case $p = 3$. The function g_3 has the Fourier coefficients

$$(\widehat{g_3})_k = n_3 \begin{cases} \frac{-12}{(k-3)(k-1)(k+1)(k+3)\pi} & \text{for } k \in 2\mathbb{Z}\setminus\{0\}, \\ 0 & \text{for } k \text{ odd}, \\ 2 - \frac{4}{3\pi} & \text{for } k = 0. \end{cases}$$

This means that only the Fourier coefficients $(\widehat{G_3^d})_{\boldsymbol{k}}$, $\boldsymbol{k} \in (2\mathbb{Z})^d$, of the tensor-product function G_3^d are non-zero. We exploit this property in our numerical tests and use weighted frequency index sets with "holes", $I_{N,\text{even}}^{d,T,\boldsymbol{\gamma}} := I_N^{d,T,\boldsymbol{\gamma}} \cap (2\mathbb{Z})^d$. Furthermore, we denote the approximated Fourier coefficients of a function $f \in \{G_{3,4}^d, G_3^d\}$ by $(\hat{\tilde{f}})_{\boldsymbol{k}}$, $\boldsymbol{k} \in I_N^{d,T,\boldsymbol{\gamma}}$.

We generate reconstructing rank-1 lattices for the weighted frequency index sets $I_N^{d,T,\boldsymbol{\gamma}}$ as well as for the weighted frequency index sets with "holes" $I_{N,\text{even}}^{d,T,\boldsymbol{\gamma}}$ using the component-by-component approach, see Section 2.3. In order to make the numerical results reproducible, which are presented in this section, the refinements N and cardinalities of the frequency index sets $I_N^{d,T,\boldsymbol{\gamma}}$ as well as the generating vector $\boldsymbol{z}$ and rank-1 lattice size M of the reconstructing rank-1 lattices $\Lambda(\boldsymbol{z}, M, I_N^{d,T,\boldsymbol{\gamma}})$ used in the examples can be found in Table 6.2, ..., 6.7. The tables of the cardinalities and the reconstructing rank-1 lattices have the form as demonstrated in Table 6.1. Table 6.1a shows the cardinalities of the index sets $I_N^{d,T,\boldsymbol{\gamma}}$ for the dimensions $d = 1, 2, 3$ and Table 6.1b shows the used reconstructing rank-1 lattices $\Lambda(\boldsymbol{z}, M, I_N^{d,T,\boldsymbol{\gamma}})$ for the dimensions $d = 1, 2, 3$. We obtain the parameters for the generating vector $\boldsymbol{z} \in \mathbb{Z}^d$ and the lattice size M of $\Lambda\left(\boldsymbol{z} = (z_1, \ldots, z_d)^\top, M = z_{d+1}, I_N^{d,T,\boldsymbol{\gamma}}\right)$, for $d = 1, 2, 3$ as follows, $\Lambda\big(z = z_1, M = z_2, I_N^{1,T,\boldsymbol{\gamma}}\big)$ in the one-dimensional case, $\Lambda\big(\boldsymbol{z} = (z_1, z_2)^\top, M = z_3, I_N^{2,T,\boldsymbol{\gamma}}\big)$ in the two-dimensional case, and $\Lambda\big(\boldsymbol{z} = (z_1, z_2, z_3)^\top, M = z_4, I_N^{3,T,\boldsymbol{\gamma}}\big)$ in the case $d = 3$. The entry "-" for $d = 5$ means that we did not compute z_5. For instance, to obtain the parameters $\boldsymbol{z}$ and M for the weighted frequency index set $I_{64}^{3,0,\mathbf{1}}$, we have to use the entries in the column $N = 64$ of Table 6.2b and find the parameter for the reconstructing rank-1 lattice $\boldsymbol{z} = (1, 129, 8451)^\top$ and $M = 47463$ in the case $d = 3$.

	N
d=1	$\lvert I_N^{1,T,\boldsymbol{\gamma}}\rvert$
d=2	$\lvert I_N^{2,T,\boldsymbol{\gamma}}\rvert$
d=3	$\lvert I_N^{3,T,\boldsymbol{\gamma}}\rvert$
d=4	-

(a) Cardinalities $|I_N^{d,T,\boldsymbol{\gamma}}|$.

	N
d=1	z_1
d=2	z_2
d=3	z_3
d=4	z_4
d=5	-

(b) Components z_d.

Table 6.1: Example for cardinalities of index sets $I_N^{d,T,\boldsymbol{\gamma}}$ and parameters for reconstructing rank-1 lattices $\Lambda\left(\boldsymbol{z} = (z_1, \ldots, z_d)^\top, M = z_{d+1}, I_N^{d,T,\boldsymbol{\gamma}}\right)$.

Example 6.1. In this example, we verify the theoretical results from Theorem 3.4 in Section 3.2 for $r = 0$, $t = 0$. We use the weighted frequency index sets $I_N^{d,0,\mathbf{1}}$ and reconstructing rank-1 lattices $\Lambda(\boldsymbol{z}, M, I_N^{d,0,\mathbf{1}})$ as well as $I_N^{d,0,\mathbf{0.5}}$ and $\Lambda(\boldsymbol{z}, M, I_N^{d,0,\mathbf{0.5}})$ as shown in Table 6.2 and 6.3, respectively. Based on these index sets and reconstructing rank-1 lattices, we compute the approximated Fourier coefficients $\hat{\tilde{f}}_{\boldsymbol{k}}$ by applying the lattice rule (3.2) and Algorithm 2. We compute the relative $L^2(\mathbb{T}^d) = \mathcal{H}^{0,0,\boldsymbol{\gamma}}(\mathbb{T}^d)$ error, i.e., $\|f - \tilde{S}_{I_N^{d,T,\boldsymbol{\gamma}}} f | L^2(\mathbb{T}^d)\| / \|f | L^2(\mathbb{T}^d)\|$, where

$$\begin{aligned}\|f - \tilde{S}_{I_N^{d,T,\boldsymbol{\gamma}}} f | L^2(\mathbb{T}^d)\| &= \big(\|f - S_{I_N^{d,T,\boldsymbol{\gamma}}} f | L^2(\mathbb{T}^d)\|^2 \qquad + \|S_{I_N^{d,T,\boldsymbol{\gamma}}} f - \tilde{S}_{I_N^{d,T,\boldsymbol{\gamma}}} f | L^2(\mathbb{T}^d)\|^2\big)^{\frac{1}{2}} \\ &= \left(\|f | L^2(\mathbb{T}^d)\|^2 - \sum_{\boldsymbol{k} \in I_N^{d,T,\boldsymbol{\gamma}}} |\hat{f}_{\boldsymbol{k}}|^2 \;+ \sum_{\boldsymbol{k} \in I_N^{d,T,\boldsymbol{\gamma}}} \left|\hat{f}_{\boldsymbol{k}} - \hat{\tilde{f}}_{\boldsymbol{k}}\right|^2\right)^{\frac{1}{2}}.\end{aligned}$$

The relative $L^2(\mathbb{T}^d)$ error corresponds to the error estimate in Theorem 3.4 with $r = t = 0$ and inequality (2.7) up to the "constant" $\|f | L^2(\mathbb{T}^d)\| / \|f | \mathcal{H}^{\alpha,\beta+\lambda,\boldsymbol{\gamma}}(\mathbb{T}^d)\| \leq 1$ since

$$\frac{\|f - \tilde{S}_{I_N^{d,T,\boldsymbol{\gamma}}} f | \mathcal{H}^{0,0,\boldsymbol{\gamma}}(\mathbb{T}^d)\|}{\|f | \mathcal{H}^{\alpha,\beta+\lambda,\boldsymbol{\gamma}}(\mathbb{T}^d)\|} = \frac{\|f | L^2(\mathbb{T}^d)\|}{\|f | \mathcal{H}^{\alpha,\beta+\lambda,\boldsymbol{\gamma}}(\mathbb{T}^d)\|} \frac{\|f - \tilde{S}_{I_N^{d,T,\boldsymbol{\gamma}}} f | L^2(\mathbb{T}^d)\|}{\|f | L^2(\mathbb{T}^d)\|}.$$

	N=1	N=2	N=4	N=8	N=16	N=32	N=64	N=128	N=256
d=1	3	5	9	17	33	65	129	257	513
d=2	9	21	49	113	265	605	1377	3093	6889
d=3	27	81	225	593	1577	4021	10113	24869	60217
d=4	81	297	945	2769	8113	22665	61889	164137	426193
d=5	243	1053	3753	12033	38193	115385	338305	958345	2644977
d=6	729	3645	14337	49761	169209	547461	1709857	5137789	14977209
d=7	2187	12393	53217	198369	716985	2465613	-	-	-
d=8	6561	41553	193185	768609	2935521	10665297	-	-	-
d=9	19683	137781	688905	2910897	11693889	-	-	-	-
d=10	59049	452709	2421009	10819089	45548649	-	-	-	-

(a) Cardinalities $|I_N^{d,0,\mathbf{1}}|$ of the unweighted symmetric hyperbolic cross index sets $I_N^{d,0,\mathbf{1}}$.

	N=1	N=2	N=4	N=8	N=16	N=32	N=64	N=128	N=256
d=1	1	1	1	1	1	1	1	1	1
d=2	3	5	9	17	33	65	129	257	513
d=3	9	23	58	163	579	2179	8451	33283	132099
d=4	27	105	343	1035	3628	11525	47463	176603	753249
d=5	81	479	1911	5727	21944	106703	475829	2244100	10561497
d=6	243	2185	10579	33769	169230	785309	3752318	20645268	136178715
d=7	729	9967	57897	191808	1105193	6897012	31829977	192757285	1400567254
d=8	2187	45465	258113	1059754	7798320	57114640	-	-	-
d=9	6561	207391	1259193	6027975	49768670	359896131	-	-	-
d=10	19683	946025	6898038	34112281	320144128	-	-	-	-
d=11	59049	4315343	30780958	194144634	2040484044	-	-	-	-

(b) z_d for reconstructing rank-1 lattices $\Lambda\left(\boldsymbol{z} = (z_1, \ldots, z_d)^\top, M = z_{d+1}, I_N^{d,0,\mathbf{1}}\right)$

Table 6.2: Cardinalities of index sets $I_N^{d,0,\mathbf{1}}$ and parameters for reconstructing rank-1 lattices $\Lambda(\boldsymbol{z}, M, I_N^{d,0,\mathbf{1}})$.

	N=1	N=2	N=4	N=8	N=16	N=32	N=64	N=128	N=256	N=512	N=1024
d=1	1	3	5	9	17	33	65	129	257	513	1025
d=2	1	5	13	29	65	145	329	733	1633	3605	7913
d=3	1	7	25	69	177	441	1097	2693	6529	15645	37025
d=4	1	9	41	137	401	1105	2977	7897	20609	52953	133905
d=5	1	11	61	241	801	2433	7073	20073	55873	152713	409825
d=6	1	13	85	389	1457	4865	15241	46069	135905	392717	1112313
d=7	1	15	113	589	2465	9017	30409	97709	304321	925445	-
d=8	1	17	145	849	3937	15713	56961	194353	637697	2034289	-
d=9	1	19	181	1177	6001	26017	101185	366289	1264513	-	-
d=10	1	21	221	1581	8801	41265	171785	659085	2391905	-	-

(a) Cardinalities $|I_N^{d,0,\mathbf{0.5}}|$ of the weighted symmetric hyperbolic cross index sets $I_N^{d,0,\mathbf{0.5}}$.

	N=1	N=2	N=4	N=8	N=16	N=32	N=64	N=128	N=256	N=512	N=1024
d=1	1	1	1	1	1	1	1	1	1	1	1
d=2	1	3	5	9	17	33	65	129	257	513	1025
d=3	1	5	13	41	145	545	2113	8321	33025	131585	525313
d=4	1	7	29	97	395	1721	5161	19788	85405	320439	1360024
d=5	1	9	49	256	1213	5815	21470	103574	463960	2422591	12274882
d=6	1	11	81	622	3062	14253	72480	346839	2178507	12286748	69234604
d=7	1	13	137	1099	6602	34117	210949	1149685	8777570	51872176	291720830
d=8	1	15	183	2063	14199	80618	523075	3640873	25496942	173740333	-
d=9	1	17	255	3470	29296	176901	1327778	10334139	88445611	586307589	-
d=10	1	19	329	5367	47863	368727	2908252	24955987	236924069	-	-
d=11	1	21	399	7935	94689	797020	7023723	66455212	557584823	-	-

(b) z_d for reconstructing rank-1 lattices $\Lambda\left(\boldsymbol{z} = (z_1, \ldots, z_d)^\top, M = z_{d+1}, I_N^{d,0,\mathbf{0.5}}\right)$.

Table 6.3: Cardinalities of index sets $I_N^{d,0,\mathbf{0.5}}$ and parameters for reconstructing rank-1 lattices $\Lambda(\boldsymbol{z}, M, I_N^{d,0,\mathbf{0.5}})$.

Figure 6.1 depicts the relative $L^2(\mathbb{T}^d)$ error with respect to the "degrees of freedom", i.e., the cardinality $|I_N^{d,T,\boldsymbol{\gamma}}|$ of the weighted frequency index sets $I_N^{d,T,\boldsymbol{\gamma}}$, for the approximation of the function $G_{3,4}^d$ using the weighted frequency index sets $I_N^{d,0,\mathbf{1}}$ and $I_N^{d,0,\mathbf{0.5}}$. The relative $L^2(\mathbb{T}^d)$ error decreases for increasing degrees of freedom. In the cases $d = 1, \ldots, 6$, using the index set $I_N^{d,0,\mathbf{0.5}}$ does not yield better errors compared to using $I_N^{d,0,\mathbf{1}}$ for similar degrees of freedom. For the cases $d = 7, \ldots, 10$, the errors are smaller, when the index set $I_N^{d,0,\mathbf{0.5}}$ is used. In general, the error decreases slower for larger dimensions d and similar degrees of

	N=1	N=2	N=4	N=8	N=16	N=32	N=64	N=128	N=256	N=512	N=1024
d=1	1	3	5	9	17	33	65	129	257	513	1025
d=2	1	5	13	29	65	145	329	733	1633	3605	7913
d=3	1	7	25	69	177	441	1097	2693	6529	15645	37025
d=4	1	9	41	137	401	1105	2977	7897	20609	52953	133905
d=5	1	11	61	241	801	2433	7073	20073	55873	152713	409825
d=6	1	13	85	389	1457	4865	15241	46069	135905	392717	1112313
d=7	1	15	113	589	2465	9017	30409	97709	304321	925445	-
d=8	1	17	145	849	3937	15713	56961	194353	637697	2034289	-
d=9	1	19	181	1177	6001	26017	101185	366289	1264513	-	-
d=10	1	21	221	1581	8801	41265	171785	659085	2391905	-	-

(a) Cardinalities $|I^{d,0,\mathbf{1}}_{N,\text{even}}|$ of the unweighted symmetric hyperbolic cross index sets $I^{d,0,\mathbf{1}}_{N,\text{even}}$.

	N=1	N=2	N=4	N=8	N=16	N=32	N=64	N=128	N=256	N=512	N=1024
d=1	1	1	1	1	1	1	1	1	1	1	1
d=2	1	3	5	9	17	33	65	129	257	513	1025
d=3	1	5	13	41	145	545	2113	8321	33025	131585	525313
d=4	1	7	29	97	395	1721	5161	21569	85405	359213	1383595
d=5	1	9	49	257	1213	5815	21535	111015	485913	2353599	11148851
d=6	1	11	81	543	3079	14253	78167	404035	2328905	12181705	70968649
d=7	1	13	137	983	6905	34117	226951	1373325	8145033	50770301	293168219
d=8	1	15	183	1643	12543	84845	574275	4068807	27910471	179044805	-
d=9	1	17	255	2895	23375	184859	1248979	11051805	84391053	600266399	-
d=10	1	19	329	4899	43581	392131	3103601	26645547	205723321	-	-
d=11	1	21	399	6753	78601	831125	7057695	69268743	493556953	-	-

(b) z_d for reconstructing rank-1 lattices $\Lambda\left(\boldsymbol{z} = (z_1, \ldots, z_d)^\top, M = z_{d+1}, I^{d,0,\mathbf{1}}_{N,\text{even}}\right)$

Table 6.4: Cardinalities of index sets $I^{d,0,\mathbf{1}}_{N,\text{even}}$ and parameters for reconstructing rank-1 lattices $\Lambda(\boldsymbol{z}, M, I^{d,0,\mathbf{1}}_{N,\text{even}})$.

	N=1	N=2	N=4	N=8	N=16	N=32	N=64	N=128	N=256
d=1	3	5	9	17	33	65	129	257	513
d=2	9	21	49	105	245	565	1253	2769	6037
d=3	27	81	225	513	1373	3565	8581	20697	48077
d=4	81	297	945	2433	6921	19289	49913	129553	317129
d=5	243	1053	3753	11073	31993	95593	261625	725025	1860185
d=6	729	3645	14337	47561	138429	443565	1288893	3751105	10057501
d=7	2187	12393	53217	194001	570741	1955061	6045021	-	-
d=8	6561	41553	193185	760769	2284689	8278129	27183025	-	
d=9	19683	137781	688905	2897841	8951121	-	-	-	-
d=10	59049	452709	2421009	10798569	34413829	-	-	-	-

(a) Cardinalities $|I^{d,\frac{1}{8},\mathbf{1}}_N|$ of the unweighted energy norm based hyperbolic cross index sets $I^{d,\frac{1}{8},\mathbf{1}}_N$.

	N=1	N=2	N=4	N=8	N=16	N=32	N=64	N=128	N=256
d=1	1	1	1	1	1	1	1	1	1
d=2	3	5	9	17	35	65	129	257	513
d=3	9	23	58	163	649	2179	8451	33283	132099
d=4	27	105	343	1035	3504	9539	44488	158624	630387
d=5	81	479	1911	5727	23505	93561	430660	1925091	9044846
d=6	243	2185	10579	33769	175564	779006	3474262	18552520	94607056
d=7	729	9967	57897	191808	1191406	5517558	32161401	190124440	985817433
d=8	2187	45465	258113	1059754	7604598	45747614	266275510	-	-
d=9	6561	207391	1259193	6027975	49211282	287397400	2106873745	-	-
d=10	19683	946025	6898038	34264592	313687524	-	-	-	-
d=11	59049	4315343	37678938	195895338	1753317137	-	-	-	-

(b) z_d for reconstructing rank-1 lattices $\Lambda\left(\boldsymbol{z} = (z_1, \ldots, z_d)^\top, M = z_{d+1}, I^{d,\frac{1}{8},\mathbf{1}}_N\right)$

Table 6.5: Cardinalities of index sets $I^{d,\frac{1}{8},\mathbf{1}}_N$ and parameters for reconstructing rank-1 lattices $\Lambda(\boldsymbol{z}, M, I^{d,\frac{1}{8},\mathbf{1}}_N)$.

freedom. This is especially due to the dependency of the cardinality of the used index sets on the dimensionality. Therefore, we also consider the relative $L^2(\mathbb{T}^d)$ error as a function of the refinement N in Figure 6.2. In the case $\boldsymbol{\gamma} = \mathbf{1}$ and $d = 1$, the error decreases like $\sim N^{-3.45}$ if we use the error values for the 5 largest refinements N. Since the function $G^d_{3,4} \in \mathcal{H}^{0,\frac{7}{2}-\epsilon,\mathbf{1}}(\mathbb{T}^d)$, $\epsilon > 0$, but $G^d_{3,4} \notin \mathcal{H}^{0,\frac{7}{2},\mathbf{1}}(\mathbb{T}^d)$, Theorem 3.4 and inequality (2.7) only guarantee that the error decreases like $\sim N^{-3+\tilde{\epsilon}}$, $\tilde{\epsilon} > 0$, due to the term $\lambda > \frac{1}{2}$ in inequality

	N=1	N=2	N=4	N=8	N=16	N=32	N=64	N=128	N=256
d=1	3	5	9	17	33	65	129	257	513
d=2	9	21	49	105	237	529	1161	2489	5301
d=3	27	81	225	513	1349	3185	7537	17121	38453
d=4	81	297	945	2433	6681	16705	42289	100593	236041
d=5	243	1053	3753	11233	30473	82433	215105	536385	1312745
d=6	729	3645	14721	48905	131013	385809	1021497	2673385	6792637
d=7	2187	12393	56801	200945	543917	1721457	4610609	-	-
d=8	6561	41553	213153	789697	2210353	7368193	20089569	-	-
d=9	19683	142389	776457	3023985	8797041	-	-	-	-
d=10	59049	509029	2757649	11405929	34231709	-	-	-	-

(a) Cardinalities $|I_N^{d,\frac{1}{4},\mathbf{1}}|$ of the unweighted energy norm based hyperbolic cross index sets $I_N^{d,\frac{1}{4},\mathbf{1}}$.

	N=1	N=2	N=4	N=8	N=16	N=32	N=64	N=128	N=256
d=1	1	1	1	1	1	1	1	1	1
d=2	3	7	11	19	37	69	133	259	515
d=3	9	38	73	201	723	2451	8979	33801	133129
d=4	27	186	467	1142	3926	12823	39413	145671	567327
d=5	81	875	2051	7183	28420	103254	377671	1650518	6650454
d=6	243	4061	12022	41098	189483	670342	3083245	13681664	72067620
d=7	729	18610	53387	242620	1100207	5000857	26272212	127034272	716418836
d=8	2187	85228	313599	1333233	7833010	37378193	192462662	-	-
d=9	6561	389560	1722123	7295852	50063120	264177289	1551093161	-	-
d=10	19683	1777940	7615741	41539092	321531624	-	-		
d=11	59049	8113191	29508919	237772651	2017562984	-	-		

(b) z_d for reconstructing rank-1 lattices $\Lambda\left(\boldsymbol{z} = (z_1, \ldots, z_d)^\top, M = z_{d+1}, I_N^{d,\frac{1}{4},\mathbf{1}}\right)$

Table 6.6: Cardinalities of index sets $I_N^{d,\frac{1}{4},\mathbf{1}}$ and parameters for reconstructing rank-1 lattices $\Lambda(\boldsymbol{z}, M, I_N^{d,\frac{1}{4},\mathbf{1}})$.

	N=1	N=2	N=4	N=8	N=16	N=32	N=64	N=128	N=256	N=512	N=1024
d=1	1	3	5	9	17	33	65	129	257	513	1025
d=2	1	5	13	21	53	129	285	645	1401	3045	6525
d=3	1	7	25	37	117	345	861	2165	4937	11653	26685
d=4	1	9	41	57	217	753	2137	5929	13921	35705	86825
d=5	1	11	61	81	361	1441	4633	14153	33953	94393	242793
d=6	1	13	85	109	557	2513	9077	30445	74617	223805	606917
d=7	1	15	113	141	813	4089	16437	60285	151497	487581	-
d=8	1	17	145	177	1137	6305	27953	111569	288897	992433	-
d=9	1	19	181	217	1537	9313	45169	195217	523393	-	-
d=10	1	21	221	261	2021	13281	69965	325845	908345	-	-

(a) Cardinalities $|I_{N,\text{even}}^{d,\frac{1}{8},\mathbf{1}}|$ of the unweighted energy norm based hyperbolic cross index sets $I_{N,\text{even}}^{d,\frac{1}{8},\mathbf{1}}$.

	N=1	N=2	N=4	N=8	N=16	N=32	N=64	N=128	N=256	N=512	N=1024
d=1	1	1	1	1	1	1	1	1	1	1	1
d=2	1	3	5	9	17	33	65	129	257	513	1025
d=3	1	5	13	41	145	545	2113	8321	33025	131585	525313
d=4	1	7	29	65	329	1213	4895	18537	73061	291691	1160717
d=5	1	9	49	95	899	4527	18469	91085	374571	1762797	8065273
d=6	1	11	81	207	1531	10833	49363	299189	1483329	7701751	40400055
d=7	1	13	137	323	3117	19739	140795	911727	5227195	31401081	-
d=8	1	15	183	433	5239	43717	321847	2271831	12811923	96109869	-
d=9	1	17	255	553	9285	84359	602127	5740897	39606511	-	-
d=10	1	19	329	777	13667	160141	1462851	14600175	94002703	-	-
d=11	1	21	399	1031	21039	264087	3058027	34837351	222875047	-	-

(b) z_d for reconstructing rank-1 lattices $\Lambda\left(\boldsymbol{z} = (z_1, \ldots, z_d)^\top, M = z_{d+1}, I_{N,\text{even}}^{d,\frac{1}{8},\mathbf{1}}\right)$

Table 6.7: Cardinalities of index sets $I_{N,\text{even}}^{d,\frac{1}{8},\mathbf{1}}$ and parameters for reconstructing rank-1 lattices $\Lambda(\boldsymbol{z}, M, I_{N,\text{even}}^{d,\frac{1}{8},\mathbf{1}})$.

(2.7). However, the observed convergence rate is about $\frac{1}{2}$ better and we do not observe the additional term λ. This difference is very likely due to estimate (3.9) in the proof of Theorem 3.4. For $d = 2, \ldots, 10$, the errors are slightly higher and decrease similarly as in the one-dimensional case. Using the weight parameter $\boldsymbol{\gamma} = \mathbf{0.5}$ and $d = 1$, the error decreases like

$\sim N^{-3.47}$ if we use the error values for the 5 largest refinements N. For $d = 2, 3$, the error decreases like in the one-dimensional case and for $d = 4, \ldots, 10$, the error decreases slower. The explanation for this slower decrease of the error is that the considered refinements N are still too small to observe the asymptotic decrease.
Additionally, we study the functions G_3^d. As mentioned, we use the index sets with "holes" $I_{N,\text{even}}^{d,T,\boldsymbol{\gamma}}$. The parameters for the corresponding reconstructing rank-1 lattices are shown in Table 6.4. The numerical results are depicted in Figure 6.3 We observe a rapid decrease of the relative $L^2(\mathbb{T}^d)$ error for increasing degrees of freedom in Figure 6.3a. Again, the order of decrease is slower for higher dimensionality. When we compare using the index sets with "holes" $I_{N,\text{even}}^{d,T,\boldsymbol{\gamma}}$ to the full index sets $I_N^{d,T,\boldsymbol{\gamma}}$, we have almost the same error values for identical refinements N and therefore smaller error values for similar degrees of freedom when using the index sets with "holes", as we see in Figure 6.3b. Figure 6.4 depicts the relative $L^2(\mathbb{T}^d)$ error as a function of the refinement N. In Figure 6.4a and 6.4b, the results for the index sets with "holes" $I_{N,\text{even}}^{d,T,\boldsymbol{\gamma}}$ and the index sets $I_N^{d,T,\boldsymbol{\gamma}}$ are displayed, respectively, which are (almost) identical. For the function G_3^d in the one-dimensional case, the error decreases like $\sim N^{-3.49}$, and similarly for $d = 2, \ldots, 10$. The expected convergence rate from Theorem 3.4 and inequality (2.7) is $\sim N^{-3+\tilde{\epsilon}}$, $\tilde{\epsilon} > 0$, since $G_3^d \in \mathcal{H}^{0,\frac{7}{2}-\epsilon,\mathbf{1}}(\mathbb{T}^d)$, $\epsilon > 0$, and the observed convergence rate is about $\frac{1}{2}$ better as we have seen before. □

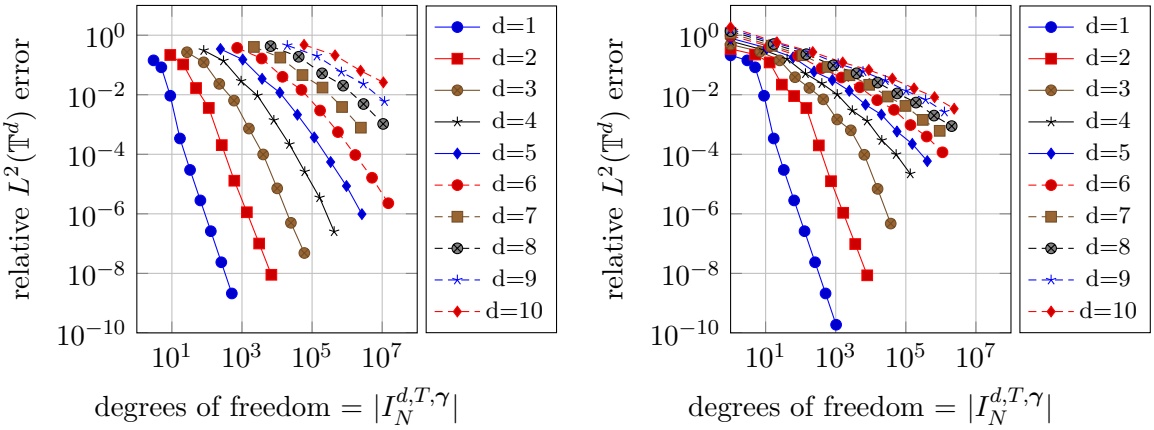

(a) $G_{3,4}^d$, $T = 0$, $\boldsymbol{\gamma} = \mathbf{1}$ (b) $G_{3,4}^d$, $T = 0$, $\boldsymbol{\gamma} = \mathbf{0.5}$

Figure 6.1: Relative $L^2(\mathbb{T}^d)$ error and "degrees of freedom" for the approximation of the function $G_{3,4}^d$.

Example 6.2. We verify the theoretical results from Theorem 3.4 for $r = 1$, $t = 0$ and inequality (2.7) using Algorithm 2. Here, we consider the relative $H^1(\mathbb{T}^d) = \mathcal{H}^{1,0,\boldsymbol{\gamma}}(\mathbb{T}^d)$ error. Similar to Example 6.1, we compute the relative $H^1(\mathbb{T}^d) = \mathcal{H}^{1,0,\boldsymbol{\gamma}}(\mathbb{T}^d)$ error $\|f - \tilde{S}_{I_N^{d,T,\boldsymbol{\gamma}}} f|H^1(\mathbb{T}^d)\|/\|f|H^1(\mathbb{T}^d)\|$ by

$$\frac{\left(\|f|H^1(\mathbb{T}^d)\|^2 - \sum_{\boldsymbol{k}\in I_N^{d,T,\boldsymbol{\gamma}}} \max(1, \|\boldsymbol{k}\|_1)^2 |\hat{f}_{\boldsymbol{k}}|^2 + \sum_{\boldsymbol{k}\in I_N^{d,T,\boldsymbol{\gamma}}} \max(1, \|\boldsymbol{k}\|_1)^2 \left|\hat{f}_{\boldsymbol{k}} - \hat{\tilde{f}}_{\boldsymbol{k}}\right|^2\right)^{\frac{1}{2}}}{\|f|H^1(\mathbb{T}^d)\|},$$

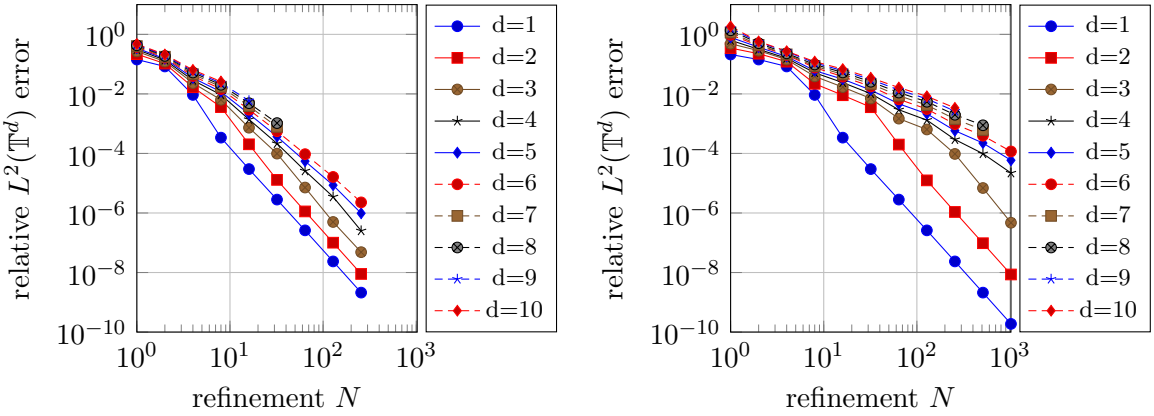

(a) $G^d_{3,4}$, $T = 0$, $\boldsymbol{\gamma} = \mathbf{1}$ (b) $G^d_{3,4}$, $T = 0$, $\boldsymbol{\gamma} = \mathbf{0.5}$

Figure 6.2: Relative $L^2(\mathbb{T}^d)$ error and refinement N for the approximation of the function $G^d_{3,4}$.

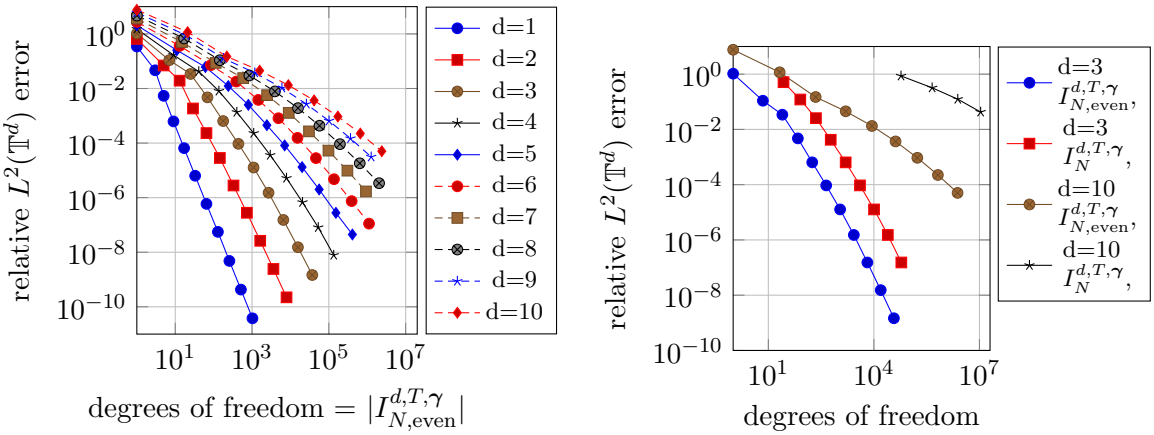

(a) G^d_3, $T = 0$, $\boldsymbol{\gamma} = \mathbf{1}$ (b) G^d_3, $T = 0$, $\boldsymbol{\gamma} = \mathbf{1}$

Figure 6.3: Relative $L^2(\mathbb{T}^d)$ error and "degrees of freedom" for the approximation of the functions G^d_3.

where we compute the $H^1(\mathbb{T}^d)$ norm explicitly. We use the unweighted symmetric hyperbolic cross index sets $I^{d,0,\mathbf{1}}_N$ and the reconstructing rank-1 lattices from Table 6.2, the unweighted energy norm based hyperbolic cross index sets $I^{d,\frac{1}{8},\mathbf{1}}_N$ and the reconstructing rank-1 lattices from Table 6.5, the unweighted energy norm based hyperbolic cross index sets $I^{d,\frac{1}{4},\mathbf{1}}_N$ and the reconstructing rank-1 lattices from Table 6.6, the weighted symmetric hyperbolic cross index sets $I^{d,0,\mathbf{0.5}}_N$ and the reconstructing rank-1 lattices from Table 6.3 as well as the unweighted energy norm based hyperbolic cross index sets with "holes" $I^{d,\frac{1}{8},\mathbf{1}}_{N,\text{even}}$ and the reconstructing rank-1 lattices from Table 6.7. Figure 6.5 shows the relative $H^1(\mathbb{T}^d)$ error with respect to the "degrees of freedom", i.e., the cardinality $|I^{d,T,\boldsymbol{\gamma}}_N|$ of the weighted frequency index sets $I^{d,T,\boldsymbol{\gamma}}_N$, for the approximation of the function $G^d_{3,4}$. The relative $H^1(\mathbb{T}^d)$ error decreases for

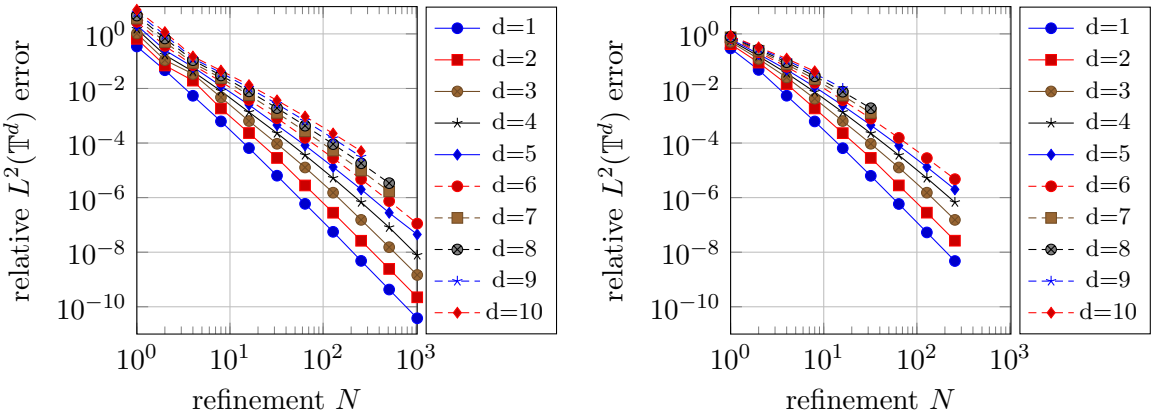

(a) G_3^d with $I_{N,\text{even}}^{d,T,\boldsymbol{\gamma}}$, $T = 0$, $\boldsymbol{\gamma} = \mathbf{1}$

(b) G_3^d with $I_N^{d,T,\boldsymbol{\gamma}}$, $T = 0$, $\boldsymbol{\gamma} = \mathbf{1}$

Figure 6.4: Relative $L^2(\mathbb{T}^d)$ error and refinement N for the approximation of the functions G_3^d.

increasing degrees of freedom. For the considered function $G_{3,4}^d$, using the energy norm based symmetric hyperbolic cross index sets $I_N^{d,\frac{1}{8},\mathbf{1}}$ and $I_N^{d,\frac{1}{4},\mathbf{1}}$ does not result in smaller error values for similar degrees of freedom, see Figure 6.5a, 6.5b and 6.5c. Furthermore, in the cases $d = 1, \ldots, 6$, using the index set $I_N^{d,0,\mathbf{0.5}}$ does not yield better errors compared to using $I_N^{d,0,\mathbf{1}}$ for similar degrees of freedom, see Figure 6.5d. For the cases $d = 7, \ldots, 10$, the errors are smaller, when the index set $I_N^{d,0,\mathbf{0.5}}$ is used. In general, the error decreases slower for larger dimensions d. This is especially due to the dependency of the cardinality of the used index sets on the dimensionality. We also consider the relative $H^1(\mathbb{T}^d)$ error as a function of the refinement N in Figure 6.6. For the unweighted symmetric hyperbolic cross index sets $I_N^{d,0,\mathbf{1}}$ and the unweighted energy norm based hyperbolic cross index sets $I_N^{d,\frac{1}{8},\mathbf{1}}$, the error decreases like $\sim N^{-2.46}$ in the one-dimensional case, if we consider the error values for the five largest refinements, and similarly for $d = 2, \ldots, 10$. In the case $T = 0$, the observed convergence rate is about $\frac{1}{2}$ better than in the theoretical results from Theorem 3.4 in combination with inequality (2.7), which state an error decrease of $\sim N^{-2+\tilde{\epsilon}}$, $\tilde{\epsilon} > 0$. In the case $T = 1/8$, the theoretical results state an error decrease of $\sim N^{-2+\tilde{\epsilon}+\frac{d-1}{d-1/8}\frac{7}{16}}$, $\tilde{\epsilon} > 0$, and again, the observed convergence rate is better than the theoretical estimate. We also consider the function G_3^d and use the frequency index sets with "holes" $I_{N,\text{even}}^{d,T,\boldsymbol{\gamma}}$. Figure 6.7 shows the relative $H^1(\mathbb{T}^d)$ error as a function of the refinement N. For the unweighted symmetric hyperbolic cross index sets with "holes" $I_{N,\text{even}}^{d,0,\mathbf{1}}$ and the unweighted energy norm based hyperbolic cross index sets $I_{N,\text{even}}^{d,\frac{1}{8},\mathbf{1}}$, the error decreases like $\sim N^{-2.45}$ in the one-dimensional case, if we consider the error values for the five largest refinements, and similarly for $d = 2, \ldots, 10$. Once more, this observed error decay is slightly better than the theoretical estimate. □

Example 6.3. In this example, we consider the computation time for some of the test cases from Example 6.1. The time measurements were performed five times using only one thread and the average value of the five time measurements was used. We consider the functions $G_{3,4}^d$ and G_3^d. For the function $G_{3,4}^d$, we use the unweighted symmetric hyperbolic cross index

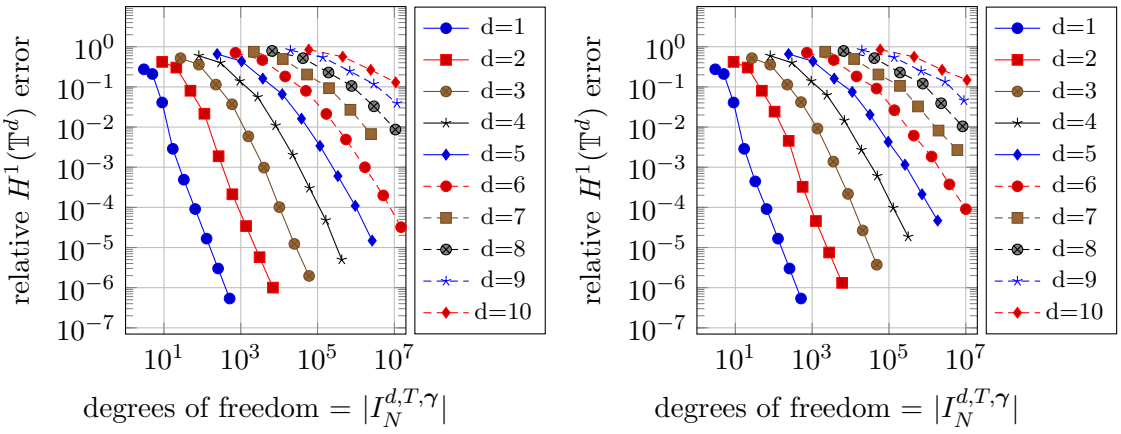

(a) $G_{3,4}^d$, $T = 0$, $\boldsymbol{\gamma} = \mathbf{1}$

(b) $G_{3,4}^d$, $T = 1/8$, $\boldsymbol{\gamma} = \mathbf{1}$

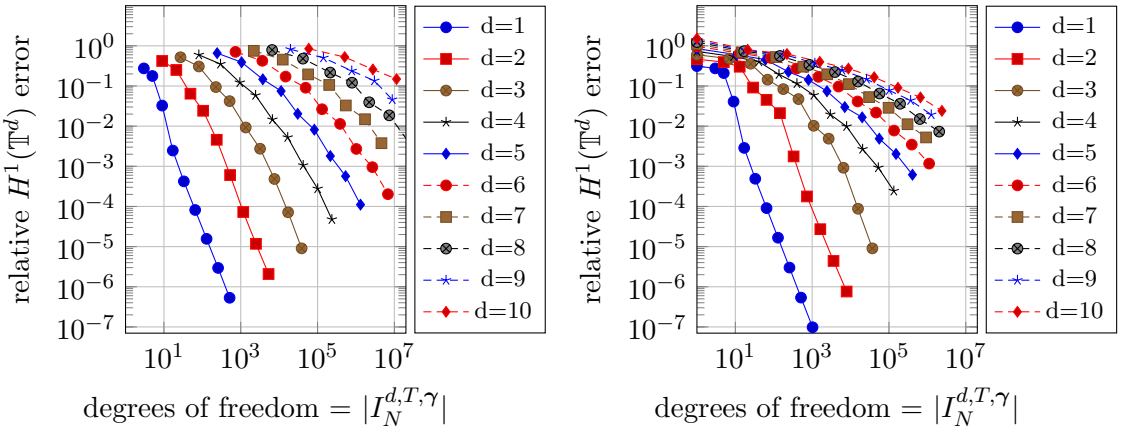

(c) $G_{3,4}^d$, $T = 1/4$, $\boldsymbol{\gamma} = \mathbf{1}$

(d) $G_{3,4}^d$, $T = 0$, $\boldsymbol{\gamma} = \mathbf{0.5}$

Figure 6.5: Relative $H^1(\mathbb{T}^d)$ error and "degrees of freedom" for the approximation of the function $G_{3,4}^d$.

sets $I_N^{d,0,\mathbf{1}}$ and reconstructing rank-1 lattices $\Lambda(\boldsymbol{z}, M, I_N^{d,0,\mathbf{1}})$ from Table 6.2. For the function G_3^d, we use the unweighted symmetric hyperbolic cross index sets with "holes" $I_{N,\text{even}}^{d,0,\mathbf{1}}$ and reconstructing rank-1 lattices $\Lambda(\boldsymbol{z}, M, I_{N,\text{even}}^{d,0,\mathbf{1}})$ from Table 6.4.
As stated in Theorem 2.1, there exists a reconstructing rank-1 lattice $\Lambda(\boldsymbol{z}, M, I)$ with lattice size $M \leq |I|^2$ for each frequency index set $I = \{I_N^{d,T,\gamma}, I_{N,\text{even}}^{d,T,\gamma}\}$. Furthermore, the arithmetic complexity of computing the approximated Fourier coefficients $\hat{\hat{f}}_{\boldsymbol{k}}$, $\boldsymbol{k} \in I$, by applying the lattice rule (3.2) and Algorithm 2 is $\mathcal{O}(M \log M + d|I|) = \mathcal{O}(|I|^2 \log |I|)$, if we assume $|I| \geq d$ and $M \leq |I|^2$. Therefore, when we visualize the computation time as a function of the cardinality $|I|$ of the frequency index set I in a double logarithmic plot, one should observe a slope of about 2 in each plot independent of the dimensionality d. Figure 6.8a shows the test results for the functions $G_{3,4}^d$ and Figure 6.8b for the function G_3^d. In both cases, we observe that the plots behave similarly independent of the dimensionality d except for smaller outliers and a slope of about 2 for larger cardinalities as the theoretical considerations suggest. □

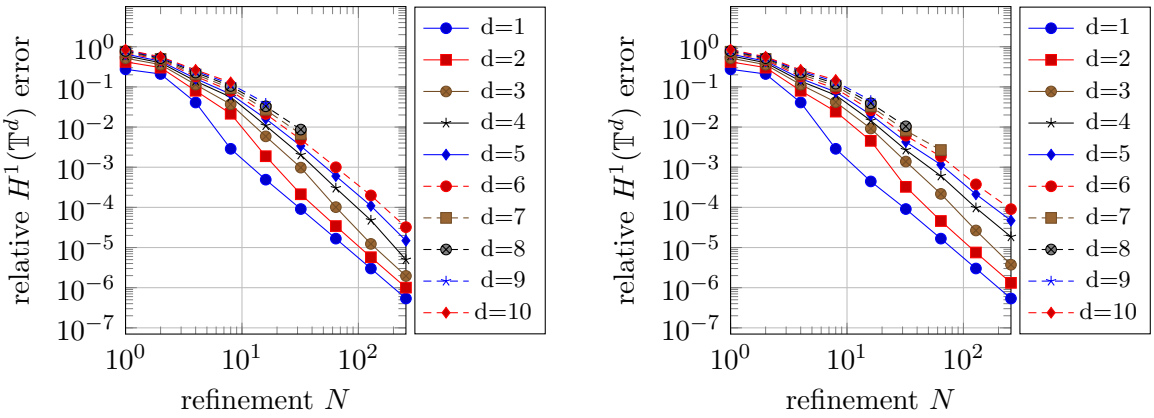

(a) $G^d_{3,4}$, $T = 0$, $\boldsymbol{\gamma} = \mathbf{1}$ (b) $G^d_{3,4}$, $T = 1/8$, $\boldsymbol{\gamma} = \mathbf{1}$

Figure 6.6: Relative $H^1(\mathbb{T}^d)$ error and refinement N for the approximation of the function $G^d_{3,4}$.

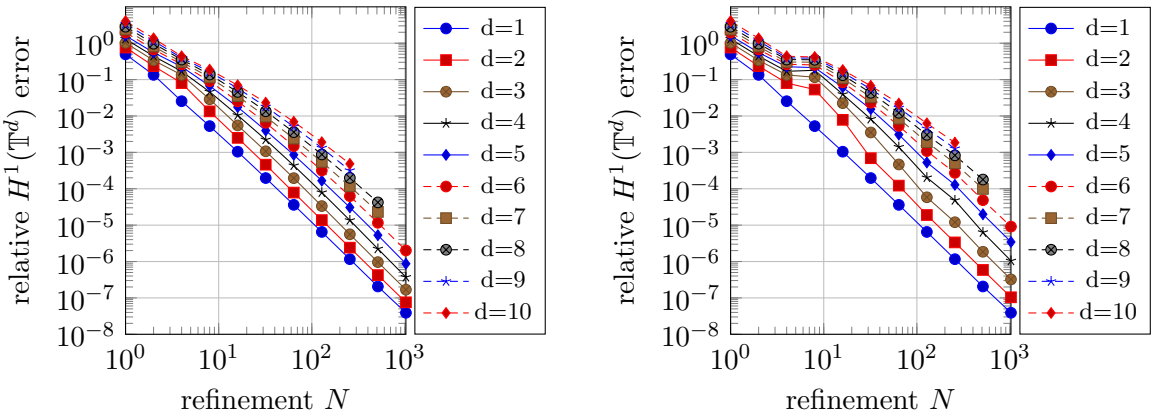

(a) G^d_3, $T = 0$, $\boldsymbol{\gamma} = \mathbf{1}$ (b) G^d_3, $T = 1/8$, $\boldsymbol{\gamma} = \mathbf{1}$

Figure 6.7: Relative $H^1(\mathbb{T}^d)$ error and refinement N for the approximation of the function G^d_3.

Example 6.4. We verify the theoretical results from Theorem 5.1 in Section 5. These results only differ from the ones of Theorem 3.4 by the additional constant $C(d, T, m)$ and the additional stability term $1/\left(2 - \mathrm{e}^{2\pi\left(d^{1+\max\left(0,\frac{T}{1-T}\right)}\right)N\varepsilon}\right)$ in the aliasing error. We use the function $G^d_{3,4}$ as well as the unweighted symmetric hyperbolic cross index sets $I_N^{d,0,\mathbf{1}}$ and the reconstructing rank-1 lattices $\Lambda(\boldsymbol{z}, M, I_N^{d,0,\mathbf{1}})$ from Table 6.2. For each reconstructing rank-1 lattice $\Lambda(\boldsymbol{z}, M, I_N^{d,0,\mathbf{1}}) = \{\boldsymbol{x}_j\}_{j=0}^{M-1}$, we uniformly randomly choose the sampling nodes $\boldsymbol{y}_j$, $j = 0, \ldots, M-1$, such that $\|\boldsymbol{y}_j - \boldsymbol{x}_j\|_\infty < \varepsilon$ with $\varepsilon = \left(2\pi dN\right)^{-1} \ln 2$. We sample the function $G^d_{3,4}$ at the sampling nodes $\boldsymbol{y}_j$ and compute the approximated Fourier coefficients $(\hat{\tilde{f}}_{\boldsymbol{k}})_{\boldsymbol{k}\in I_N^{d,T,\boldsymbol{\gamma}}}$ using the approximate LSQR algorithm (lsqr function from MATLAB) in combination with Algorithm 3 and its adjoint version. Since $G^d_{3,4} \in \mathcal{H}^{0,\frac{7}{2}-\epsilon,\mathbf{1}}(\mathbb{T}^d)$, $\epsilon > 0$, the prerequisites of

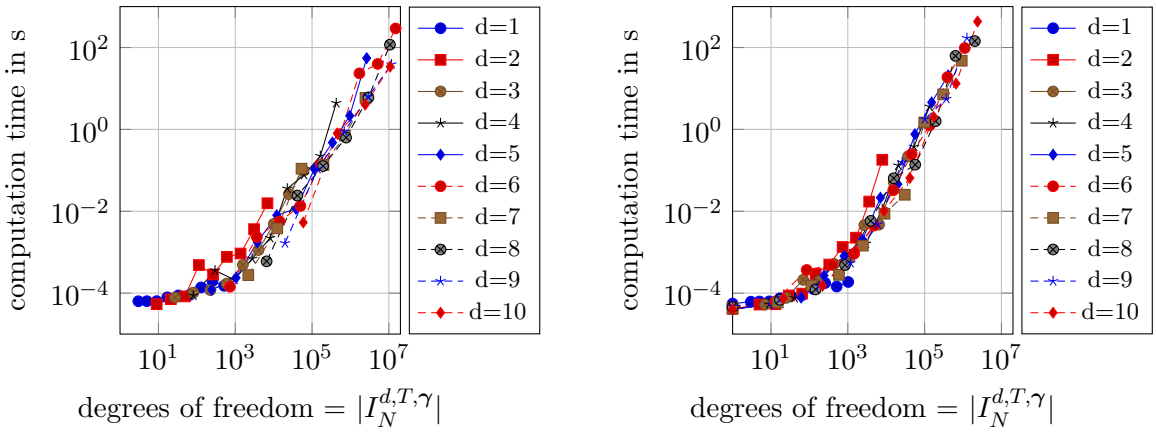

(a) $G_{3,4}^d$, $T = 0$, $\boldsymbol{\gamma} = \mathbf{1}$

(b) G_3^d, $T = 0$, $\boldsymbol{\gamma} = \mathbf{1}$

Figure 6.8: Computation time and "degrees of freedom" for the approximation of the functions $G_{3,4}^d$ and G_3^d.

Theorem 5.1 require to choose $m = 4$ in order to obtain a guaranteed order of convergence of $\sim N^{-\frac{7}{2}+\epsilon}$. Therefore, we run the numerical tests for $m = 4$. The numerical results for the relative $L^2(\mathbb{T}^d)$ error are depicted in Figure 6.9c and the observed relative $L^2(\mathbb{T}^d)$ errors are (almost) identical to those of the unperturbed case, see Figure 6.1a of Example 6.1. Additionally, we consider the cases $m = 2$ and $m = 3$. The corresponding numerical results are shown in Figure 6.9a and 6.9b. For $m = 3$, the observed relative $L^2(\mathbb{T}^d)$ errors are (almost) identical to the case $m = 4$ and to the unperturbed case. For $m = 2$, the errors are larger in the cases $d = 1, 2, 3$ for higher degrees of freedom and similar for the cases $d = 4, \dots, 10$. In Figure 6.9d, the results of the cases $m = 2$ and $m = 3$ as well as for the unperturbed case ("R1L") are compared for $d = 2, 3, 6$. In Figure 6.10, the numerical results for the relative $H^1(\mathbb{T}^d)$ error are depicted. We observe the same behavior as in the case of the relative $L^2(\mathbb{T}^d)$ error when we compare the relative $H^1(\mathbb{T}^d)$ errors from this example with the results from Example 6.2.
Additionally, we increase the perturbation parameter to $\varepsilon = \big(2\pi N\big)^{-1} \ln 2$, i.e., we set it independently of the dimensionality d, which is larger than the prerequisites of Theorem 5.1 allow. The numerical results are shown in Figure 6.11. We observe almost the same behavior as with the smaller perturbation in Figure 6.9. Only for low degrees of freedom and higher dimensionality, we observe a larger relative $L^2(\mathbb{T}^d)$ error. □

7 Conclusion

In this paper, we developed a method for the approximation of functions from subspaces of the Wiener algebra by sampling on rank-1 lattices and on perturbed rank-1 lattices. We used reconstructing rank-1 lattices which guarantee good approximation properties. Based on the decay property of the Fourier coefficients of functions, we proved error estimates and presented numerical results. Our main focus in future research will be the development of good strategies for finding reconstructing lattice rules, as well as the development of algorithms for reconstructing trigonometric polynomials with frequencies supported on an index set I by

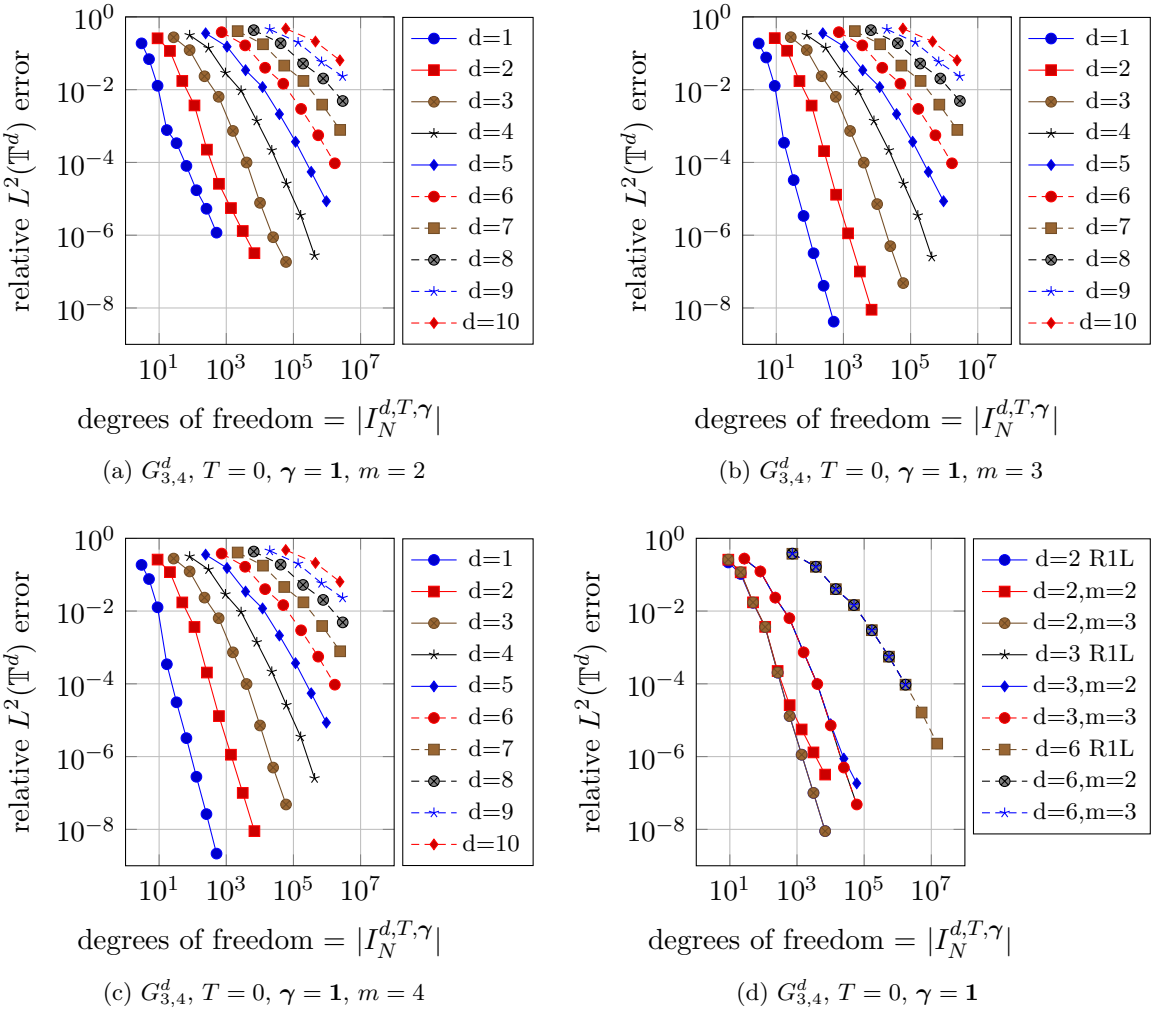

(a) $G_{3,4}^d$, $T = 0$, $\boldsymbol{\gamma} = \mathbf{1}$, $m = 2$

(b) $G_{3,4}^d$, $T = 0$, $\boldsymbol{\gamma} = \mathbf{1}$, $m = 3$

(c) $G_{3,4}^d$, $T = 0$, $\boldsymbol{\gamma} = \mathbf{1}$, $m = 4$

(d) $G_{3,4}^d$, $T = 0$, $\boldsymbol{\gamma} = \mathbf{1}$

Figure 6.9: Relative $L^2(\mathbb{T}^d)$ error and "degrees of freedom" for the approximation of the function $G_{3,4}^d$ by sampling at perturbed rank-1 lattice nodes ($\varepsilon = \left(2\pi dN\right)^{-1} \ln 2$) and unperturbed rank-1 lattice nodes ("R1L").

using only $\mathcal{O}(|I|)$ values from a corresponding reconstructing lattice rule. We refer to the impressive results of the sparse FFT, cf. [17, 16]. The authors present methods which allow the reconstruction with high probability in $\mathcal{O}(|I| \log |I|)$. We will combine our rank-1 lattice approach with these methods. The main advantage is that after using the rank-1 lattice we have a one-dimensional problem, where in addition the support of the one-dimensional Fourier transform is known.

Acknowledgements

The authors thank the referees for their valuable suggestions and gratefully acknowledge support by the German Research Foundation (DFG) within the Priority Program 1324, project PO 711/10-2.

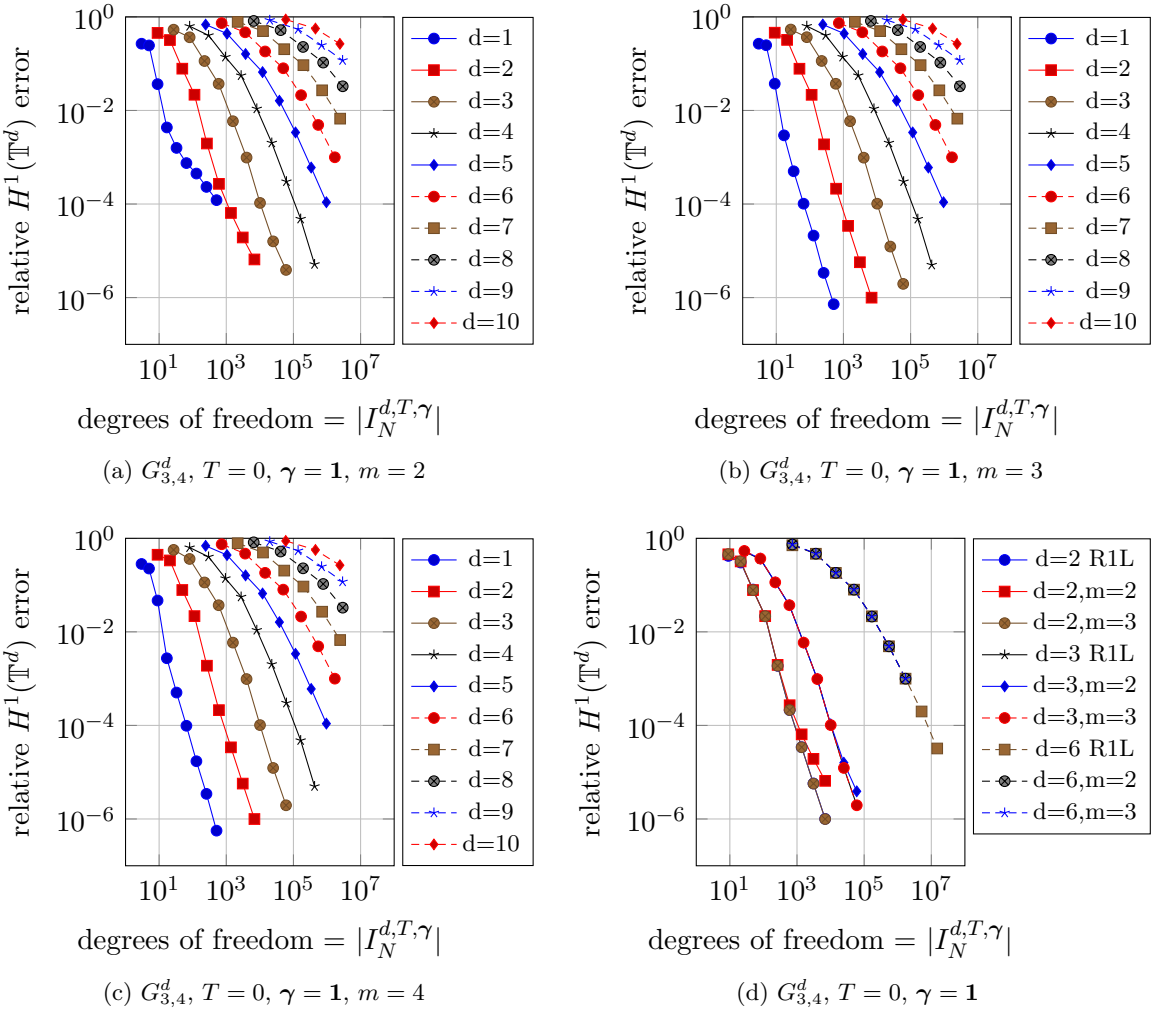

(a) $G_{3,4}^d$, $T = 0$, $\boldsymbol{\gamma} = \mathbf{1}$, $m = 2$

(b) $G_{3,4}^d$, $T = 0$, $\boldsymbol{\gamma} = \mathbf{1}$, $m = 3$

(c) $G_{3,4}^d$, $T = 0$, $\boldsymbol{\gamma} = \mathbf{1}$, $m = 4$

(d) $G_{3,4}^d$, $T = 0$, $\boldsymbol{\gamma} = \mathbf{1}$

Figure 6.10: Relative $H^1(\mathbb{T}^d)$ error and "degrees of freedom" for the approximation of the function $G_{3,4}^d$ by sampling at perturbed rank-1 lattice nodes ($\varepsilon = \left(2\pi dN\right)^{-1} \ln 2$) and unperturbed rank-1 lattice nodes ("R1L").

References

[1] C. Anderson and M. Dahleh. Rapid computation of the discrete Fourier transform. *SIAM J. Sci. Comput.*, 17:913 – 919, 1996.

[2] G. Baszenski and F.-J. Delvos. A discrete Fourier transform scheme for Boolean sums of trigonometric operators. In C. K. Chui, W. Schempp, and K. Zeller, editors, *Multivariate Approximation Theory IV*, ISNM 90, pages 15 – 24. Birkhäuser, Basel, 1989.

[3] Å. Björck. *Numerical Methods for Least Squares Problems.* SIAM, Philadelphia, PA, USA, 1996.

[4] H.-J. Bungartz and M. Griebel. A note on the complexity of solving Poisson's equation for spaces of bounded mixed derivatives. *J. Complexity*, 15:167 – 199, 1999.

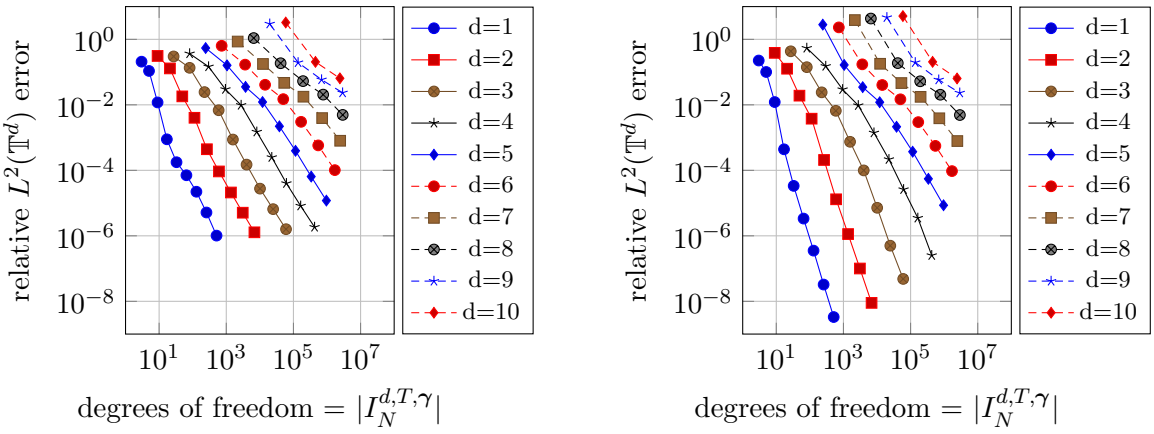

(a) $G_{3,4}^d$, $T = 0$, $\boldsymbol{\gamma} = \mathbf{1}$, $m = 2$

(b) $G_{3,4}^d$, $T = 0$, $\boldsymbol{\gamma} = \mathbf{1}$, $m = 3$

(c) $G_{3,4}^d$, $T = 0$, $\boldsymbol{\gamma} = \mathbf{1}$, $m = 4$

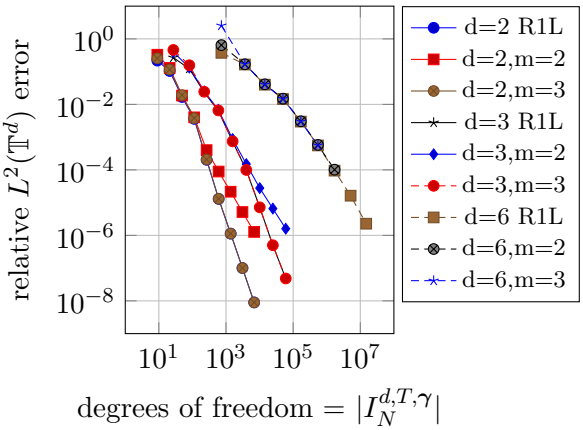

(d) $G_{3,4}^d$, $T = 0$, $\boldsymbol{\gamma} = \mathbf{1}$

Figure 6.11: Relative $L^2(\mathbb{T}^d)$ error and "degrees of freedom" for the approximation of the function $G_{3,4}^d$ by sampling at perturbed rank-1 lattice nodes ($\varepsilon = \left(2\pi N\right)^{-1} \ln 2$) and unperturbed rank-1 lattice nodes ("R1L").

[5] H.-J. Bungartz and M. Griebel. Sparse grids. *Acta Numer.*, 13:147 – 269, 2004.

[6] R. Cools, F. Y. Kuo, and D. Nuyens. Constructing lattice rules based on weighted degree of exactness and worst case error. *Computing*, 87:63 – 89, 2010.

[7] R. Cools and D. Nuyens. Fast algorithms for component-by-component construction of rank-1 lattice rules in shift-invariant reproducing kernel Hilbert spaces. *Math. Comp.*, 75:903 – 920, 2004.

[8] J. Dick, F. Y. Kuo, and I. H. Sloan. High-dimensional integration: The quasi-Monte Carlo way. *Acta Numer.*, 22:133 – 288, 2013.

[9] M. Döhler, S. Kunis, and D. Potts. Nonequispaced hyperbolic cross fast Fourier transform. *SIAM J. Numer. Anal.*, 47:4415 – 4428, 2010.

[10] H. G. Feichtinger and K. Gröchenig. Theory and practice of irregular sampling. In J. Benedetto and M. Frazier, editors, *Wavelets: Mathematics and Applications*, pages 305 – 363, CRC Press, 1993.

[11] V. Gradinaru. Fourier transform on sparse grids: Code design and the time dependent Schrödinger equation. *Computing*, 80:1 – 22, 2007.

[12] M. Griebel and J. Hamaekers. Fast discrete Fourier transform on generalized sparse grids. In J. Garcke and D. Pflger, editors, *Sparse Grids and Applications - Munich 2012*, volume 97 of *Lect. Notes Comput. Sci. Eng.*, pages 75 – 107. Springer International Publishing, 2014.

[13] M. Griebel and S. Knapek. Optimized Tensor-Product Approximation Spaces. *Constructive Approximation*, 16(4):525–540, 2000.

[14] K. Gröchenig. Reconstruction algorithms in irregular sampling. *Math. Comput.*, 59:181 – 194, 1992.

[15] K. Hallatschek. Fouriertransformation auf dünnen Gittern mit hierarchischen Basen. *Numer. Math.*, 63:83 – 97, 1992.

[16] H. Hassanieh, P. Indyk, D. Katabi, and E. Price. Nearly optimal sparse Fourier transform. In *Proceedings of the Forty-fourth Annual ACM Symposium on Theory of Computing*, pages 563 – 578. ACM, 2012.

[17] H. Hassanieh, P. Indyk, D. Katabi, and E. Price. Simple and practical algorithm for sparse Fourier transform. In *Proceedings of the Twenty-third Annual ACM-SIAM Symposium on Discrete Algorithms*, pages 1183 – 1194. SIAM, 2012.

[18] R. A. Horn and C. R. Johnson. *Topics in Matrix Analysis*. Cambridge University Press, Cambridge, UK, 1991.

[19] Y. Jiang and Y. Xu. Fast discrete algorithms for sparse Fourier expansions of high dimensional functions. *J. Complexity*, 26:51 – 81, 2010.

[20] L. Kämmerer. Reconstructing hyperbolic cross trigonometric polynomials by sampling along rank-1 lattices. *SIAM J. Numer. Anal.*, 51:2773 – 2796, 2013.

[21] L. Kämmerer. Reconstructing multivariate trigonometric polynomials from samples along rank-1 lattices. In G. E. Fasshauer and L. L. Schumaker, editors, *Approximation Theory XIV: San Antonio 2013*, pages 255 – 271. Springer International Publishing, 2014.

[22] L. Kämmerer and S. Kunis. On the stability of the hyperbolic cross discrete Fourier transform. *Numer. Math.*, 117:581 – 600, 2011.

[23] L. Kämmerer, S. Kunis, and D. Potts. Interpolation lattices for hyperbolic cross trigonometric polynomials. *J. Complexity*, 28:76 – 92, 2012.

[24] S. Knapek. Approximation und Kompression mit Tensorprodukt-Multiskalenräumen. Dissertation, Universität Bonn, 2000.

[25] T. Kühn, W. Sickel, and T. Ullrich. Approximation numbers of Sobolev embeddings—sharp constants and tractability. *J. Complexity*, 30:95 – 116, 2014.

[26] S. Kunis. Nonequispaced fast Fourier transforms without oversampling. *Proc. Appl. Math. Mech.*, 8:10977 – 10978, 2008.

[27] D. Li and F. J. Hickernell. Trigonometric spectral collocation methods on lattices. In S. Y. Cheng, C.-W. Shu, and T. Tang, editors, *Recent Advances in Scientific Computing and Partial Differential Equations*, volume 330 of *Contemp. Math.*, pages 121 – 132. AMS, 2003.

[28] H. Munthe-Kaas and T. Sørevik. Multidimensional pseudo-spectral methods on lattice grids. *Appl. Numer. Math.*, 62:155 – 165, 2012.

[29] E. Novak and H. Woźniakowski. *Tractability of Multivariate Problems Volume II: Standard Information for Functionals.* Eur. Math. Society, EMS Tracts in Mathematics Vol 12, 2010.

[30] D. Potts and M. Tasche. Numerical stability of nonequispaced fast Fourier transforms. *J. Comput. Appl. Math.*, 222:655 – 674, 2008.

[31] W. Sickel and T. Ullrich. The Smolyak algorithm, sampling on sparse grids and function spaces of dominating mixed smoothness. *East J. Approx.*, 13:387 – 425, 2007.

[32] I. H. Sloan and S. Joe. *Lattice methods for multiple integration.* Oxford Science Publications. The Clarendon Press Oxford University Press, New York, 1994.

[33] I. H. Sloan and A. V. Reztsov. Component-by-component construction of good lattice rules. *Math. Comp.*, 71:263 – 273, 2002.

[34] F. Sprengel. A class of function spaces and interpolation on sparse grids. *Numer. Funct. Anal. Optim.*, 21:273 – 293, 2000.

[35] V. N. Temlyakov. Approximation of functions with bounded mixed derivative. *Proc. Steklov Inst. Math.*, 1989. A translation of Trudy Mat. Inst. Steklov 178 (1986).

[36] T. Volkmer. Taylor and rank-1 lattice based nonequispaced fast Fourier transform. In *10th international conference on Sampling Theory and Applications (SampTA 2013)*, pages 576 – 579, Bremen, Germany, 2013.

[37] C. Zenger. Sparse grids. In *Parallel algorithms for partial differential equations (Kiel, 1990)*, volume 31 of *Notes Numer. Fluid Mech.*, pages 241 – 251. Vieweg, Braunschweig, Germany, 1991.